Algorithmic Lung Nodule Analysis in Chest Tomography Images

A Statistical Extension of the Level Set Method for Image Segmentation

Matthew C. Hancock

Department of Mathematics
Florida State University

Major Professor: Jerry F. Magnan

November 9, 2017

Mortality Rates of Cancer by Anatomical Location

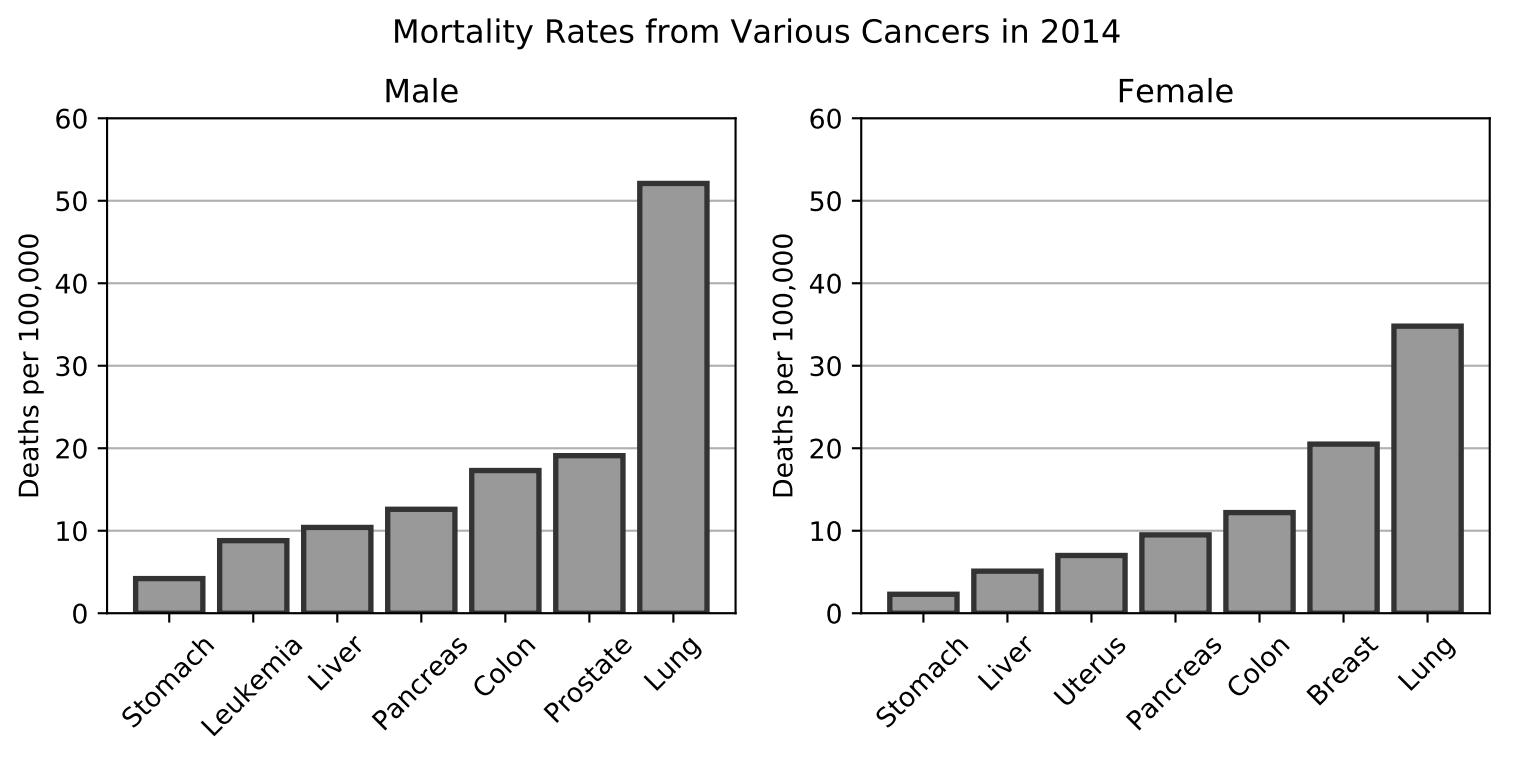

Medical Motivation for Computer-Aided Diagnosis

- Early detection of lung cancer increases survival rate [3]
- NLST [1] (study of 53,454 patients): low-dose CT screening reduced mortality rate by a relative reduction of 20% compared to traditional radiography screening.
- Lung CAD may aid in early detection and understanding of characteristics of malignant nodules to potentially improve survival rates
- Large dataset necessary for validating lung CAD methods prompts collection of LIDC dataset (1018 annotated chest CT scans) [2]

Medical Motivation for Computer-Aided Diagnosis

- Early detection of lung cancer increases survival rate [3]
- NLST [1] (study of 53,454 patients): low-dose CT screening reduced mortality rate by a relative reduction of 20% compared to traditional radiography screening.
- Lung CAD may aid in early detection and understanding of characteristics of malignant nodules to potentially improve survival rates
- Large dataset necessary for validating lung CAD methods prompts collection of LIDC dataset (1018 annotated chest CT scans) [2]

Medical Motivation for Computer-Aided Diagnosis

- Early detection of lung cancer increases survival rate [3]
- NLST [1] (study of 53,454 patients): low-dose CT screening reduced mortality rate by a relative reduction of 20% compared to traditional radiography screening.
- Lung CAD may aid in early detection and understanding of characteristics of malignant nodules to potentially improve survival rates
- Large dataset necessary for validating lung CAD methods prompts collection of LIDC dataset (1018 annotated chest CT scans) [2]

Medical Motivation for Computer-Aided Diagnosis

- Early detection of lung cancer increases survival rate [3]
- NLST [1] (study of 53,454 patients): low-dose CT screening reduced mortality rate by a relative reduction of 20% compared to traditional radiography screening.
- Lung CAD may aid in early detection and understanding of characteristics of malignant nodules to potentially improve survival rates
- Large dataset necessary for validating lung CAD methods prompts collection of LIDC dataset (1018 annotated chest CT scans) [2]

Primary Object of Interest

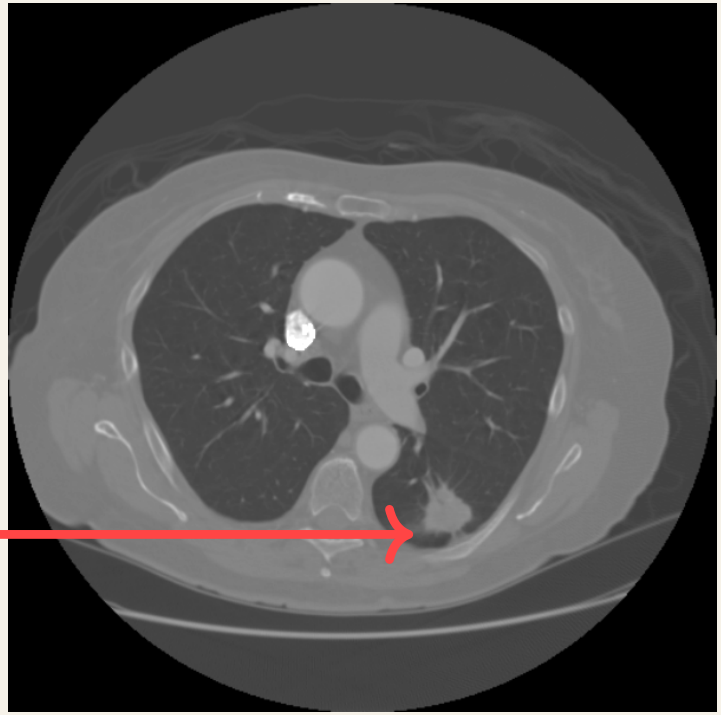

- **Lung nodule**: small to medium sized (roughly, 3 mm to 30 mm), abnormal region with a somewhat well-defined boundary [8]

Lung CAD Paradigm for Nodules from Chest CT

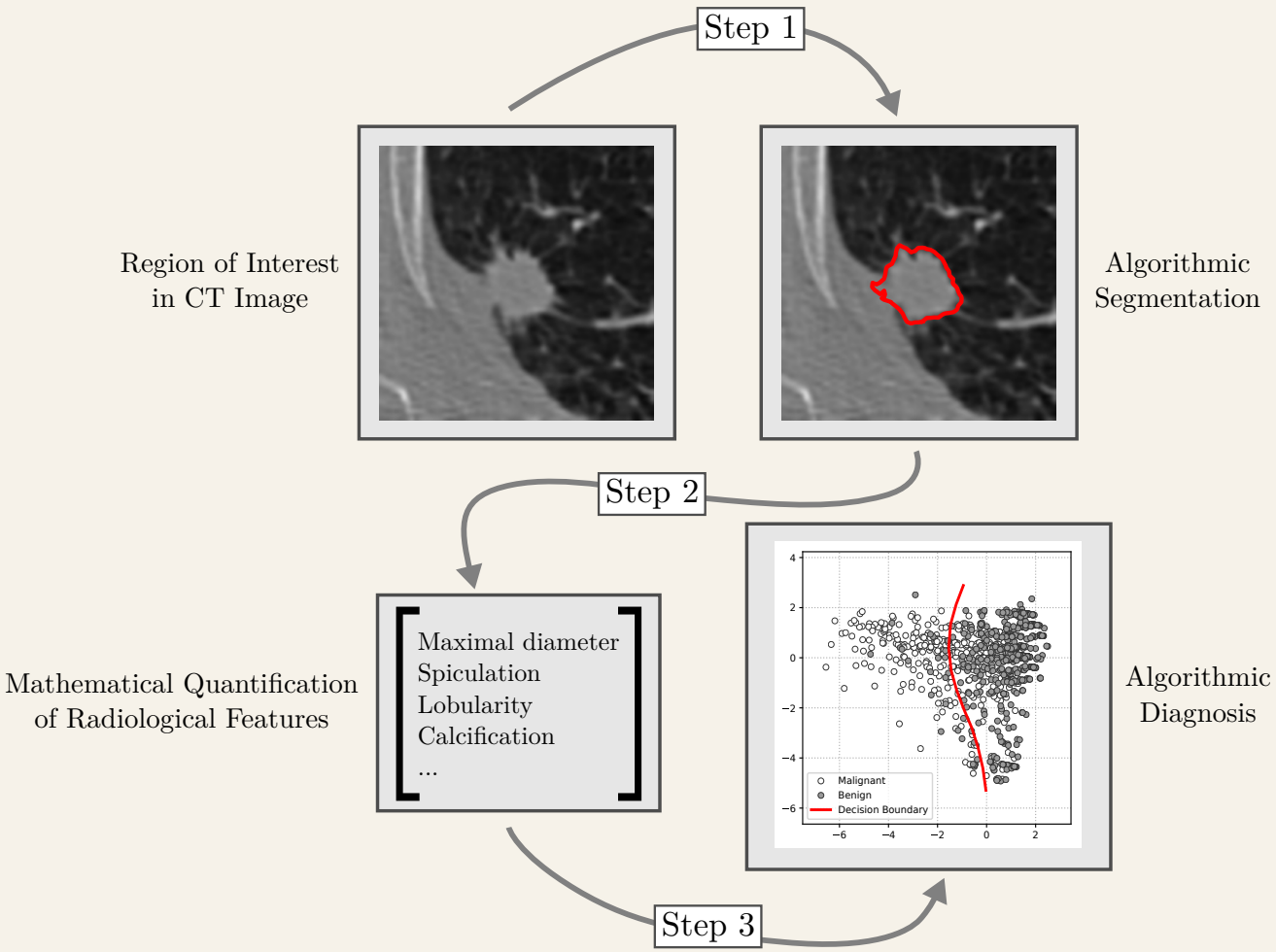

Lung CAD Paradigm for Nodules from Chest CT

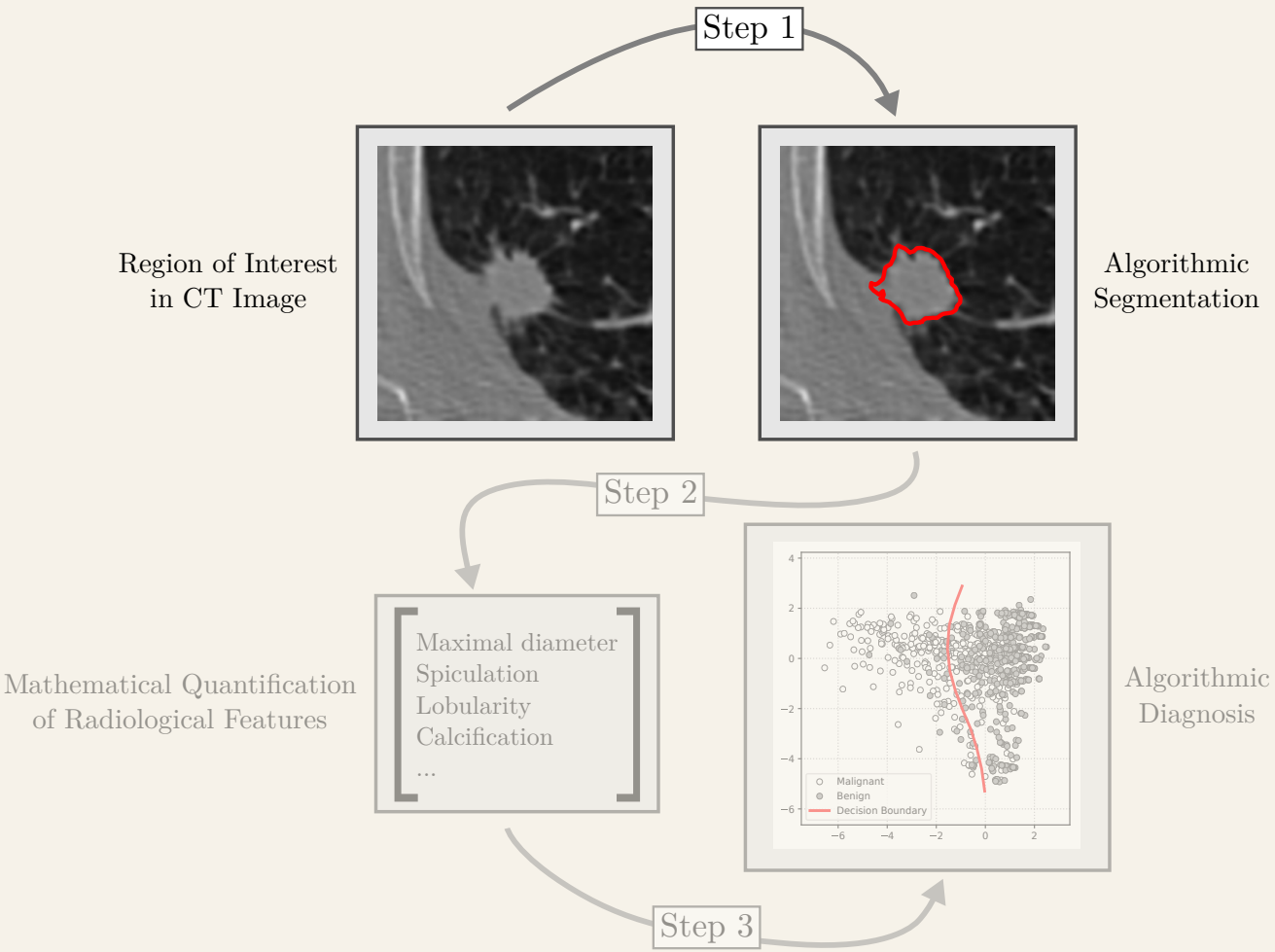

Lung CAD Paradigm for Nodules from Chest CT

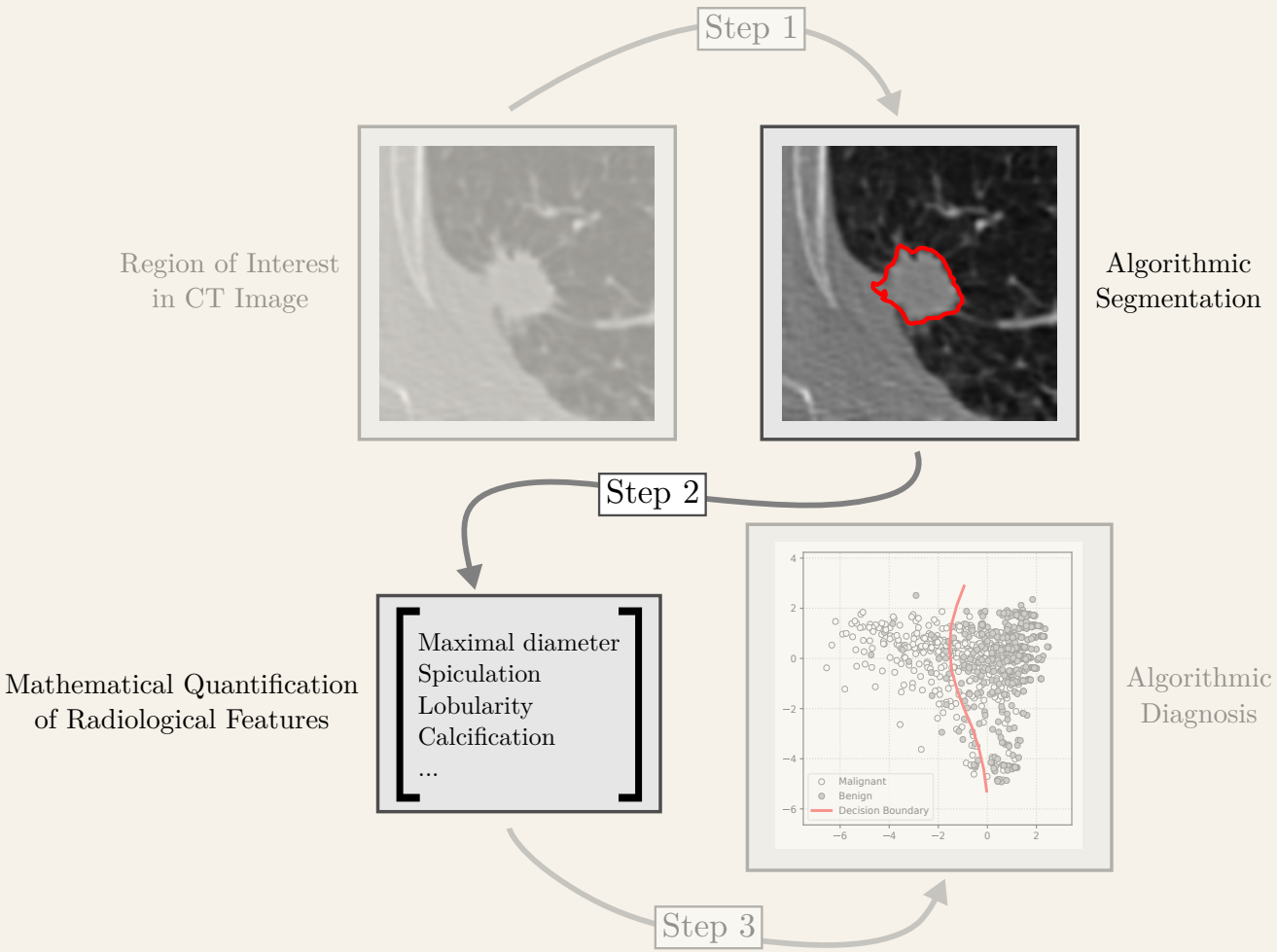

Lung CAD Paradigm for Nodules from Chest CT

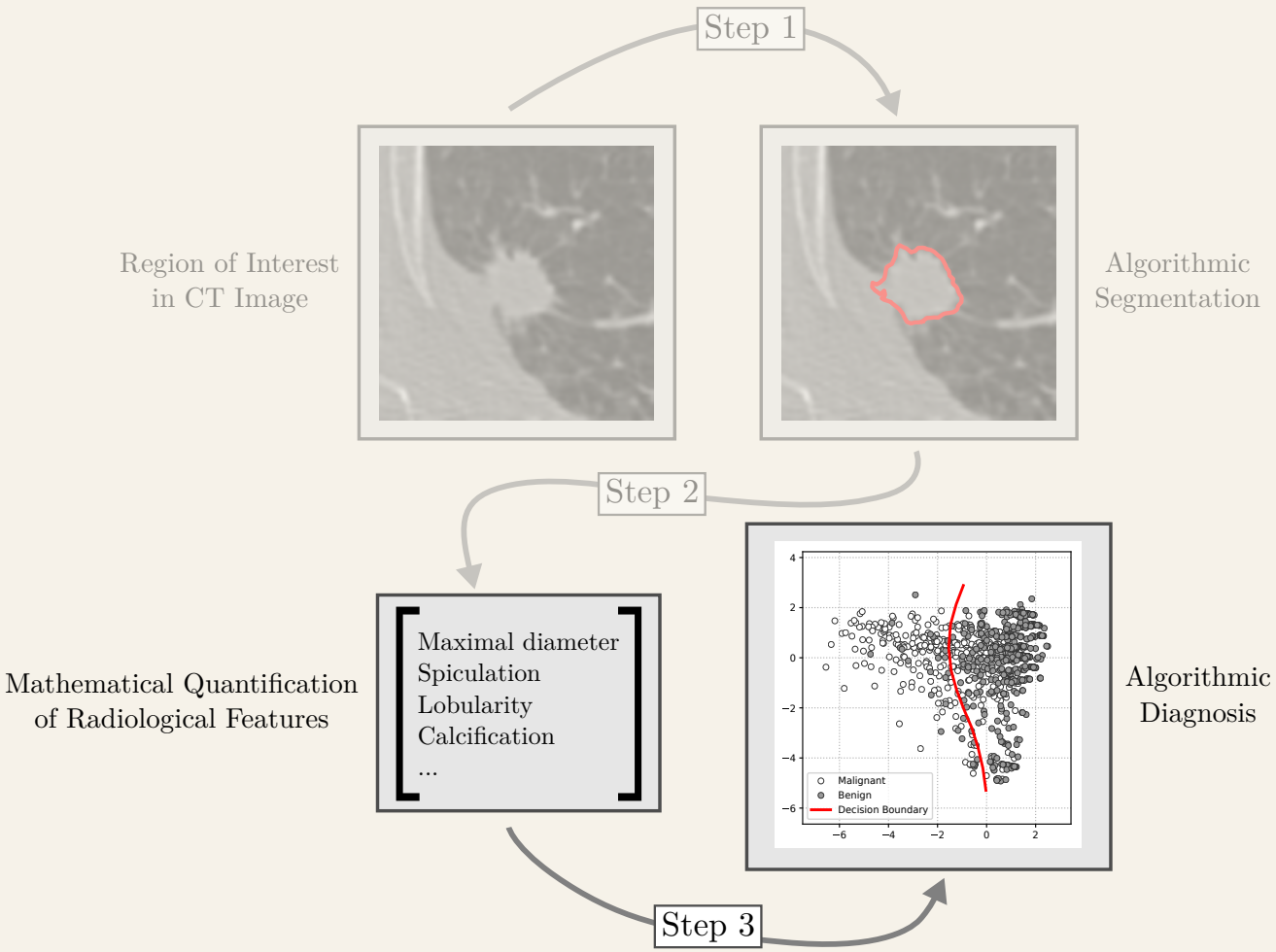

Active Contours

- Parameterized contour evolves to minimize shape and image functionals (Kass et al. [4])

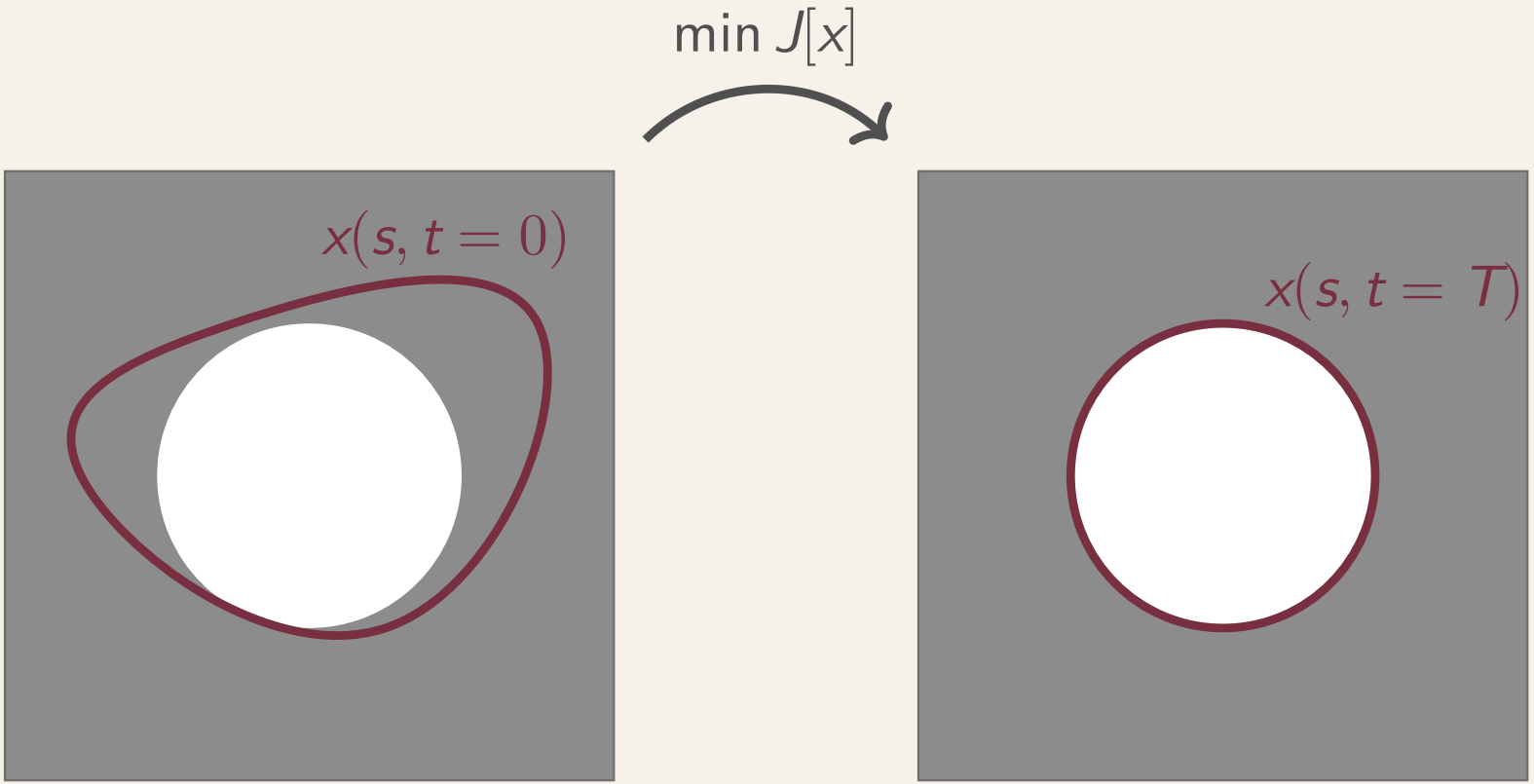

Level Set Formulation

- Contour as zero level set of $\phi : \mathbb{R}^2 \to \mathbb{R}$ (Malladi and Sethian [7])
- Enforce level curves evolve in normal direction with speed ν

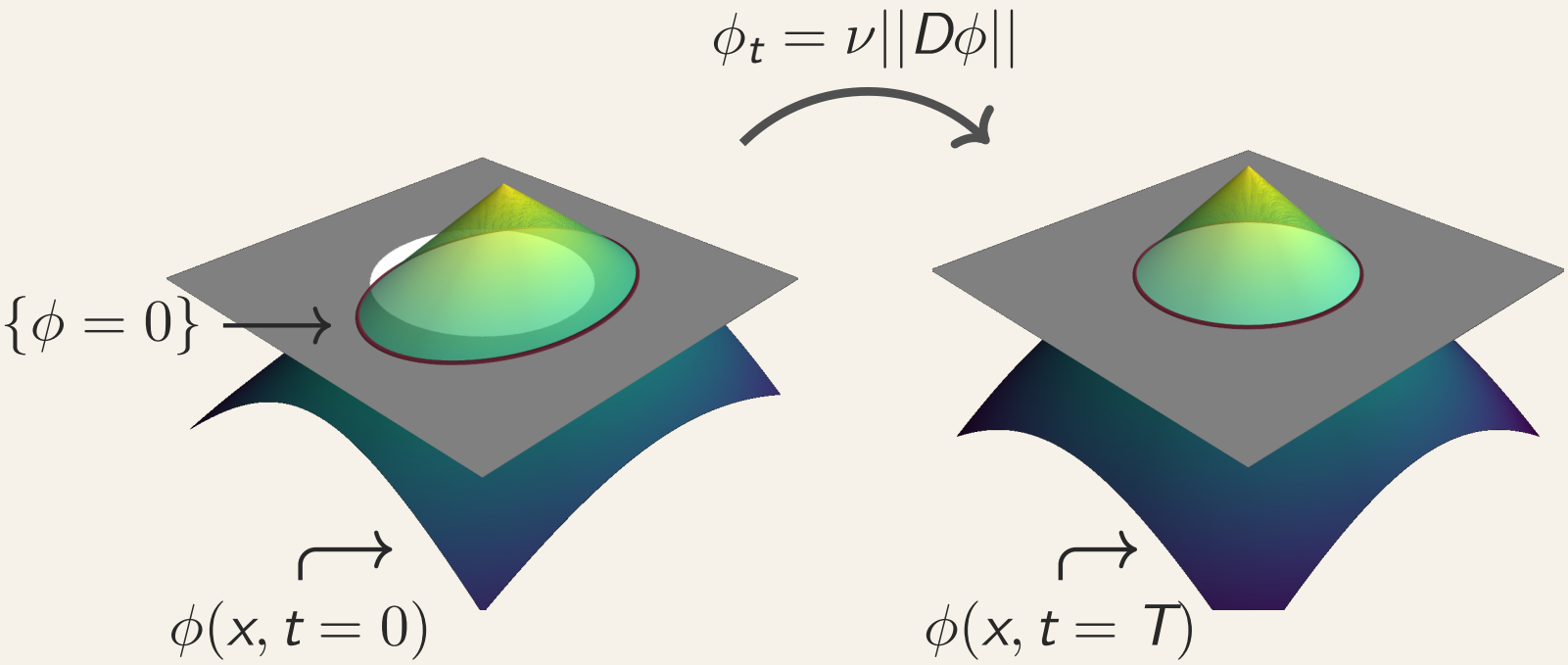

Level Set Formulation: Advantages

- Discretization over regular spatial grid ϕ_{ij}, rather than discretized parametrized curve $x(s_i) = (x_1(s_i), x_2(s_i))$
- Extra book-keeping unnecessary for curves that merge / split
- Indifference to dimension

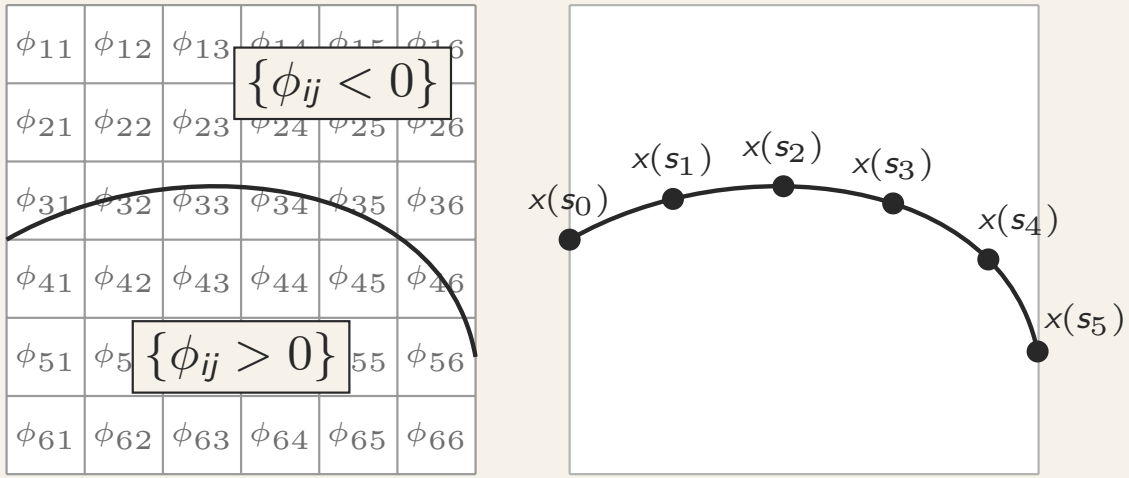

Choosing the Speed Term $\nu(x)$

- Need:
  1. Contraction outside of object
  2. Expansion inside object
  3. $\nu(x) \to 0$ near border of object
- In general, depends on expected object shape and appearance
- Contract/expand where image dark/light. Stop at image edges:

$$\nu(x) = \text{sign}\Big(\underbrace{M(x)}_{\text{Image}}\Big) \exp\Big(-\lambda \underbrace{||D(M * G_\sigma)(x)||}_{\text{Image edge strength}}\Big)$$

Choosing the Speed Term $\nu(x)$

- Need:
  1. Contraction outside of object
  2. Expansion inside object
  3. $\nu(x) \to 0$ near border of object
- In general, depends on expected object shape and appearance
- Contract/expand where image dark/light. Stop at image edges:

$$\nu(x) = \text{sign}\Big(\underbrace{M(x)}_{\text{Image}}\Big) \exp\Big(-\lambda \underbrace{||D(M * G_\sigma)(x)||}_{\text{Image edge strength}}\Big)$$

Choosing the Speed Term $\nu(x)$

- Need:
  1. Contraction outside of object
  2. Expansion inside object
  3. $\nu(x) \to 0$ near border of object
- In general, depends on expected object shape and appearance
- Contract/expand where image dark/light. Stop at image edges:

$$\nu(x) = \text{sign}\Big(\underbrace{M(x)}_{\text{Image}}\Big) \exp\Big(-\lambda \underbrace{||D(M * G_\sigma)(x)||}_{\text{Image edge strength}}\Big)$$

Choosing the Speed Term $\nu(x)$

- Contract/expand where image dark/light. Stop at image edges:

$$\nu(x) = \text{sign}\Big(\underbrace{M(x)}_{\text{Image}}\Big) \exp\Big(-\lambda \underbrace{||D(M * G_\sigma)(x)||}_{\text{Image edge strength}}\Big)$$

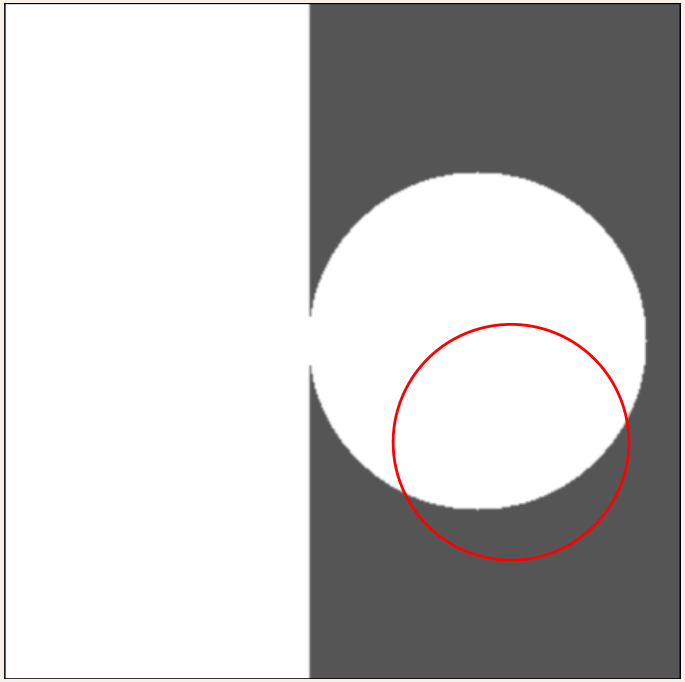

Choosing the Speed Term $\nu(x)$

- Contract/expand where image dark/light. Stop at image edges:

$$\nu(x) = \text{sign}\Big(\underbrace{M(x)}_{\text{Image}}\Big)\exp\Big(-\lambda\underbrace{||D(M * G_\sigma)(x)||}_{\text{Image edge strength}}\Big)$$

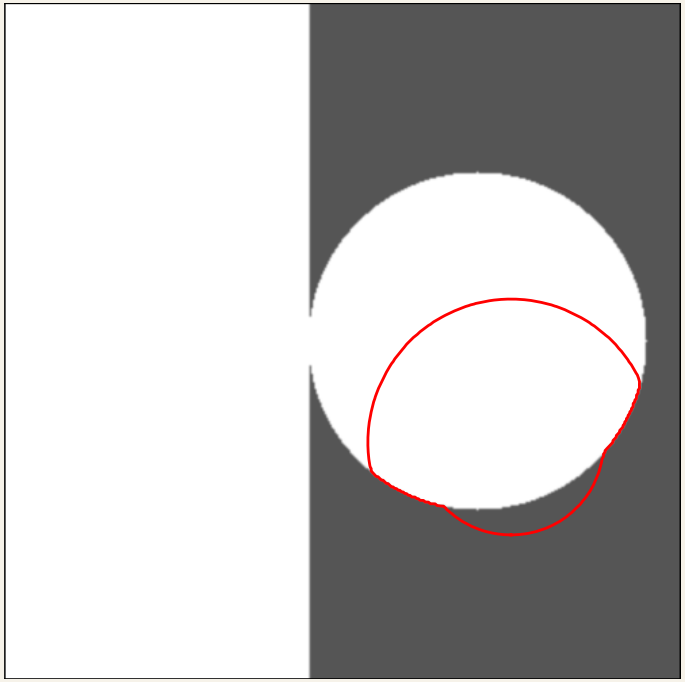

Choosing the Speed Term $\nu(x)$

- Contract/expand where image dark/light. Stop at image edges:

$$\nu(x) = \text{sign}\Big(\underbrace{M(x)}_{\text{Image}}\Big) \exp\Big(-\lambda \underbrace{||D(M * G_\sigma)(x)||}_{\text{Image edge strength}}\Big)$$

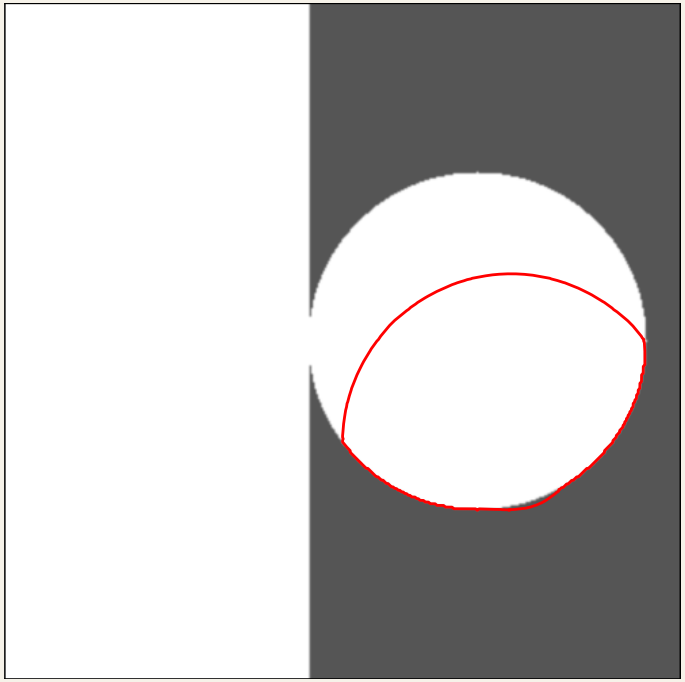

Choosing the Speed Term $\nu(x)$

- Contract/expand where image dark/light. Stop at image edges:

$$\nu(x) = \text{sign}\Big(\underbrace{M(x)}_{\text{Image}}\Big) \exp\Big(-\lambda \underbrace{||D(M * G_\sigma)(x)||}_{\text{Image edge strength}}\Big)$$

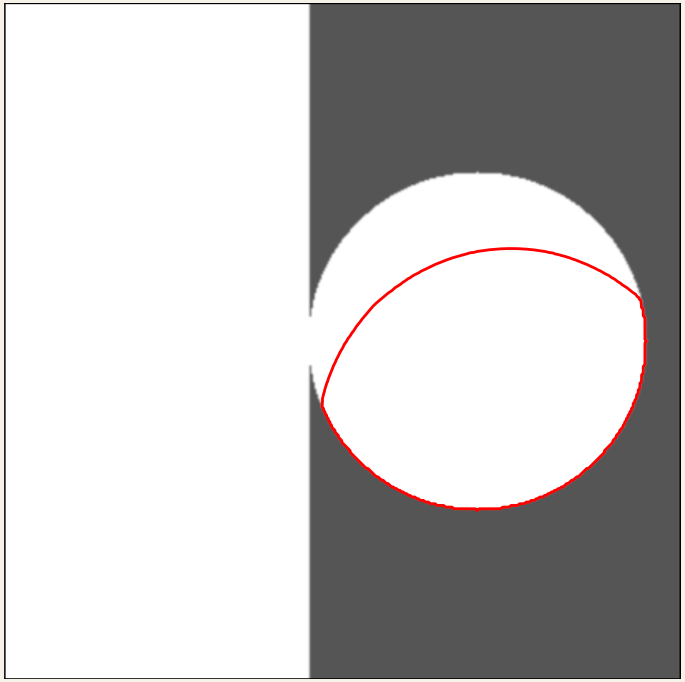

Choosing the Speed Term $\nu(x)$

- Contract/expand where image dark/light. Stop at image edges:

$$\nu(x) = \text{sign}\Big(\underbrace{M(x)}_{\text{Image}}\Big) \exp\Big(-\lambda \underbrace{||D(M * G_\sigma)(x)||}_{\text{Image edge strength}}\Big)$$

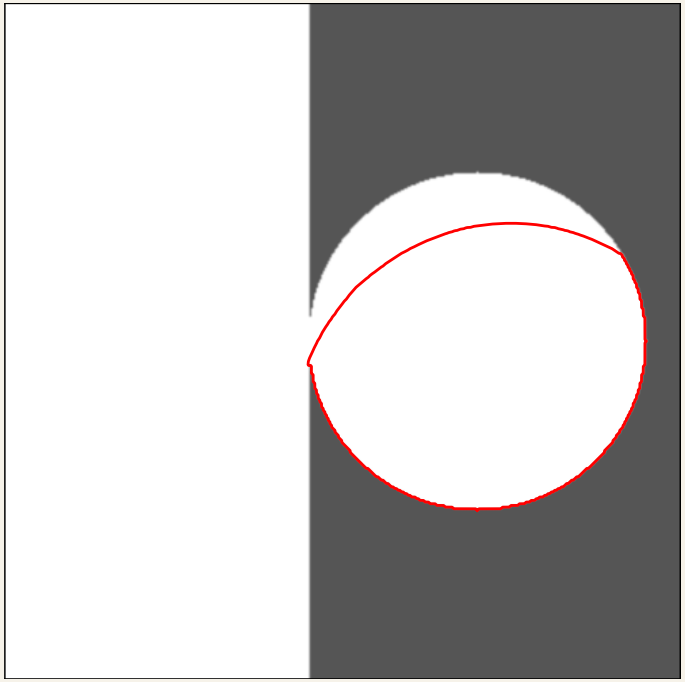

Choosing the Speed Term $\nu(x)$

- Contract/expand where image dark/light. Stop at image edges:

$$\nu(x) = \text{sign}\Big(\underbrace{M(x)}_{\text{Image}}\Big) \exp\Big(-\lambda \underbrace{||D(M * G_\sigma)(x)||}_{\text{Image edge strength}}\Big)$$

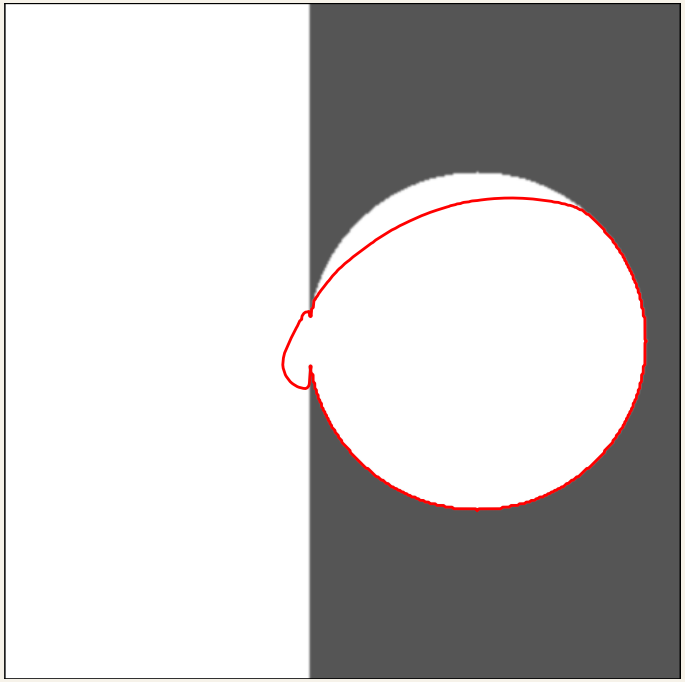

Choosing the Speed Term $\nu(x)$

- Contract/expand where image dark/light. Stop at image edges:

$$\nu(x) = \text{sign}\Big(\underbrace{M(x)}_{\text{Image}}\Big) \exp\Big(-\lambda \underbrace{||D(M * G_\sigma)(x)||}_{\text{Image edge strength}}\Big)$$

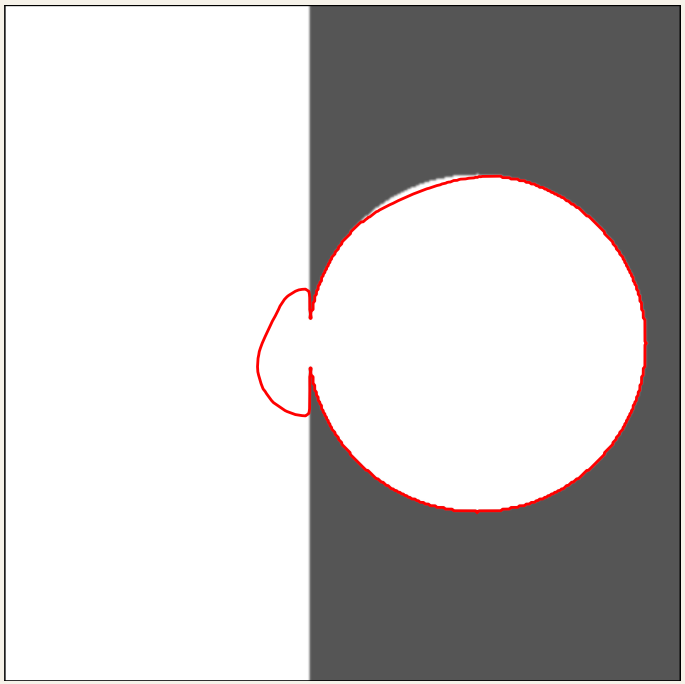

Choosing the Speed Term $\nu(x)$

- Contract/expand where image dark/light. Stop at image edges:

$$\nu(x) = \text{sign}\Big(\underbrace{M(x)}_{\text{Image}}\Big) \exp\Big(-\lambda \underbrace{||D(M * G_\sigma)(x)||}_{\text{Image edge strength}}\Big)$$

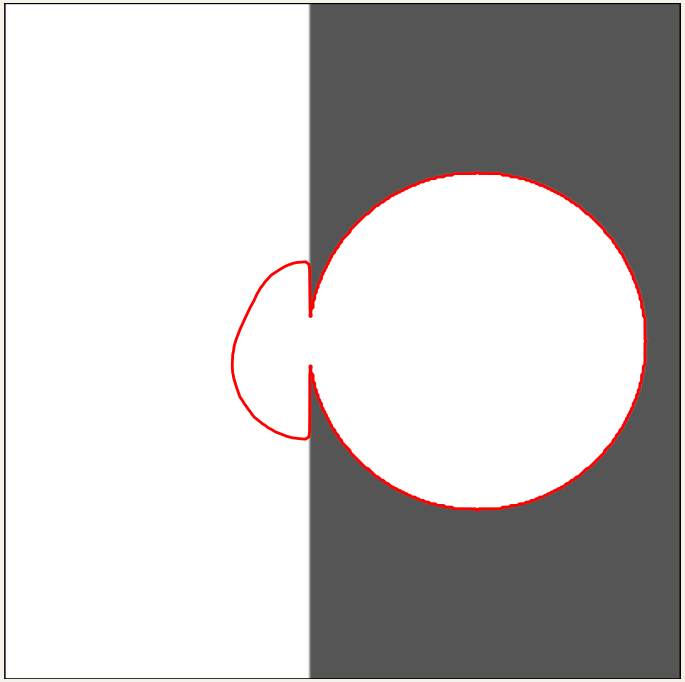

Choosing the Speed Term $\nu(x)$

- Contract/expand where image dark/light. Stop at image edges:

$$\nu(x) = \text{sign}\Big(\underbrace{M(x)}_{\text{Image}}\Big) \exp\Big(-\lambda \underbrace{||D(M * G_\sigma)(x)||}_{\text{Image edge strength}}\Big)$$

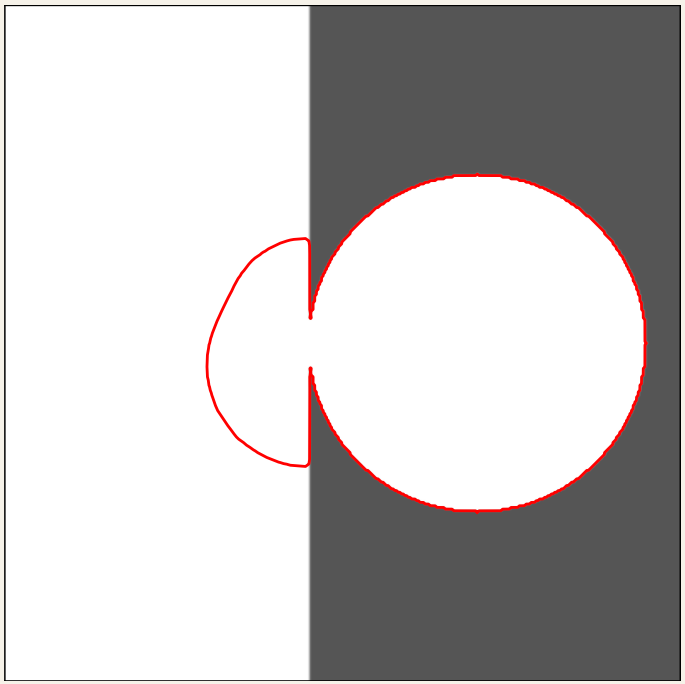

Choosing the Speed Term $\nu(x)$

- Contract/expand where image dark/light. Stop at image edges:

$$\nu(x) = \text{sign}\Big(\underbrace{M(x)}_{\text{Image}}\Big)\exp\Big(-\lambda\underbrace{||D(M * G_\sigma)(x)||}_{\text{Image edge strength}}\Big)$$

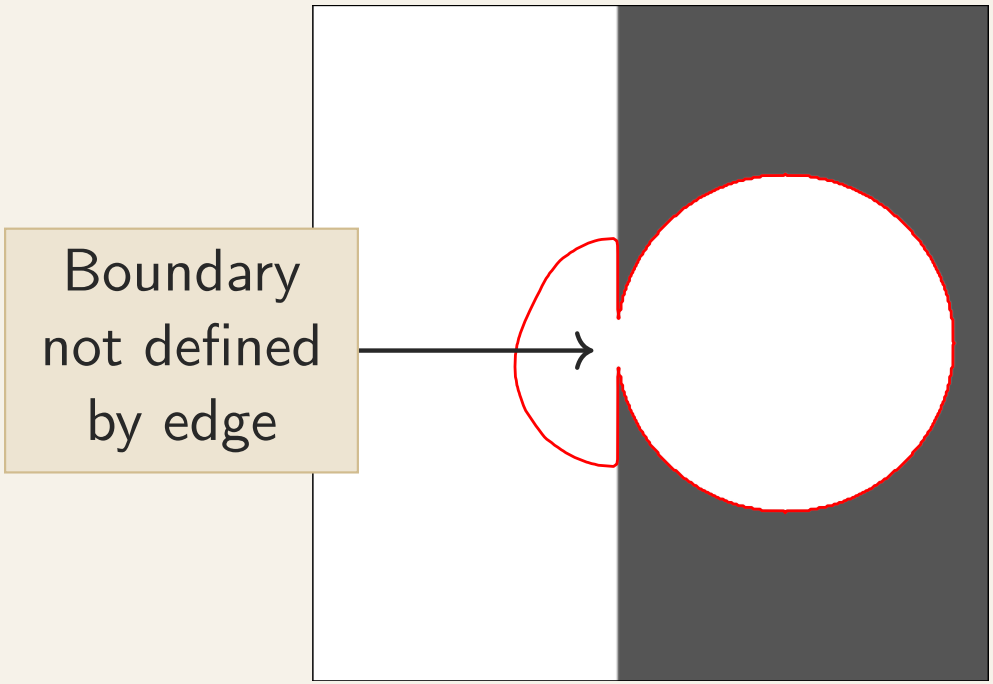

Statistically-Calibrated Level Set (SCLS) Method

- Basic idea: use dataset of images and ground truth segmentations $\left(M(k), B(k)\right)_{k=1}^{N}$ to approximate $\nu(x)$
- How should data influence the estimate of $\nu(x)$?

SCLS Method: Motivating Choice of $\nu(x)$

- Discretize the PDE:

$$\phi_{ij}^{n+1} = \phi_{ij}^{n} + \eta s_{ij} ||D\phi_{ij}^{n}|| \qquad (1)$$

- If s_{ij} is a signed representation of the target segmentation B, then (1) converges to signed representation of B*

*(with minor caveats on η and ϕ^0)

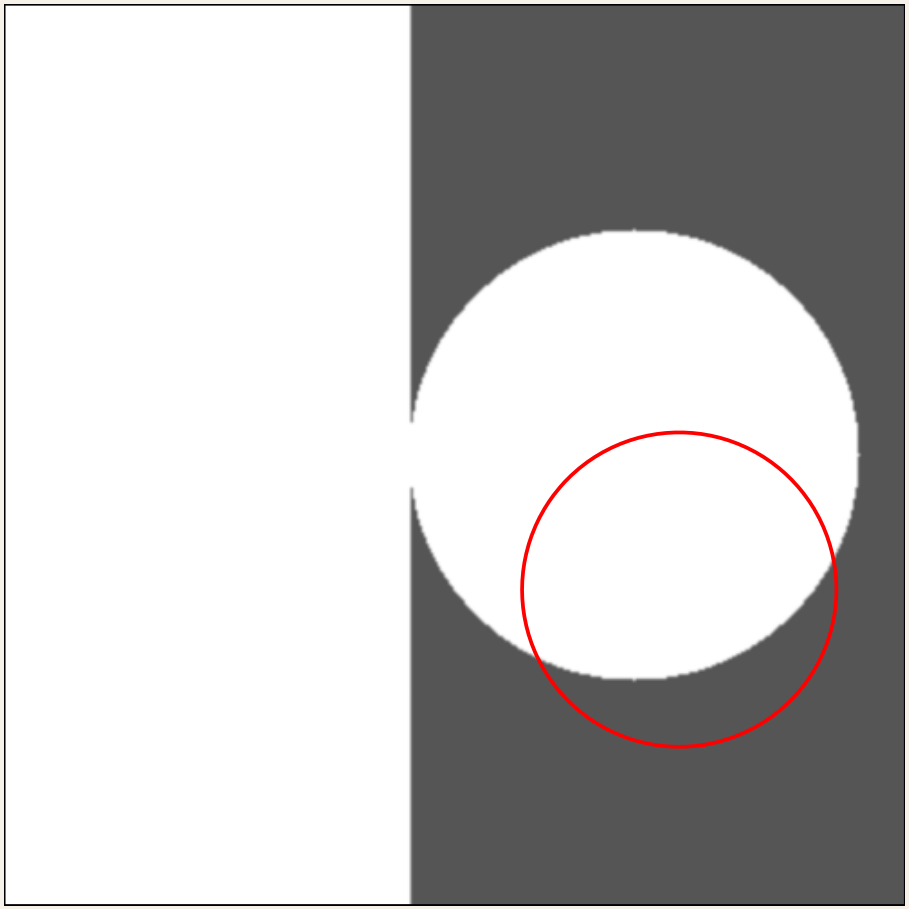

SCLS Method: Motivating Choice of $\nu(x)$

- Discretize the PDE:

$$\phi_{ij}^{n+1} = \phi_{ij}^{n} + \eta s_{ij} ||D\phi_{ij}^{n}|| \qquad (1)$$

- If s_{ij} is a signed representation of the target segmentation B, then (1) converges to signed representation of B*

*(with minor caveats on η and ϕ^0)

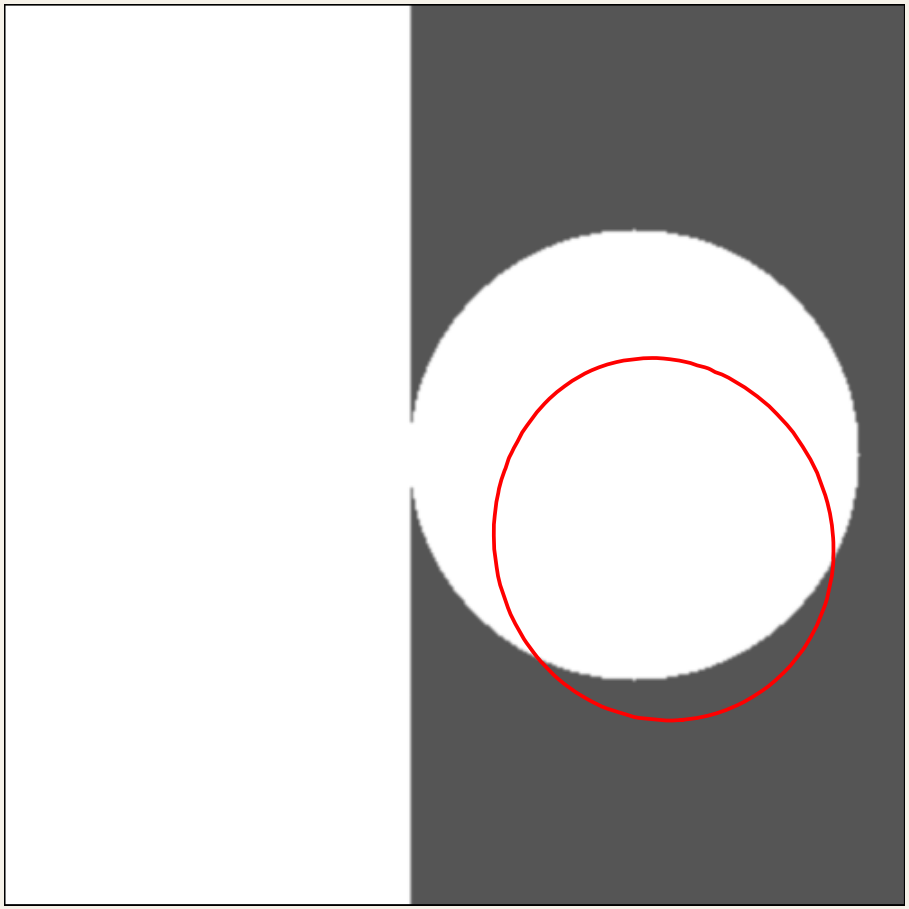

SCLS Method: Motivating Choice of $\nu(x)$

- Discretize the PDE:

$$\phi_{ij}^{n+1} = \phi_{ij}^{n} + \eta s_{ij} ||D\phi_{ij}^{n}|| \qquad (1)$$

- If s_{ij} is a signed representation of the target segmentation B, then (1) converges to signed representation of B*

*(with minor caveats on η and ϕ^0)

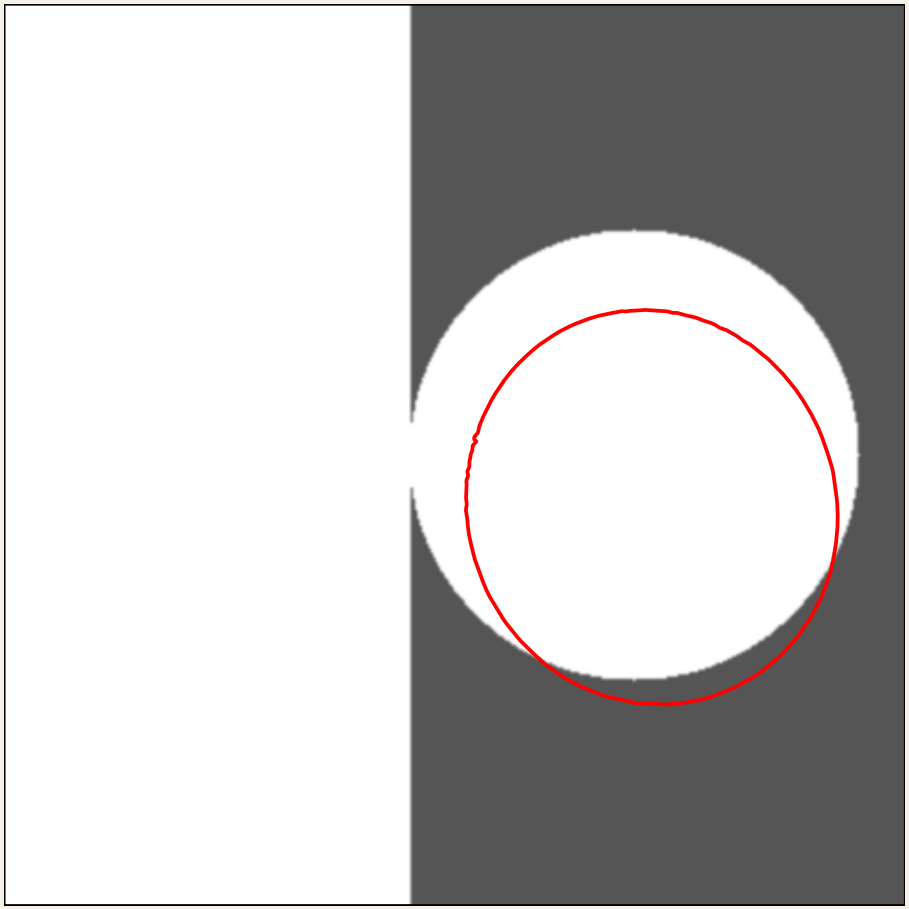

SCLS Method: Motivating Choice of $\nu(x)$

- Discretize the PDE:

$$\phi_{ij}^{n+1} = \phi_{ij}^{n} + \eta s_{ij} ||D\phi_{ij}^{n}|| \qquad (1)$$

- If s_{ij} is a signed representation of the target segmentation B, then (1) converges to signed representation of B*

*(with minor caveats on η and ϕ^0)

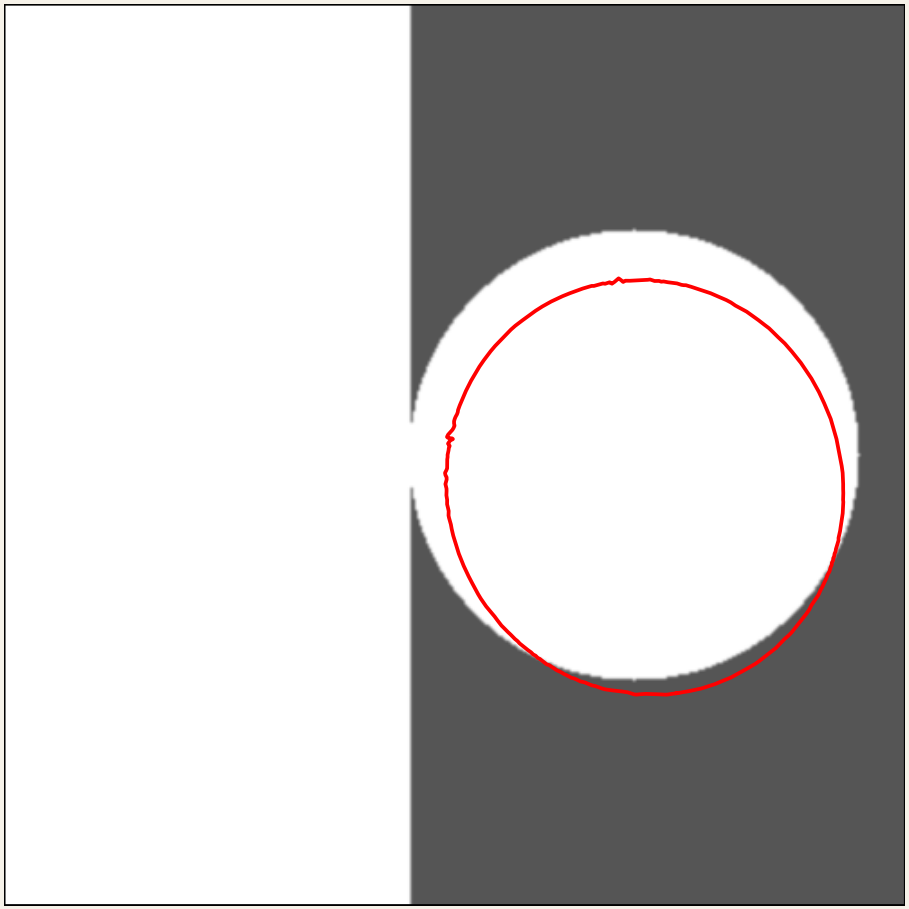

SCLS Method: Motivating Choice of $\nu(x)$

- Discretize the PDE:

$$\phi_{ij}^{n+1} = \phi_{ij}^{n} + \eta s_{ij} ||D\phi_{ij}^{n}|| \qquad (1)$$

- If s_{ij} is a signed representation of the target segmentation B, then (1) converges to signed representation of B*

*(with minor caveats on η and ϕ^0)

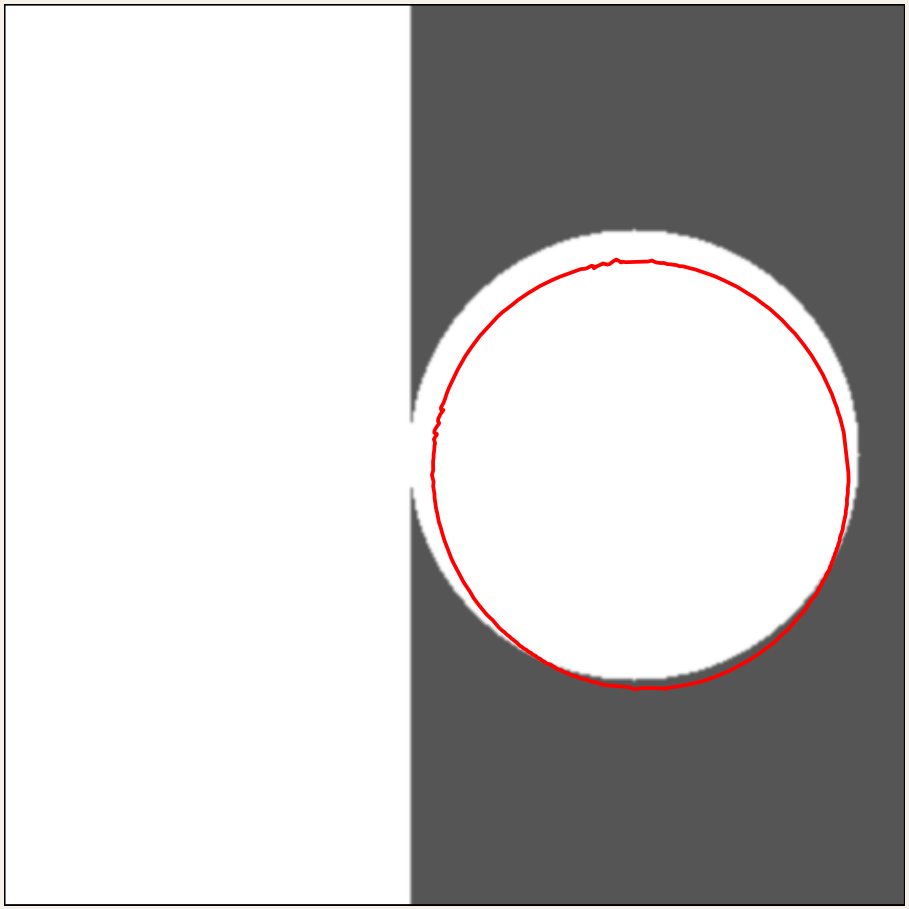

SCLS Method: Motivating Choice of $\nu(x)$

- Discretize the PDE:

$$\phi_{ij}^{n+1} = \phi_{ij}^{n} + \eta s_{ij} ||D\phi_{ij}^{n}|| \qquad (1)$$

- If s_{ij} is a signed representation of the target segmentation B, then (1) converges to signed representation of B*

*(with minor caveats on η and ϕ^0)

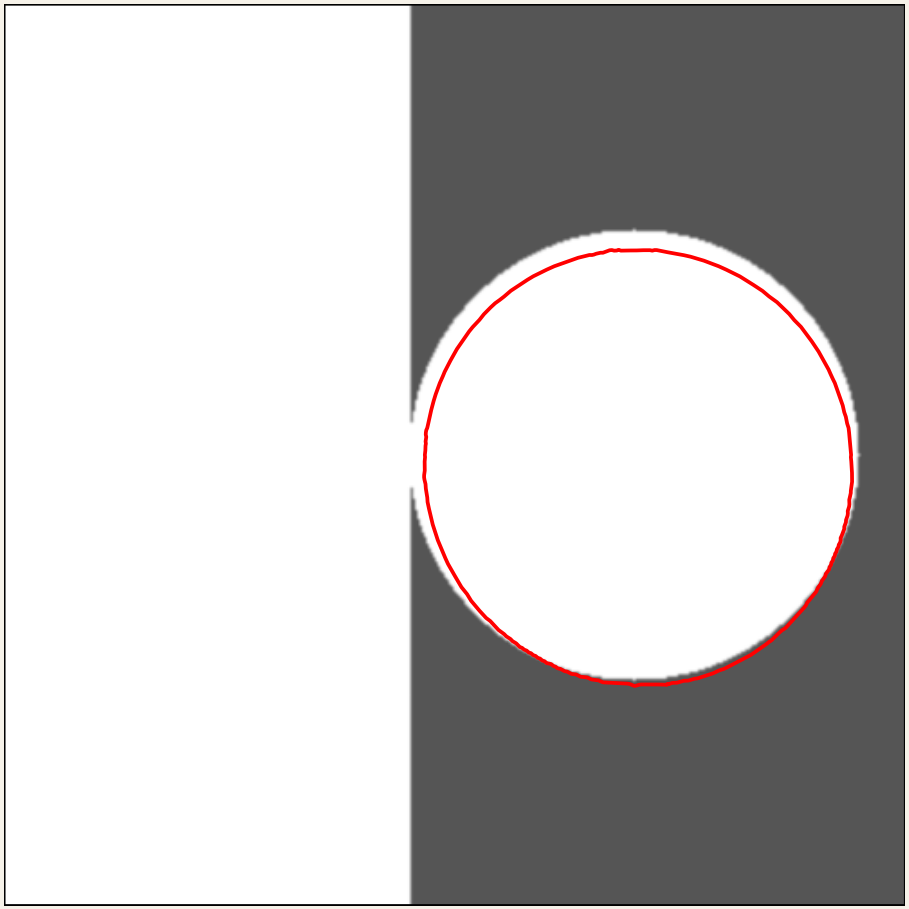

SCLS Method: Motivating Choice of $\nu(x)$

- Discretize the PDE:

$$\phi_{ij}^{n+1} = \phi_{ij}^{n} + \eta s_{ij} ||D\phi_{ij}^{n}|| \qquad (1)$$

- If s_{ij} is a signed representation of the target segmentation B, then (1) converges to signed representation of B*

*(with minor caveats on η and ϕ^0)

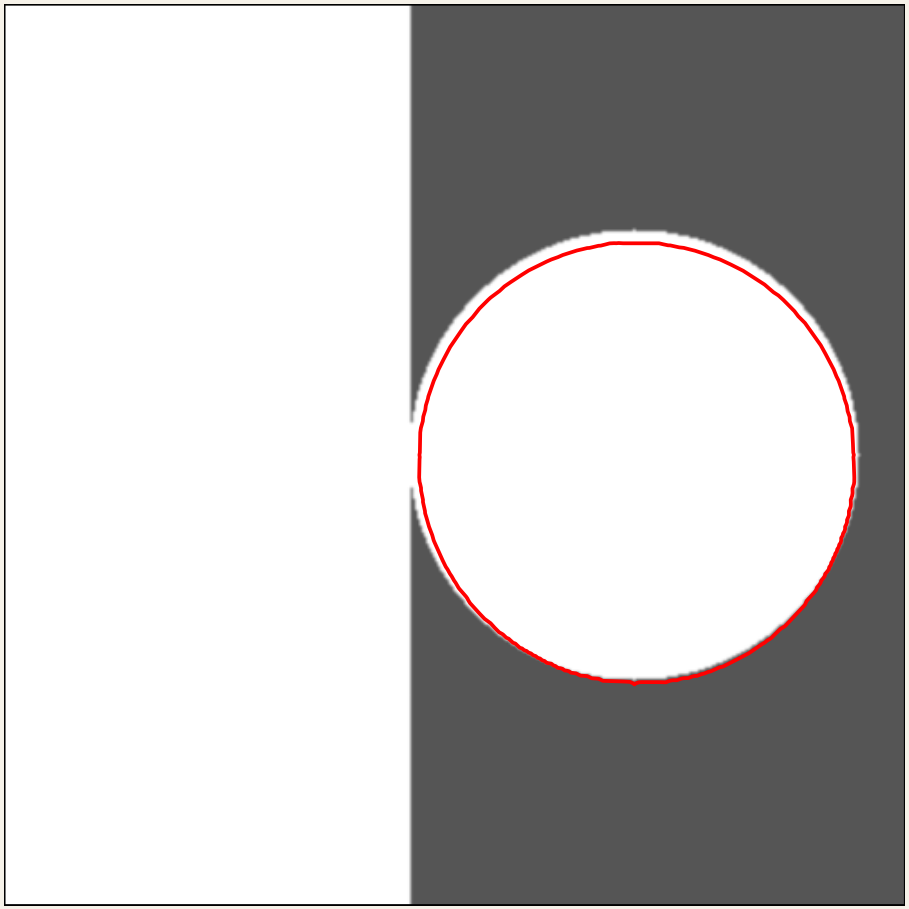

SCLS Method: Motivating Choice of $\nu(x)$

- Discretize the PDE:

$$\phi_{ij}^{n+1} = \phi_{ij}^{n} + \eta s_{ij} ||D\phi_{ij}^{n}|| \qquad (1)$$

- If s_{ij} is a signed representation of the target segmentation B, then (1) converges to signed representation of B*

*(with minor caveats on η and ϕ^0)

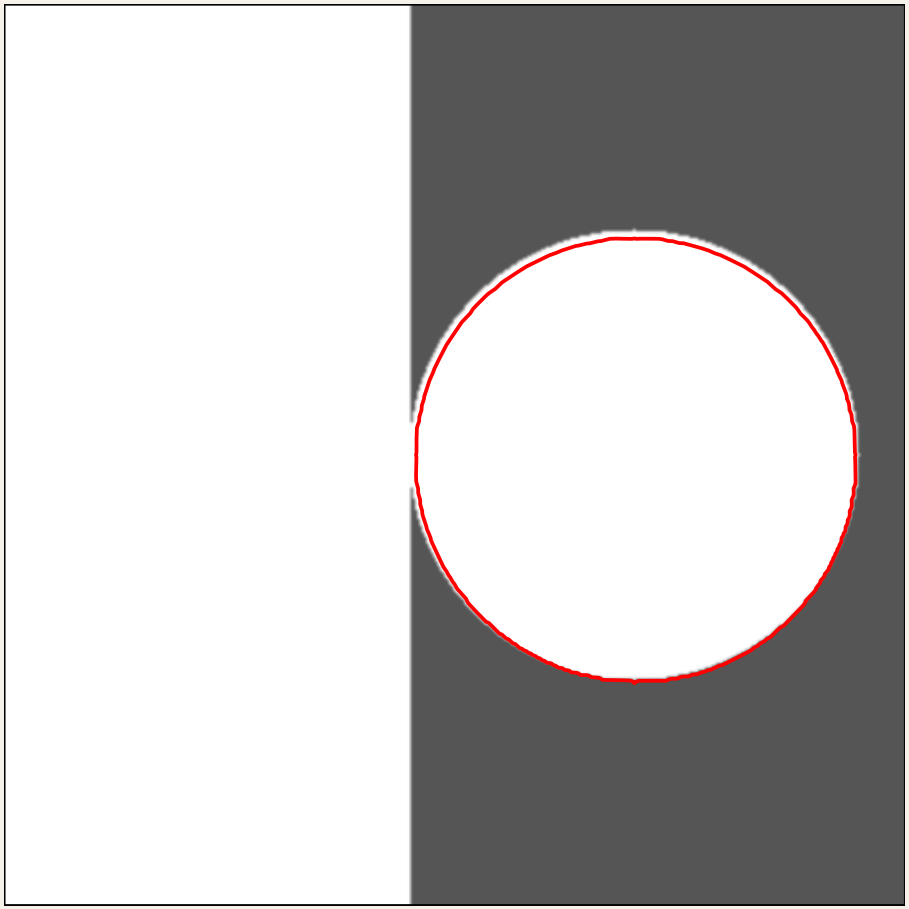

SCLS Method: Motivating Choice of $\nu(x)$

- Discretize the PDE:

$$\phi_{ij}^{n+1} = \phi_{ij}^{n} + \eta s_{ij} ||D\phi_{ij}^{n}|| \qquad (1)$$

- If s_{ij} is a signed representation of the target segmentation B, then (1) converges to signed representation of B*

*(with minor caveats on η and ϕ^0)

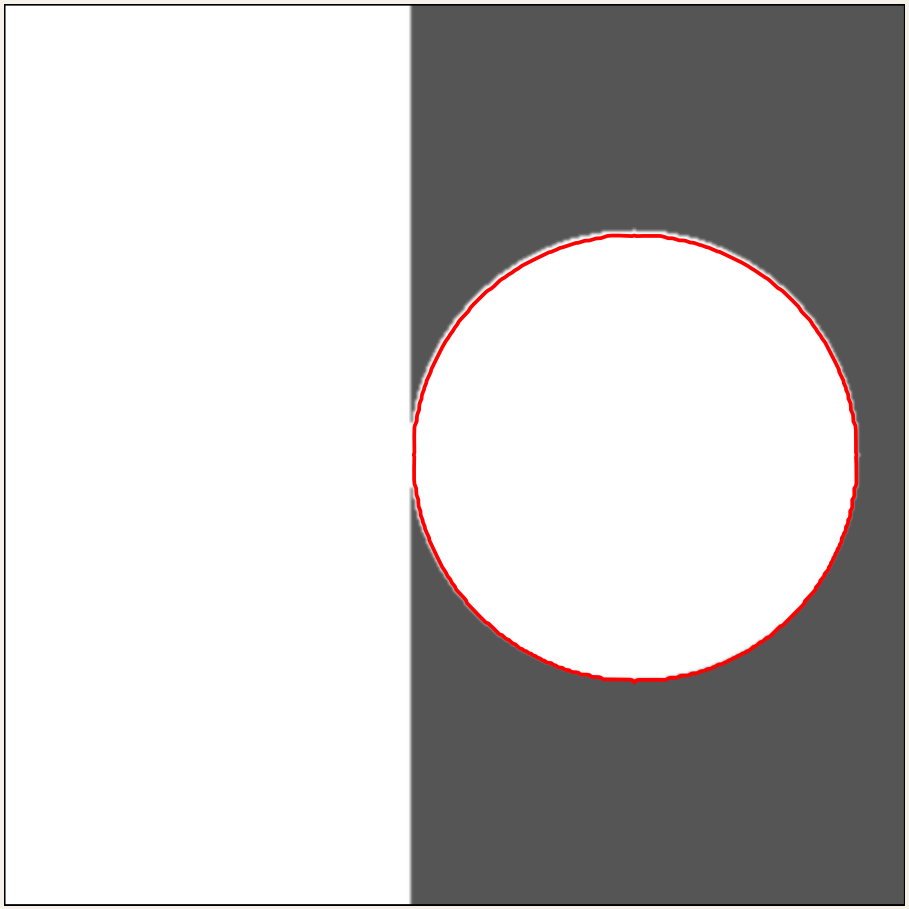

SCLS Method: Motivating Choice of $\nu(x)$

- Discretize the PDE:

$$\phi_{ij}^{n+1} = \phi_{ij}^{n} + \eta s_{ij} ||D\phi_{ij}^{n}|| \qquad (1)$$

- If s_{ij} is a signed representation of the target segmentation B, then (1) converges to signed representation of B*

*(with minor caveats on η and ϕ^0)

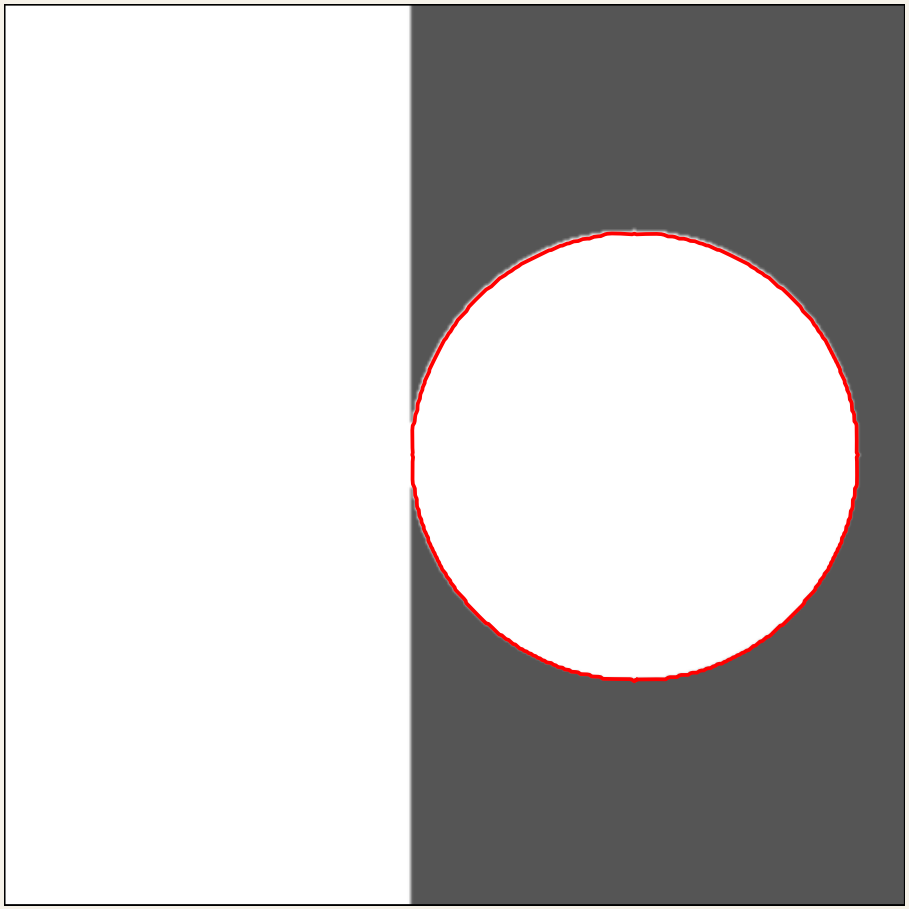

SCLS Method: An Iterative Approximation Scheme

$$\phi_{ij}^{n+1} = \phi_{ij}^{n} + \eta s_{ij} ||D\phi_{ij}^{n}||$$

- Approximate $s_{ij} \approx \hat{s}_{ij}^{n} = V^{n}(F|\theta_n)$
- V^n is a regression model
- $F = F(i, j, \phi, M)$ is feature map
- V^n : Features $\rightarrow$ Level set speed

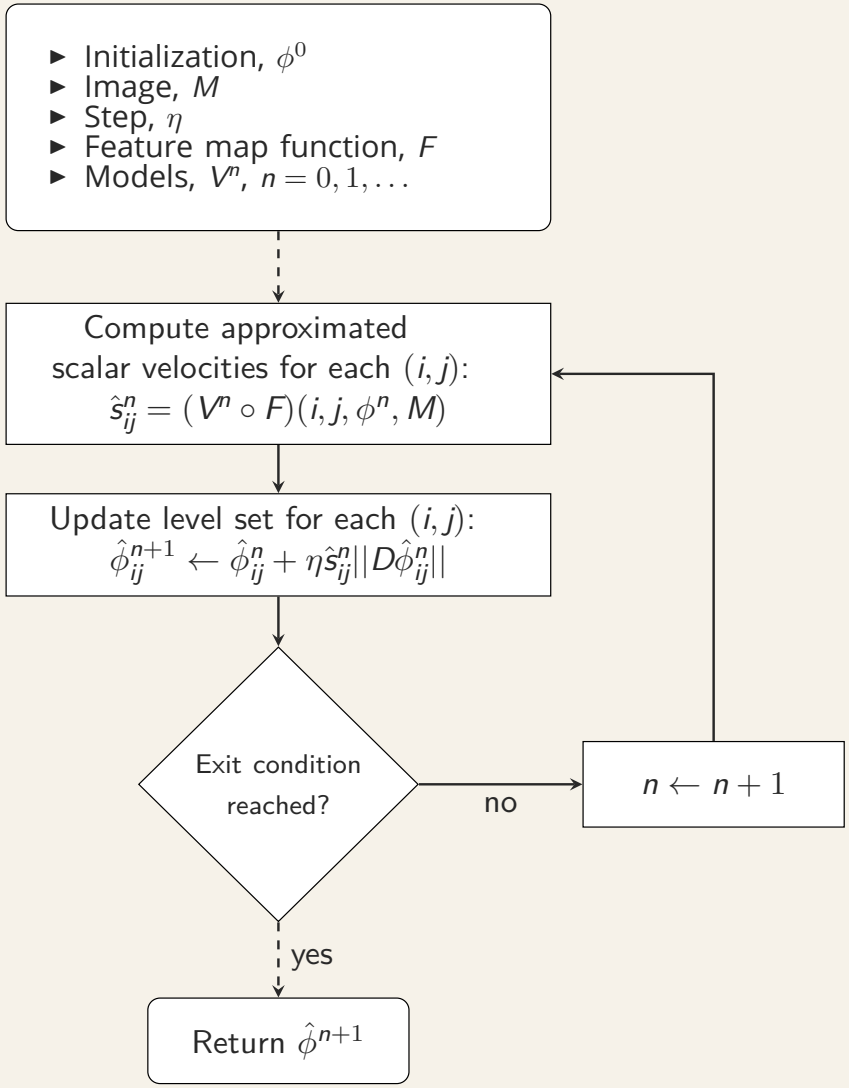

SCLS Method: An Iterative Approximation Scheme

$$\phi_{ij}^{n+1} = \phi_{ij}^{n} + \eta s_{ij} ||D\phi_{ij}^{n}||$$

- Approximate $s_{ij} \approx \hat{s}_{ij}^{n} = V^{n}(F \mid \theta_{n})$
- V^{n} is a regression model
- $F = F(i, j, \phi, M)$ is feature map
- V^{n} : Features $\rightarrow$ Level set speed

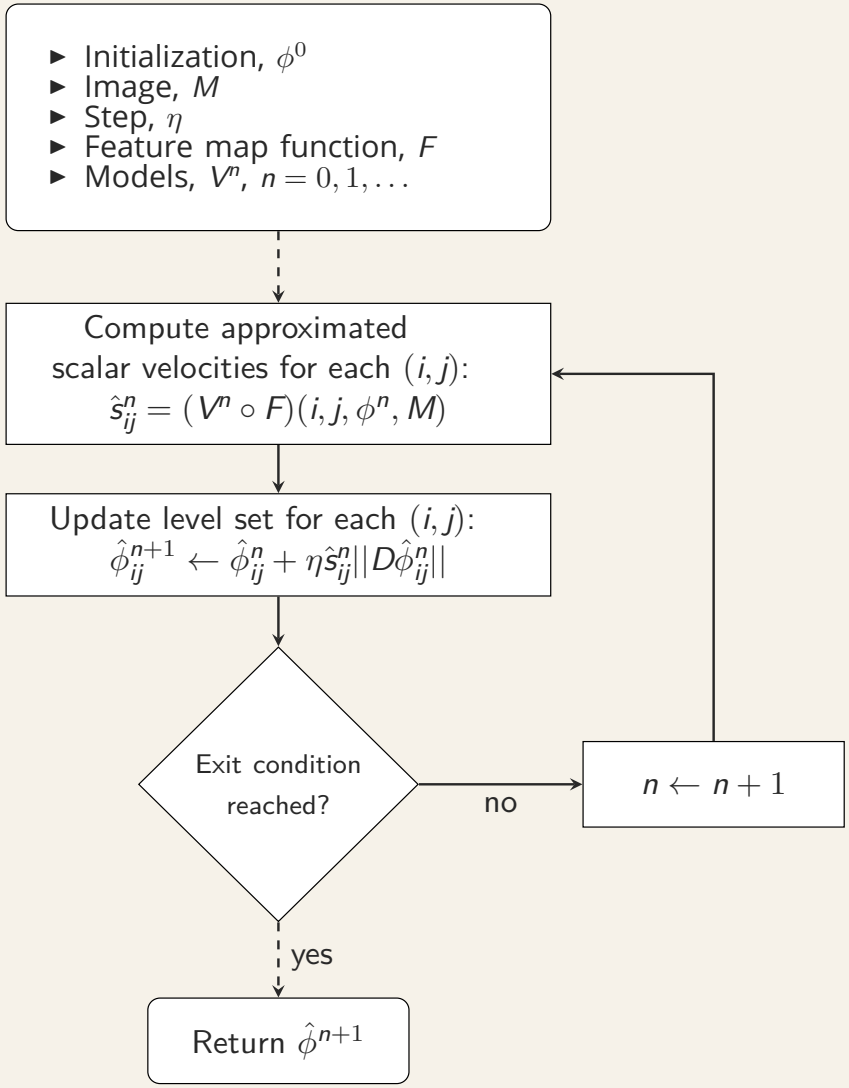

SCLS Method: An Iterative Approximation Scheme

$$\phi_{ij}^{n+1} = \phi_{ij}^{n} + \eta s_{ij} ||D\phi_{ij}^{n}||$$

- Approximate $s_{ij} \approx \hat{s}_{ij}^{n} = V^{n}(F \mid \theta_{n})$
- V^{n} is a regression model
- $F = F(i, j, \phi, M)$ is feature map
- V^{n} : Features $\rightarrow$ Level set speed

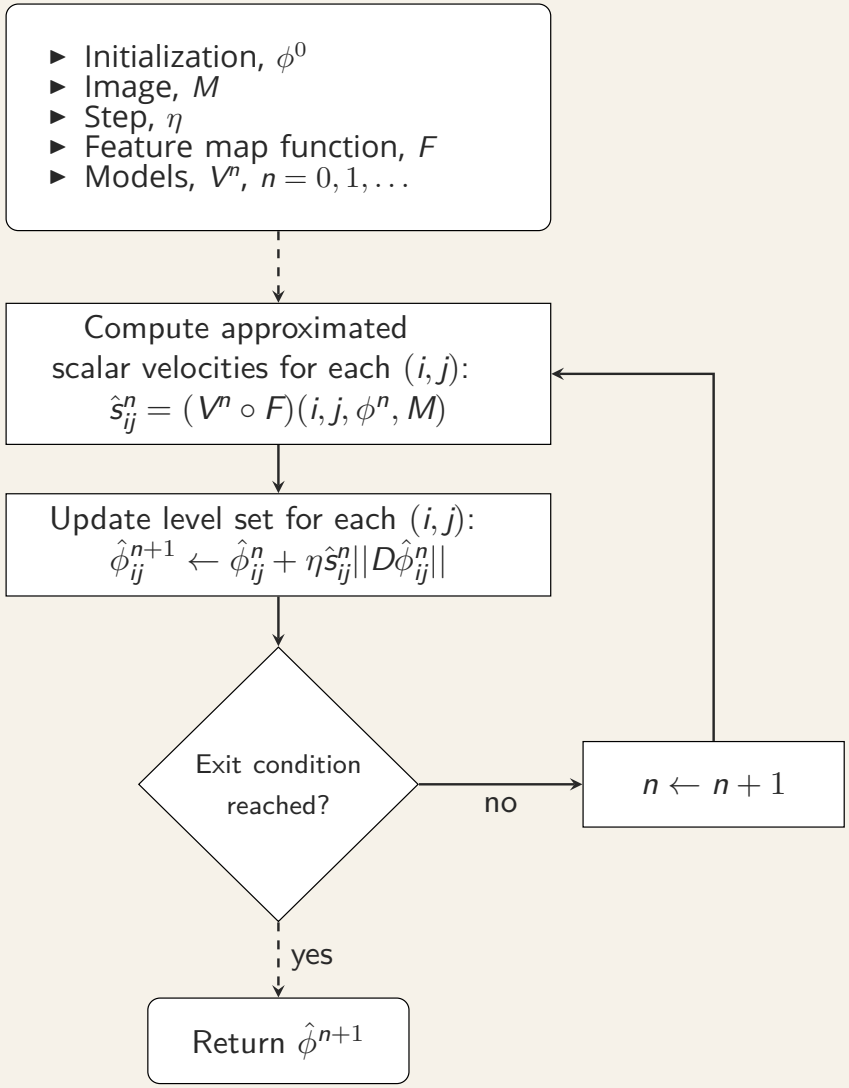

SCLS Method: An Iterative Approximation Scheme

$$\phi_{ij}^{n+1} = \phi_{ij}^{n} + \eta s_{ij} ||D\phi_{ij}^{n}||$$

- Approximate $s_{ij} \approx \hat{s}_{ij}^{n} = V^{n}(F \,|\, \theta_n)$
- V^n is a regression model
- $F = F(i, j, \phi, M)$ is feature map
- V^n : Features $\rightarrow$ Level set speed

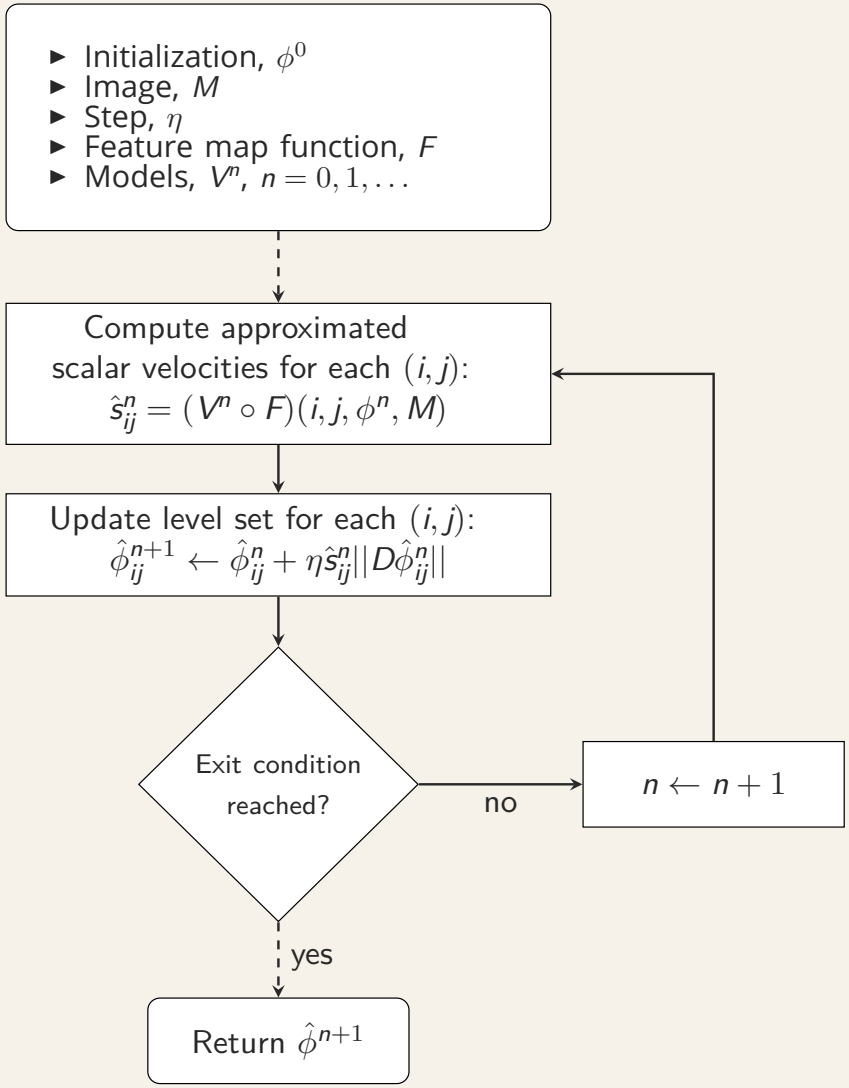

SCLS Method: Training Process

- $F = F(i, j, \phi, M)$ is a feature map of our choosing, e.g.,

$$F(i, j, \phi, M) = \begin{bmatrix} (G_\sigma * M)_{ij} \\ \sum_{uv} H(\phi_{uv}) \end{bmatrix}$$

- Parameters θ_n obtained via sequential optimization:

$$\theta_n^* = \underset{\theta}{\operatorname{argmin}} \sum_{ijk} (s_{ij} - V^n(F \mid \theta_n))^2$$

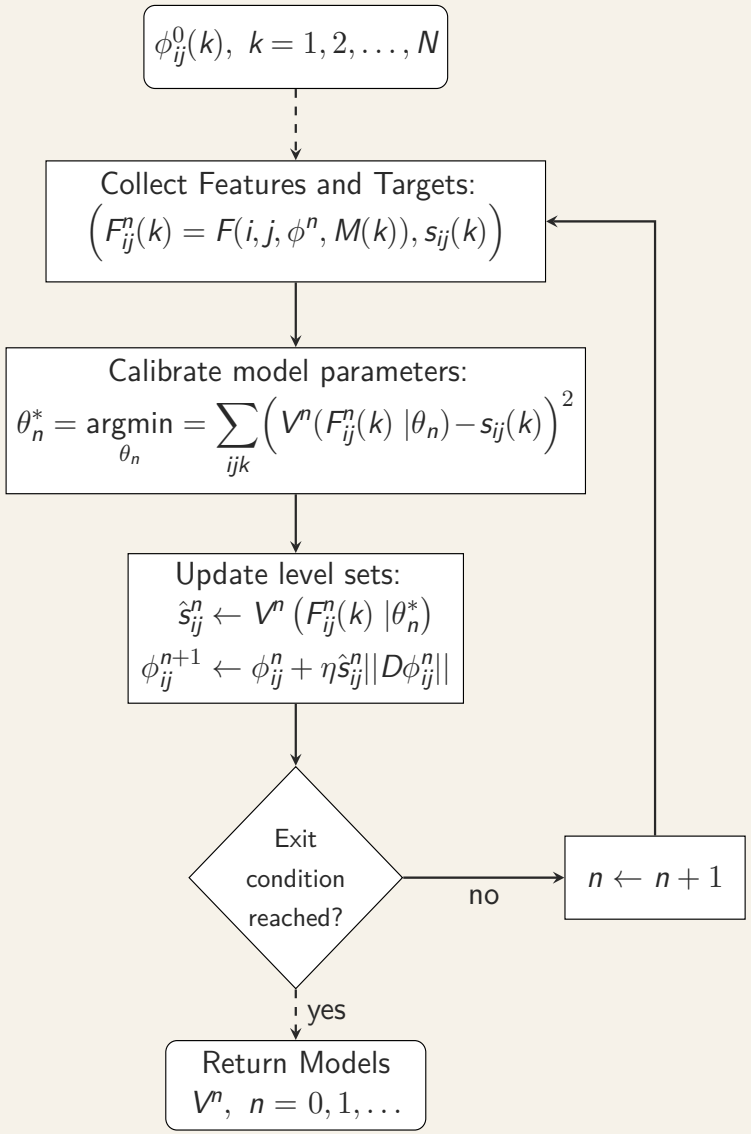

SCLS Method: Training Process

- $F = F(i, j, \phi, M)$ is a feature map of our choosing, e.g.,

$$F(i, j, \phi, M) = \begin{bmatrix} (G_\sigma * M)_{ij} \\ \sum_{uv} H(\phi_{uv}) \end{bmatrix}$$

- Parameters θ_n obtained via sequential optimization:

$$\theta_n^* = \underset{\theta}{\operatorname{argmin}} \sum_{ijk} (s_{ij} - V^n(F \mid \theta_n))^2$$

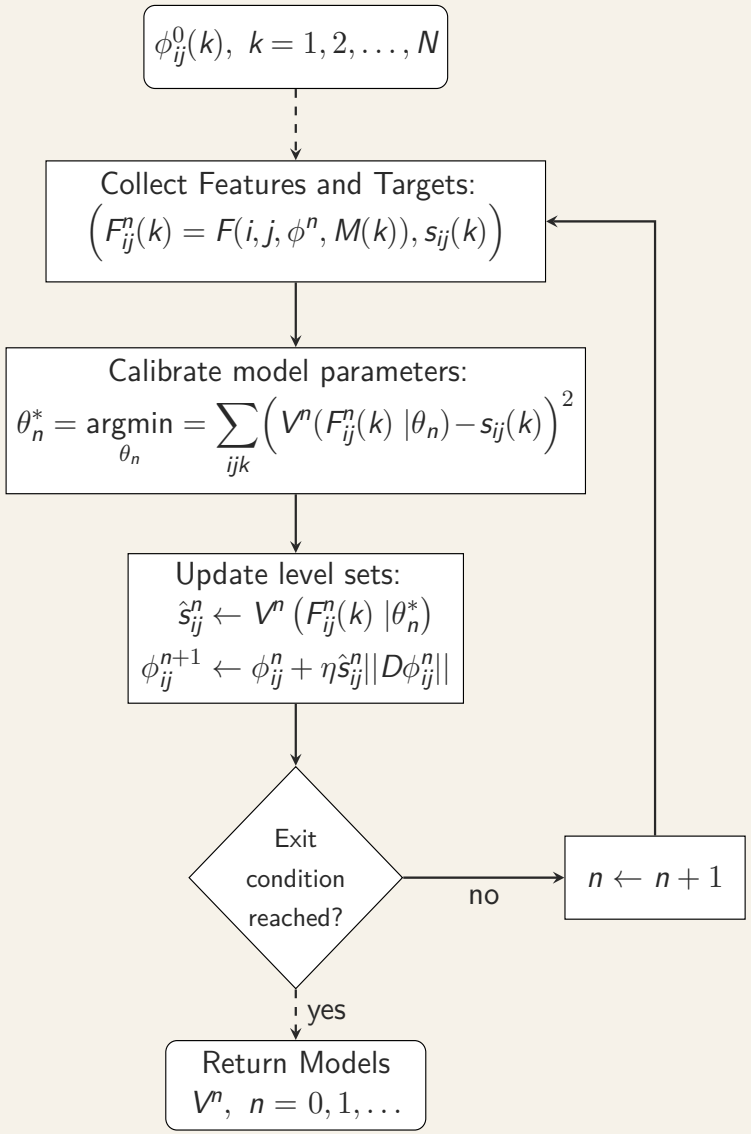

SCLS: Details

- Choice of regression model: neural network
- Step size choice $\eta = 0.1$ works well empirically
- Initialization choice ϕ^0 is application dependent

SCLS: Details

- Choice of regression model: neural network
- Step size choice $\eta = 0.1$ works well empirically
- Initialization choice ϕ^0 is application dependent

SCLS: Details

- Choice of regression model: neural network
- Step size choice $\eta = 0.1$ works well empirically
- Initialization choice ϕ^0 is application dependent

Synthetic Data: Partitioned Circles

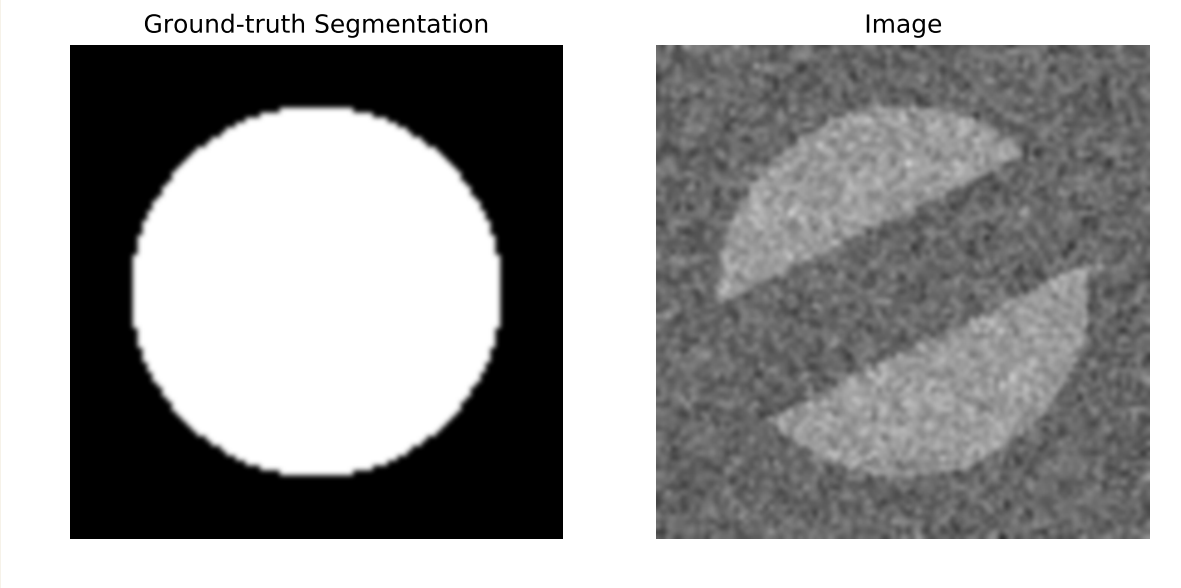

- 100/50/50 randomly generated image and segmentation pairs for training/validation/testing datasets

Synthetic Data: Partitioned Circles, Feature Maps Tested

Table: Feature Map 1

Feature	Local	Global
Image value	✓	
Image edge	✓	

Table: Feature Map 2

Feature	Local	Global
Area		✓
Boundary length		✓
Isoperimetric ratio		✓
Seg. moments, $p = 1, 2$		✓
Dist. from center of mass	✓	✓
Image value mean in seg.		✓
Image value std. in seg.		✓
Image value	✓	
Image edge	✓	

Image features are computed at four scales, $\sigma \in \{0, 1, 2, 3\}$

Synthetic Data: Partitioned Circles, Results

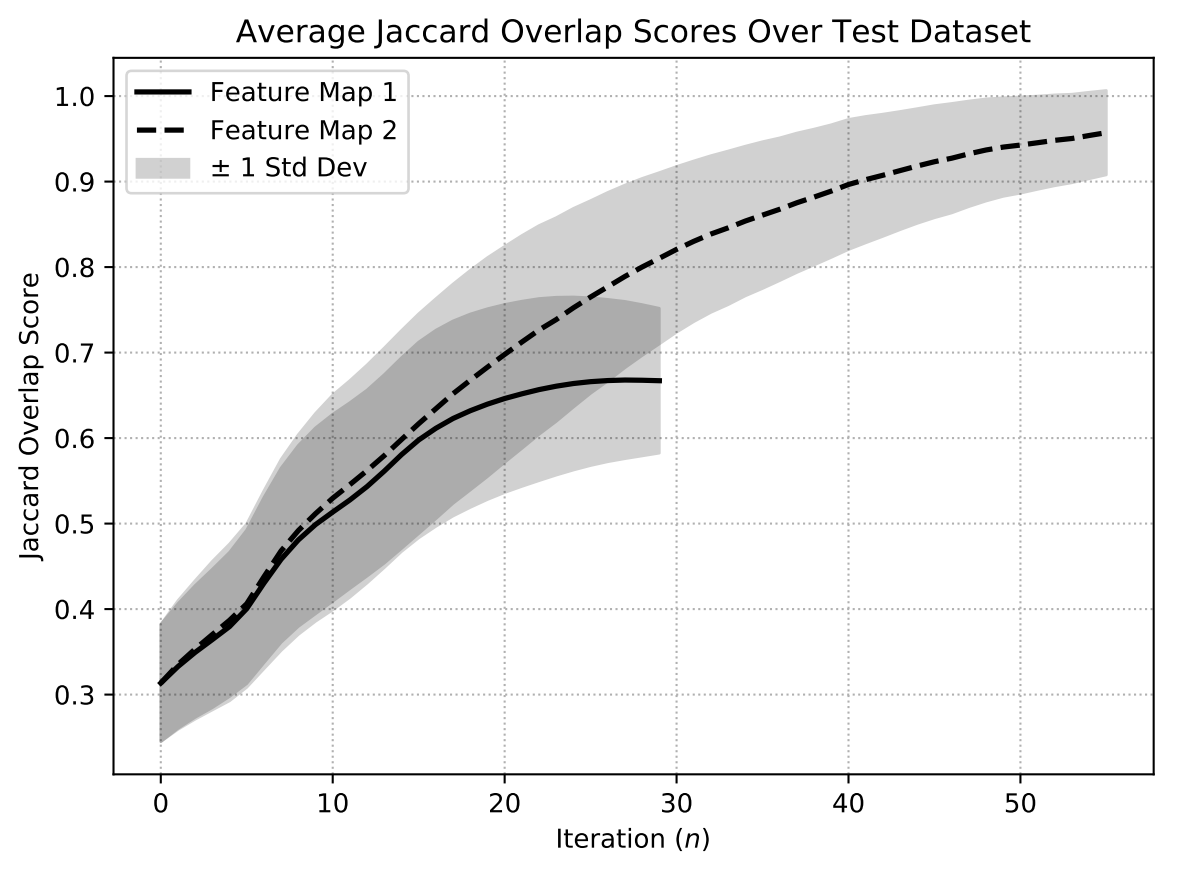

Synthetic Data: Partitioned Circles, Results

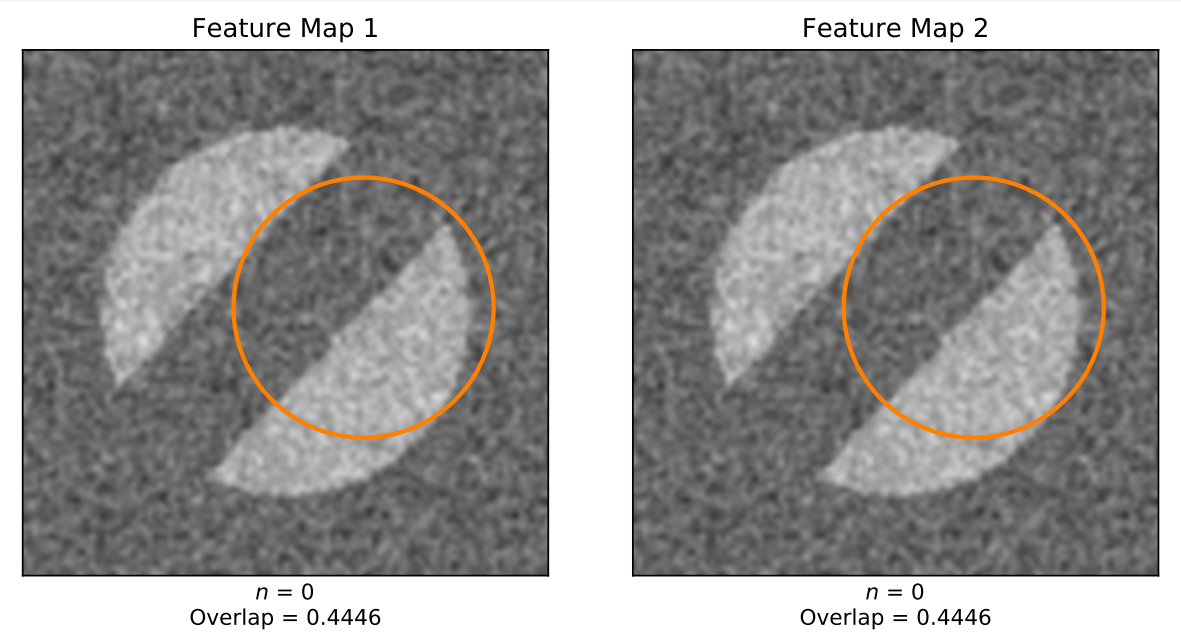

Synthetic Data: Partitioned Circles, Results

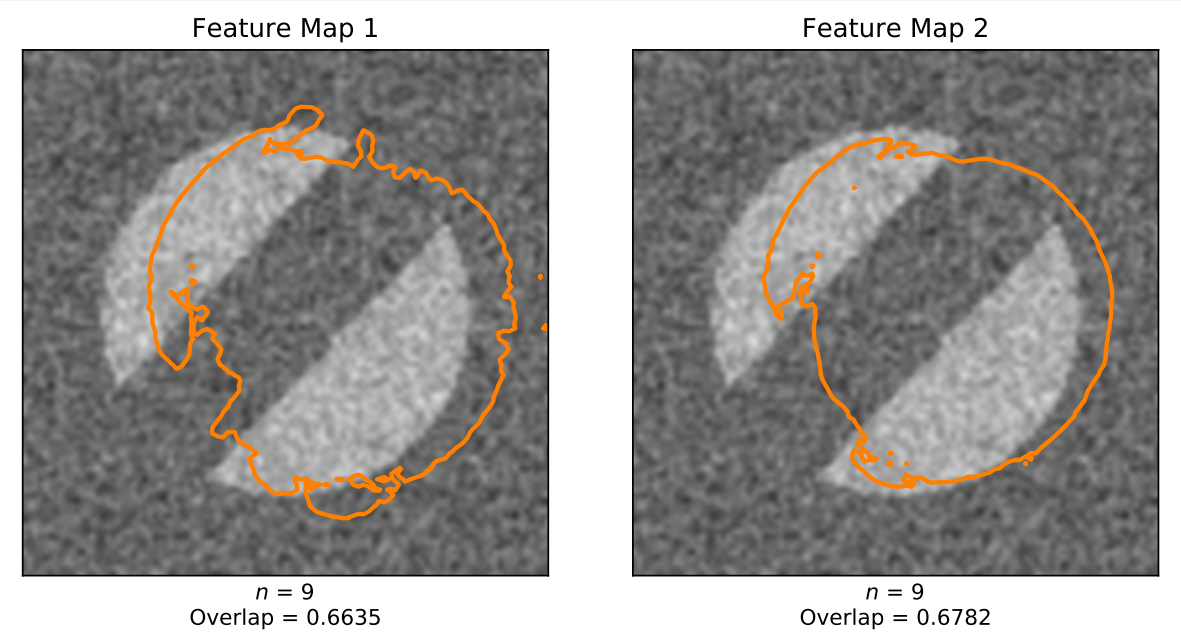

Synthetic Data: Partitioned Circles, Results

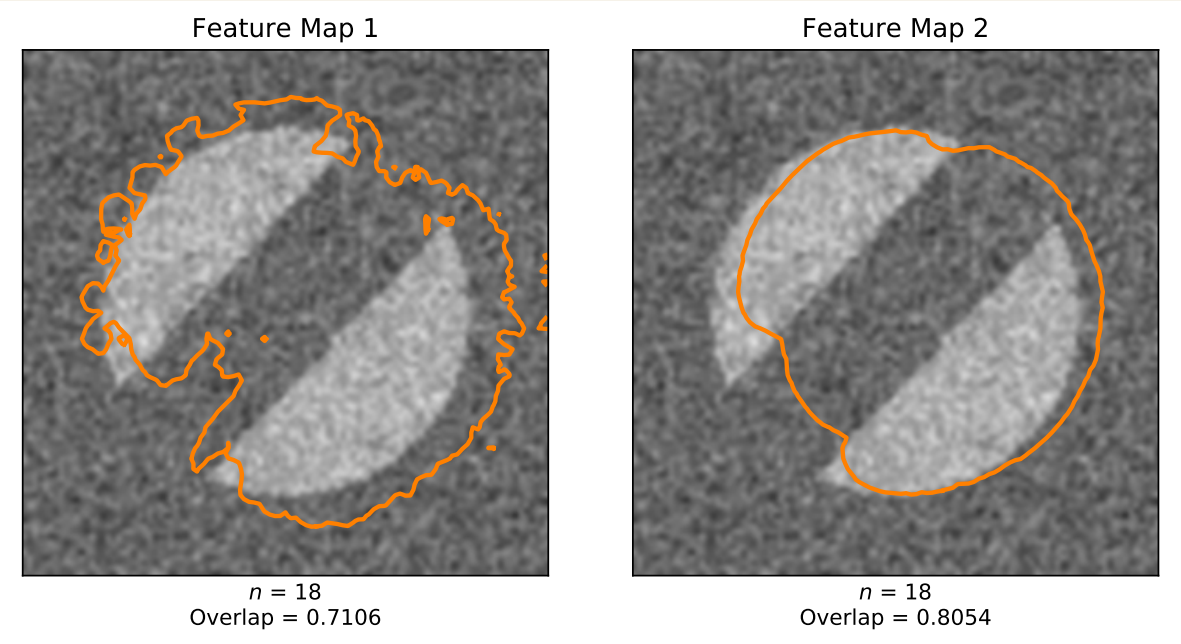

Synthetic Data: Partitioned Circles, Results

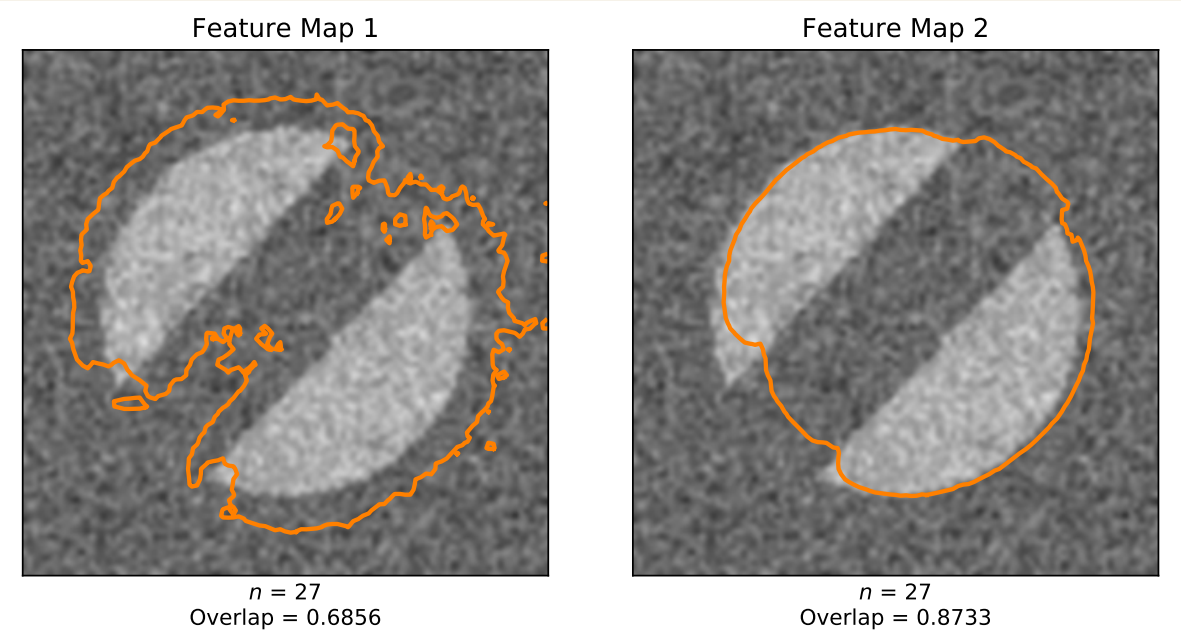

Synthetic Data: Partitioned Circles, Results

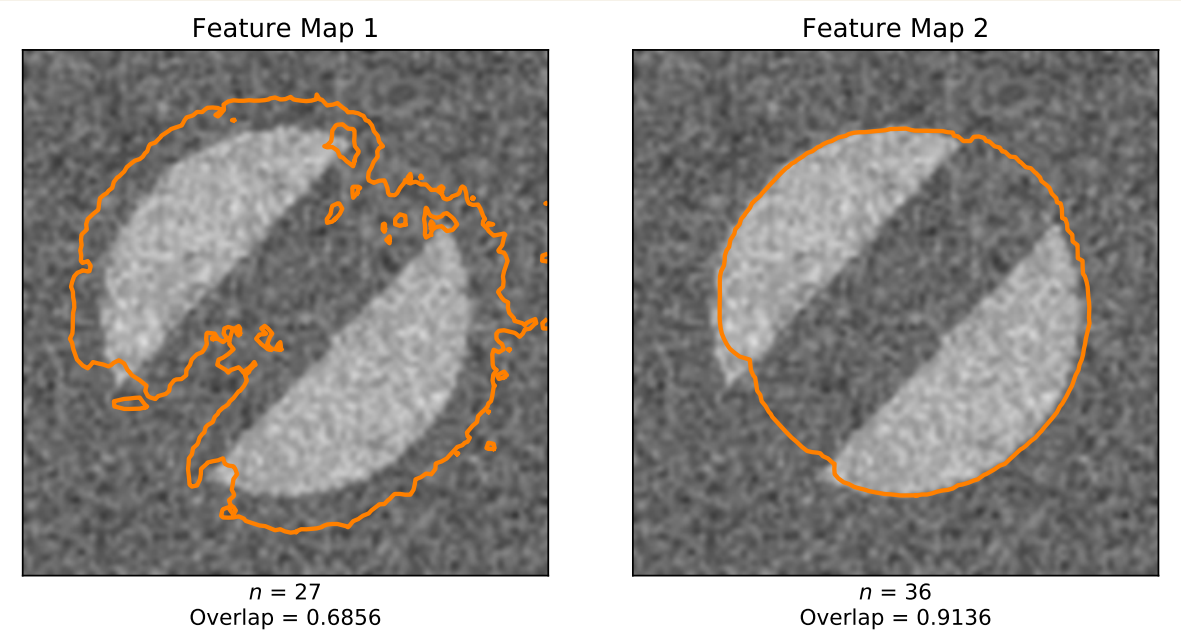

Synthetic Data: Partitioned Circles, Results

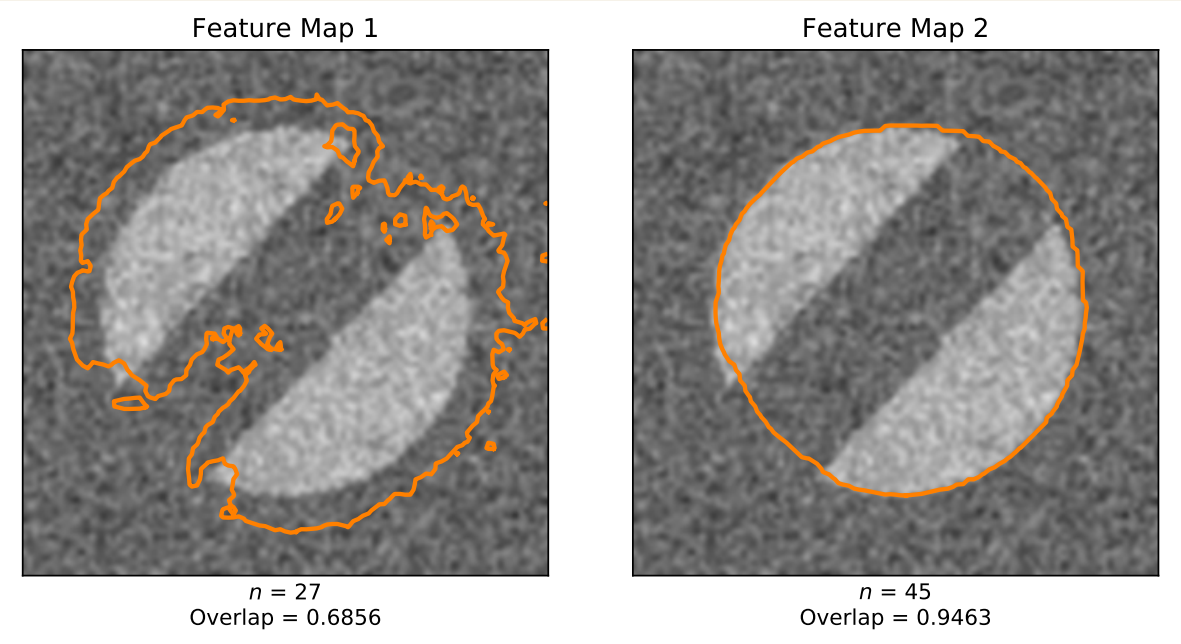

Synthetic Data: Partitioned Circles, Results

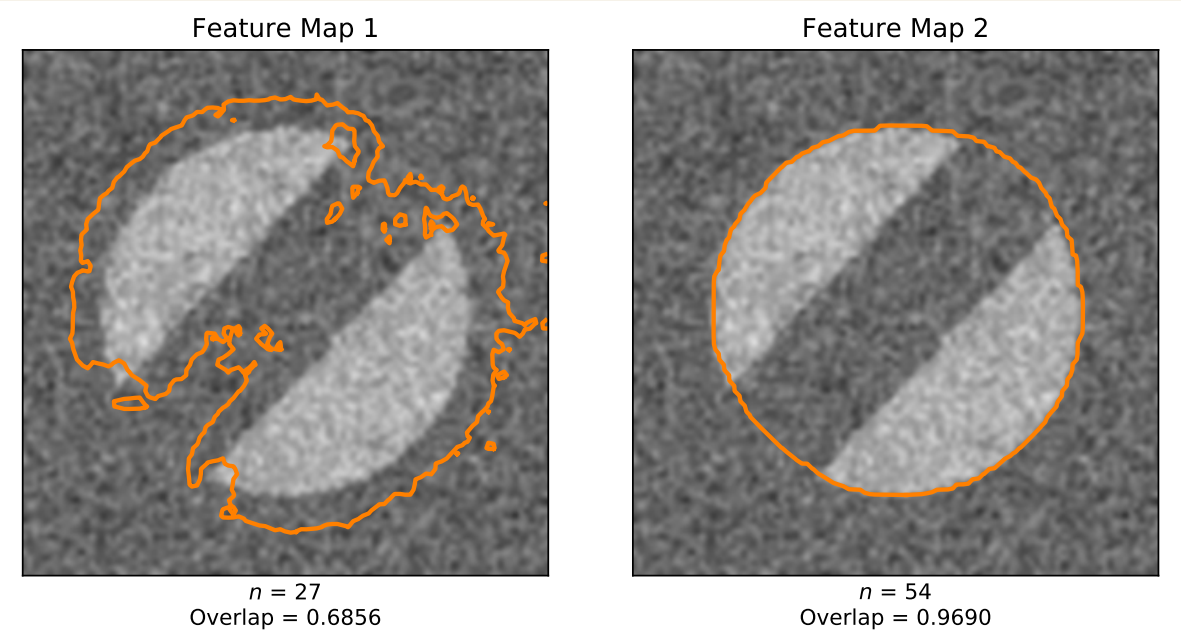

Synthetic Data: Illusory Triangles

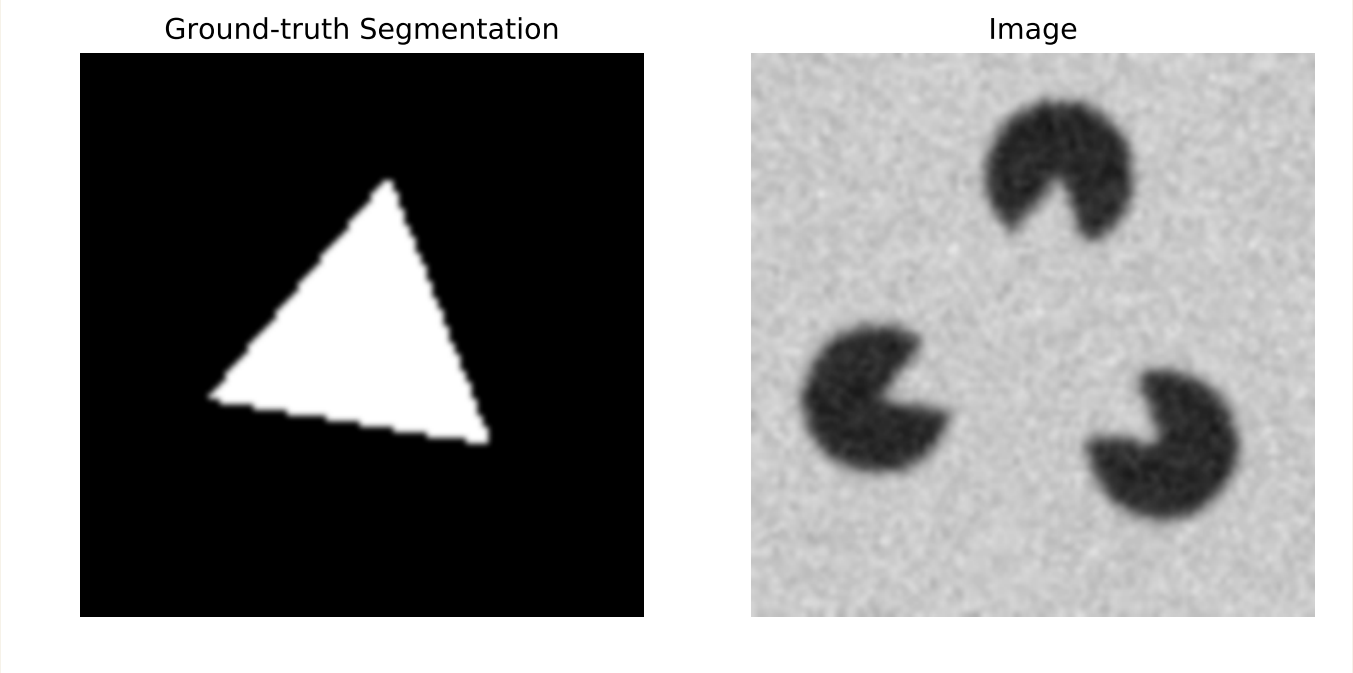

- 100/50/50 randomly generated image and segmentation pairs for training/validation/testing datasets

Synthetic Data: Illusory Triangles, Feature Maps Tested

Table: Feature Map 1

Feature	Local	Global
Area		✓
Boundary length		✓
Isoperimetric ratio		✓
Seg. moments, $p = 1, 2$		✓
Dist. from center of mass	✓	✓
Image value mean in seg.		✓
Image value std. in seg.		✓
Image value	✓	
Image edge	✓	

Table: Feature Map 2

Feature	Local	Global
Area		✓
Boundary length		✓
Isoperimetric ratio		✓
Seg. moments, $p = 1, 2$		✓
Dist. from center of mass	✓	✓
Image value mean in seg.		✓
Image value std. in seg.		✓
Image value	✓	
Image edge	✓	
Corner response	✓	
Frenet frame	✓	

Image features are computed at four scales, $\sigma \in \{0, 1, 2, 3\}$

Synthetic Data: Illusory Triangles, Results

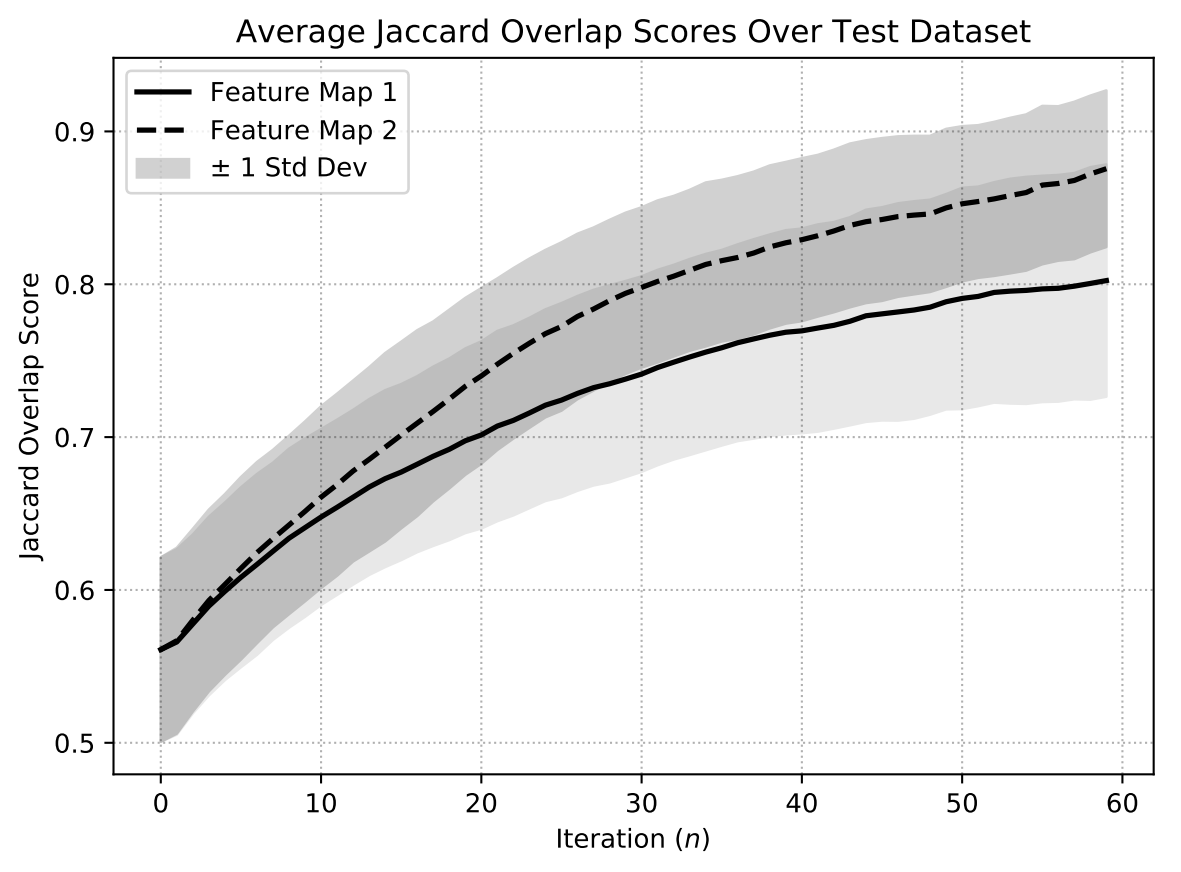

Synthetic Data: Illusory Triangles, Results

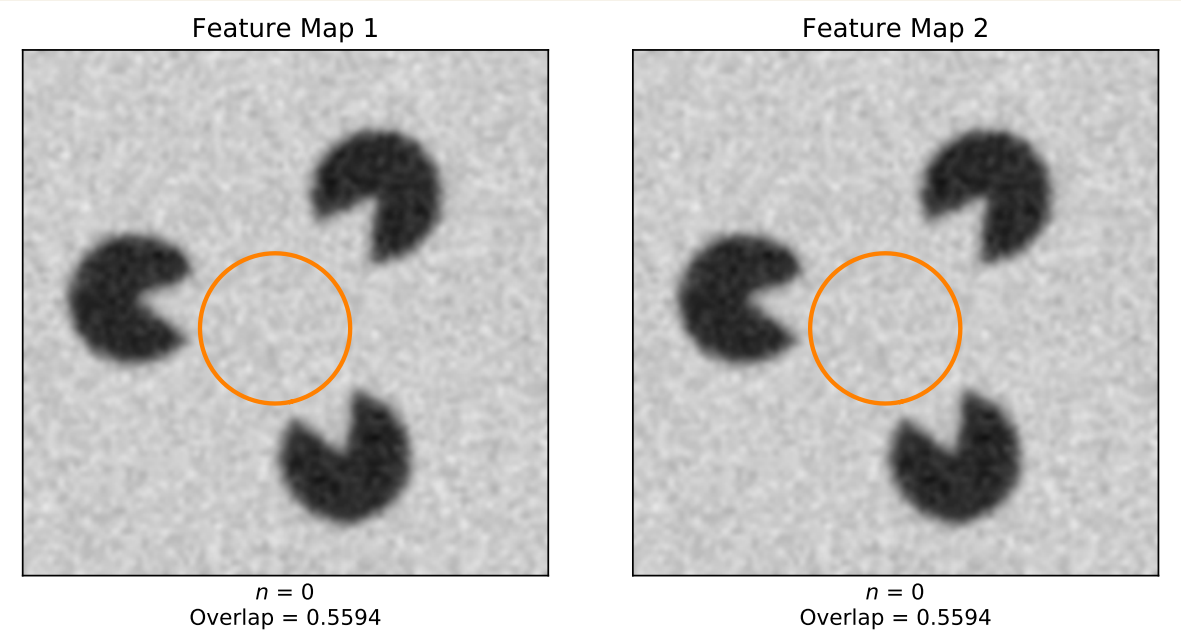

Synthetic Data: Illusory Triangles, Results

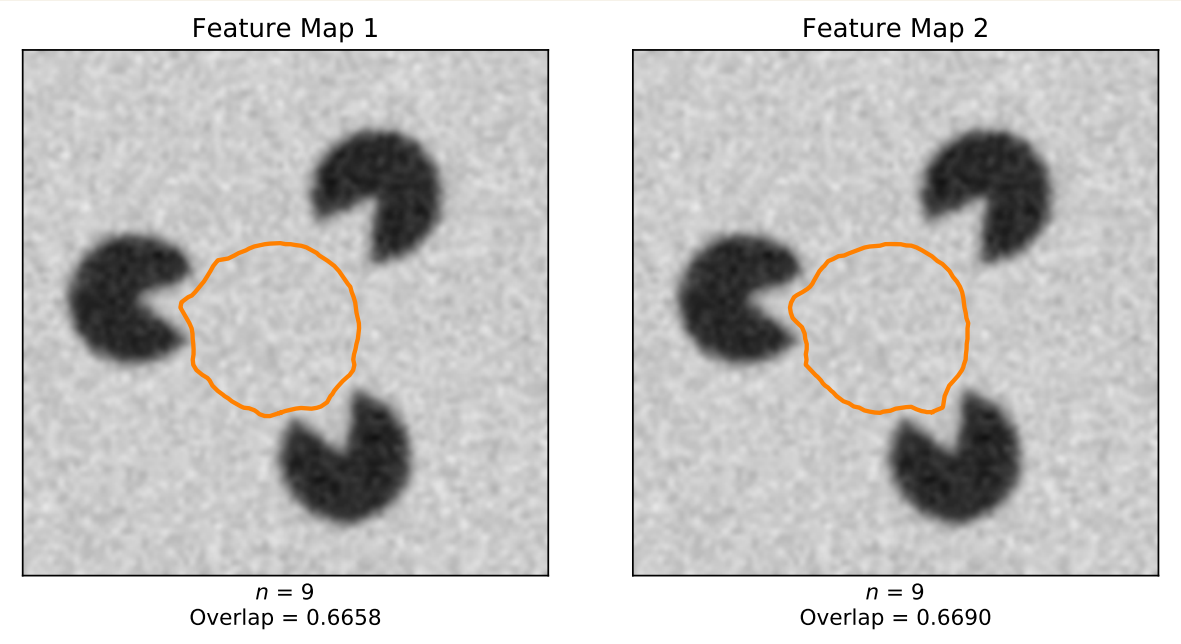

Synthetic Data: Illusory Triangles, Results

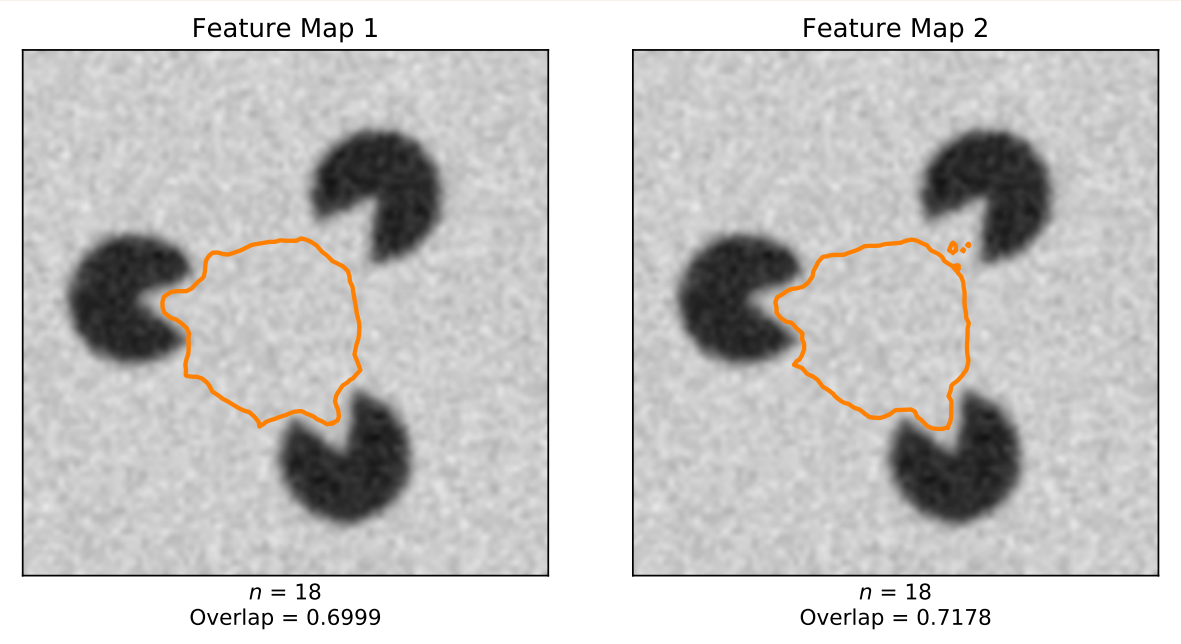

Synthetic Data: Illusory Triangles, Results

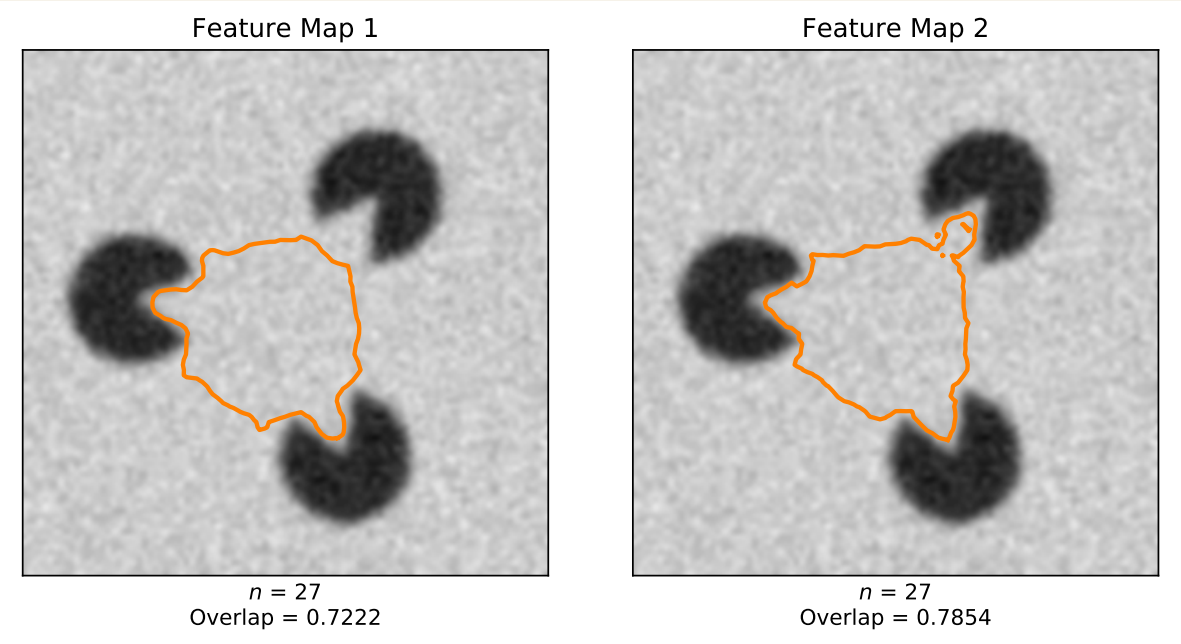

Synthetic Data: Illusory Triangles, Results

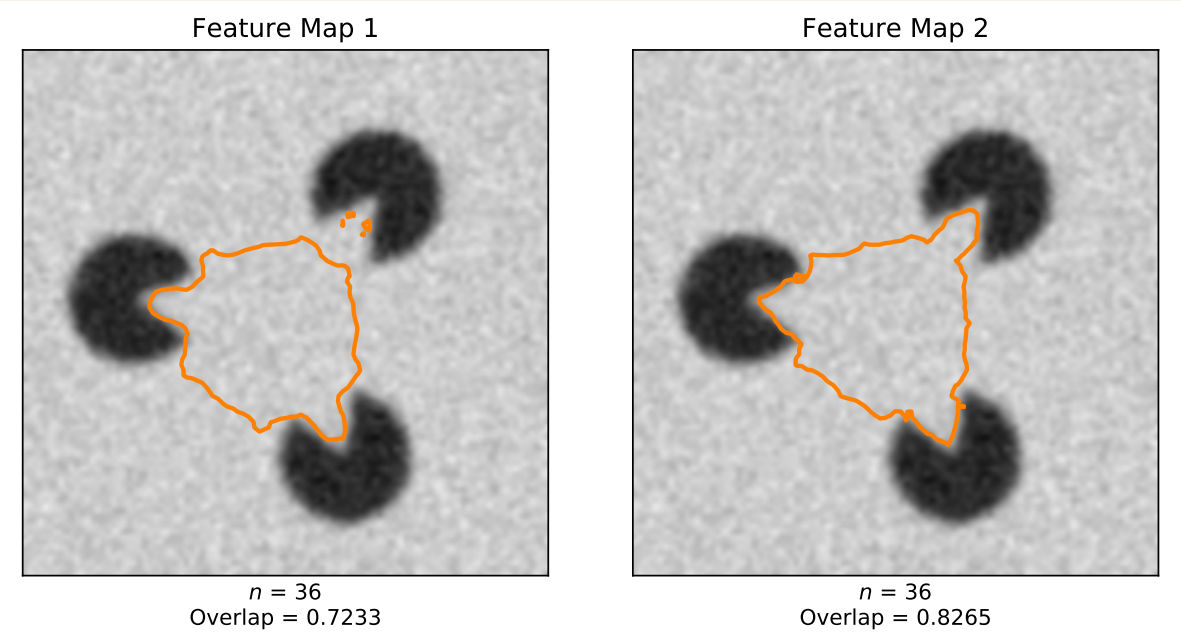

Synthetic Data: Illusory Triangles, Results

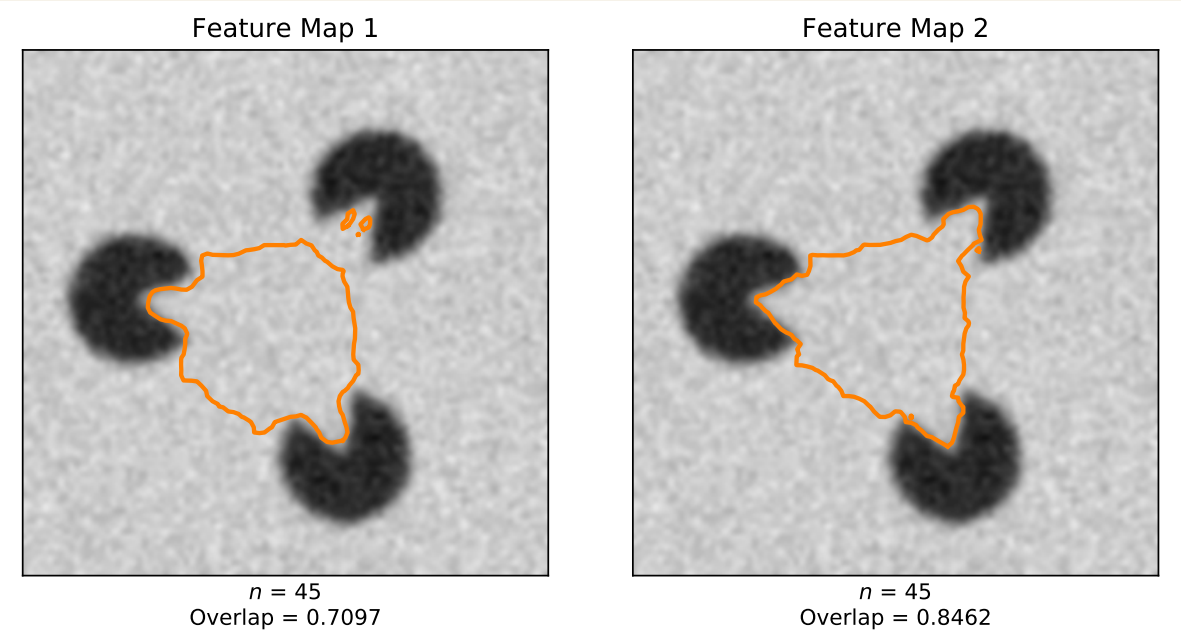

Synthetic Data: Illusory Triangles, Results

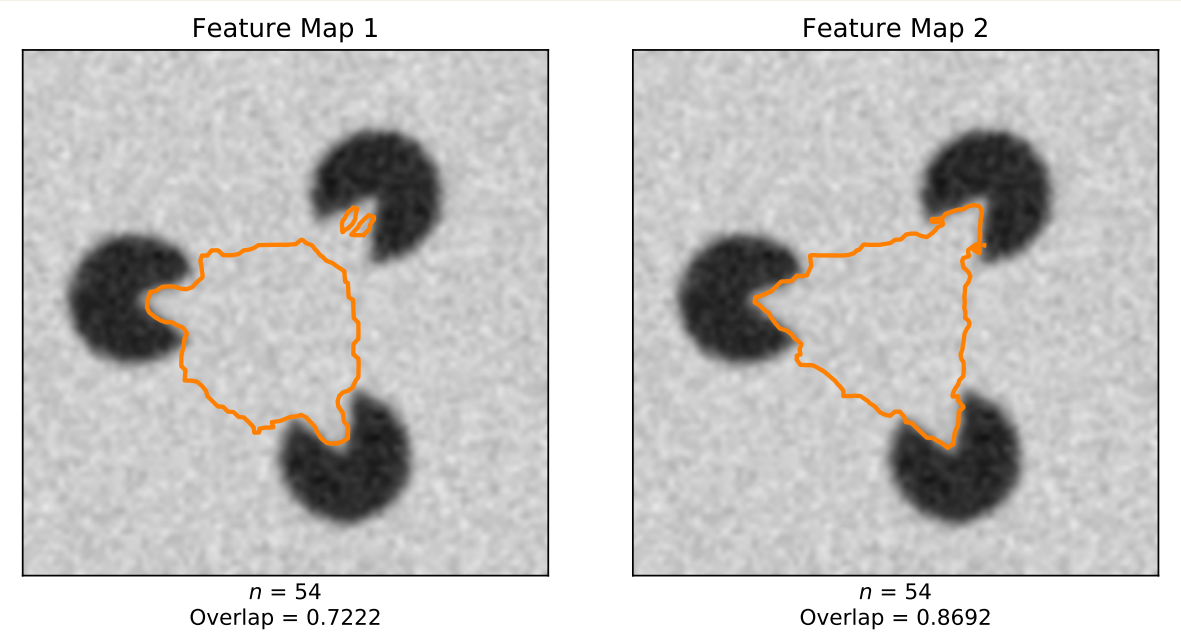

Lung Nodule Segmentation: LIDC Dataset

- 891 nodules where 4 annotators agree on existence of nodule at that location
- Sample 200/100/100 nodules for training/validation/testing
- Preprocess data:
  1. Transform annotation contours to boolean-valued images
  2. Interpolate images to uniform (1 mm) pixel spacing
- For each nodule 10 random seed points chosen

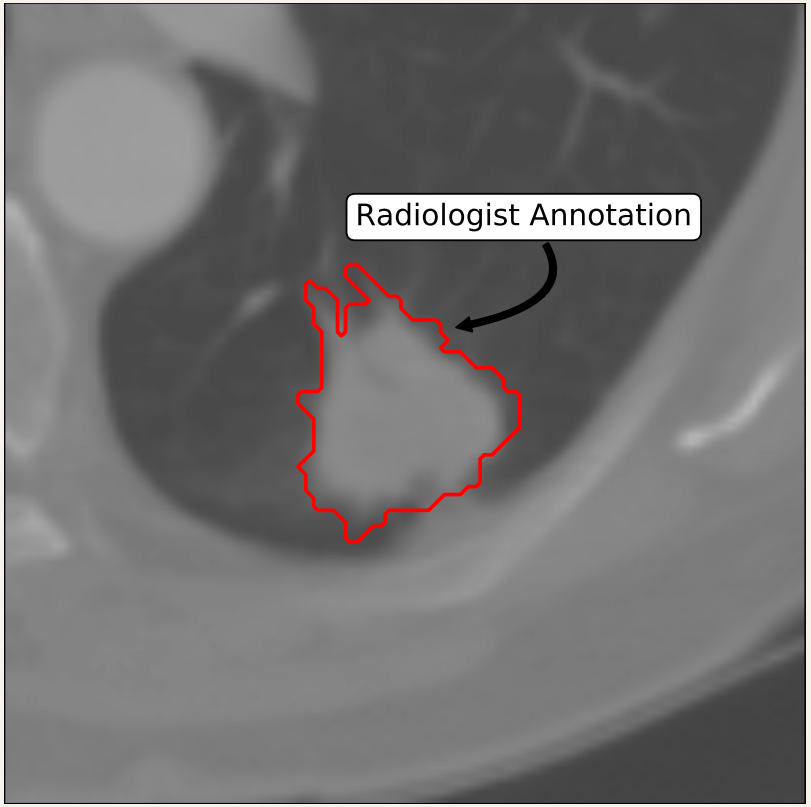

Lung Nodule Segmentation: LIDC Dataset

- 891 nodules where 4 annotators agree on existence of nodule at that location
- Sample 200/100/100 nodules for training/validation/testing
- Preprocess data:
  1. Transform annotation contours to boolean-valued images
  2. Interpolate images to uniform (1 mm) pixel spacing
- For each nodule 10 random seed points chosen

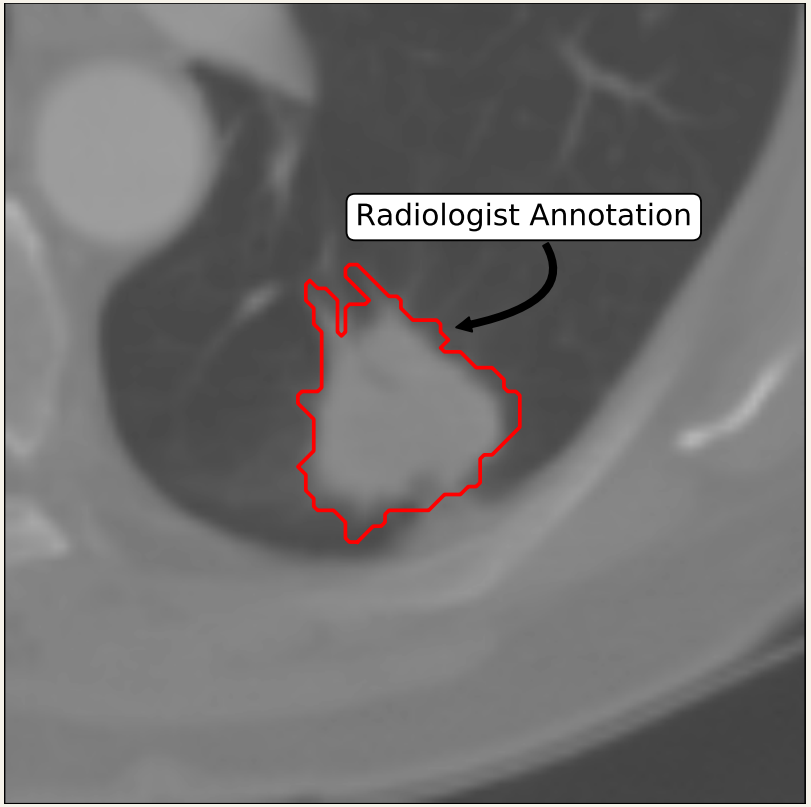

Lung Nodule Segmentation: LIDC Dataset

- 891 nodules where 4 annotators agree on existence of nodule at that location
- Sample 200/100/100 nodules for training/validation/testing
- Preprocess data:
  1. Transform annotation contours to boolean-valued images
  2. Interpolate images to uniform (1 mm) pixel spacing
- For each nodule 10 random seed points chosen

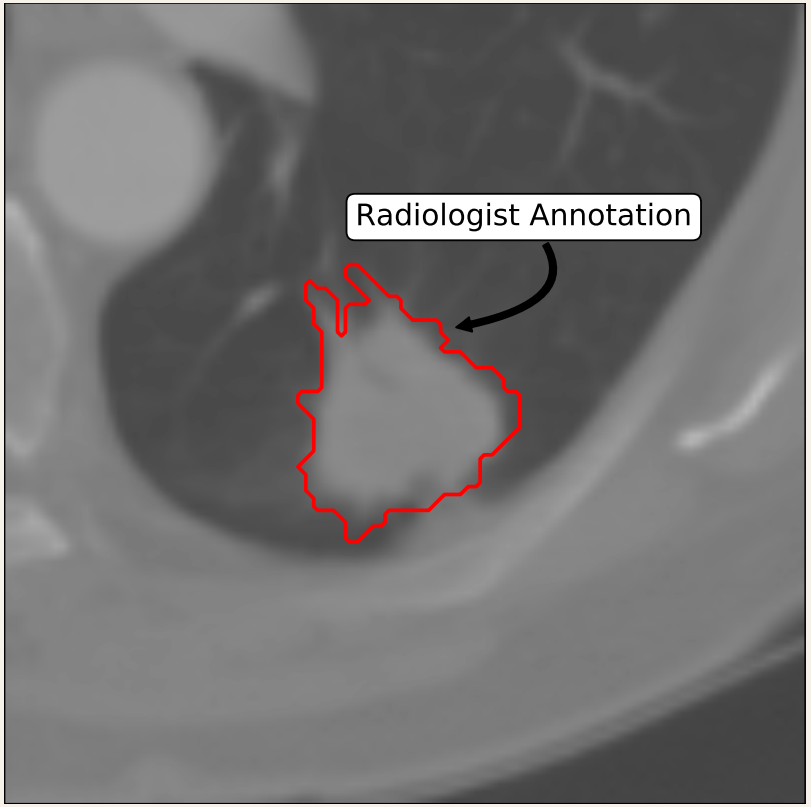

Lung Nodule Segmentation: LIDC Dataset

- 891 nodules where 4 annotators agree on existence of nodule at that location
- Sample 200/100/100 nodules for training/validation/testing
- Preprocess data:
  1. Transform annotation contours to boolean-valued images
  2. Interpolate images to uniform (1 mm) pixel spacing
- For each nodule 10 random seed points chosen

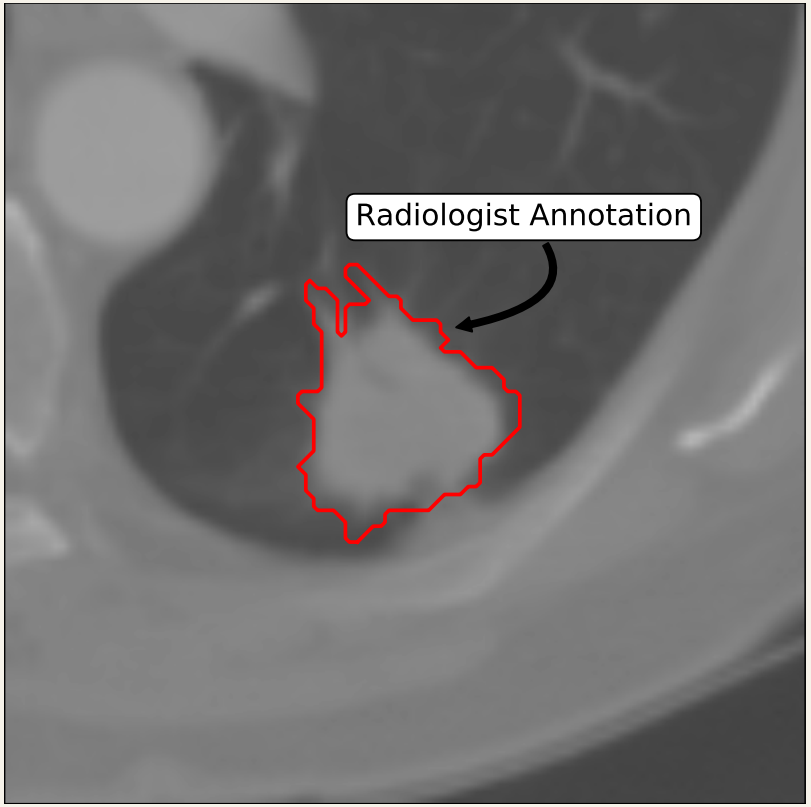

Lung Nodule Segmentation: LIDC Dataset

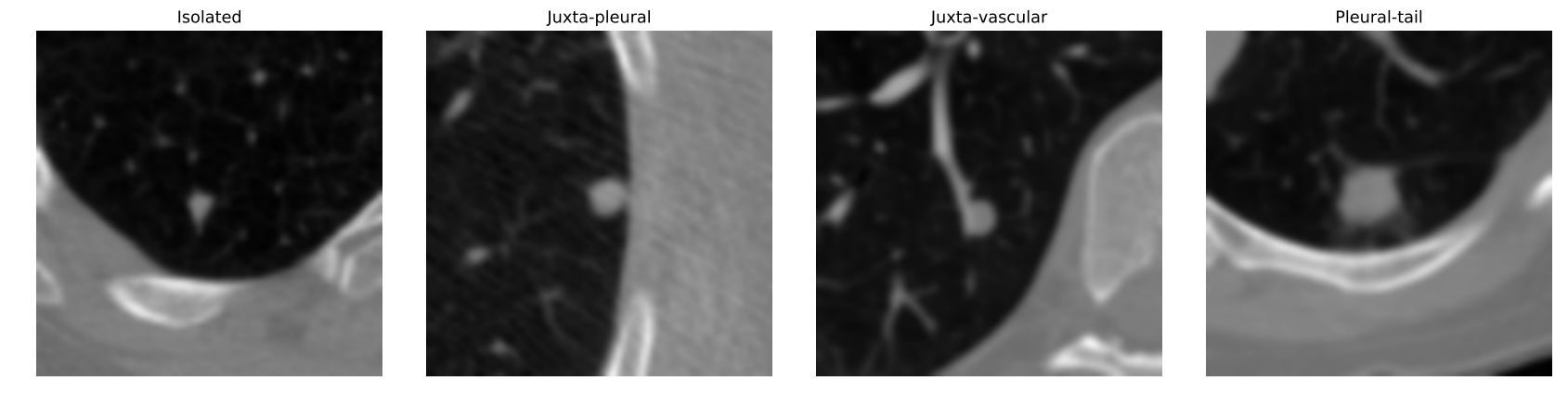

(a) Example nodules of various anatomical location types.

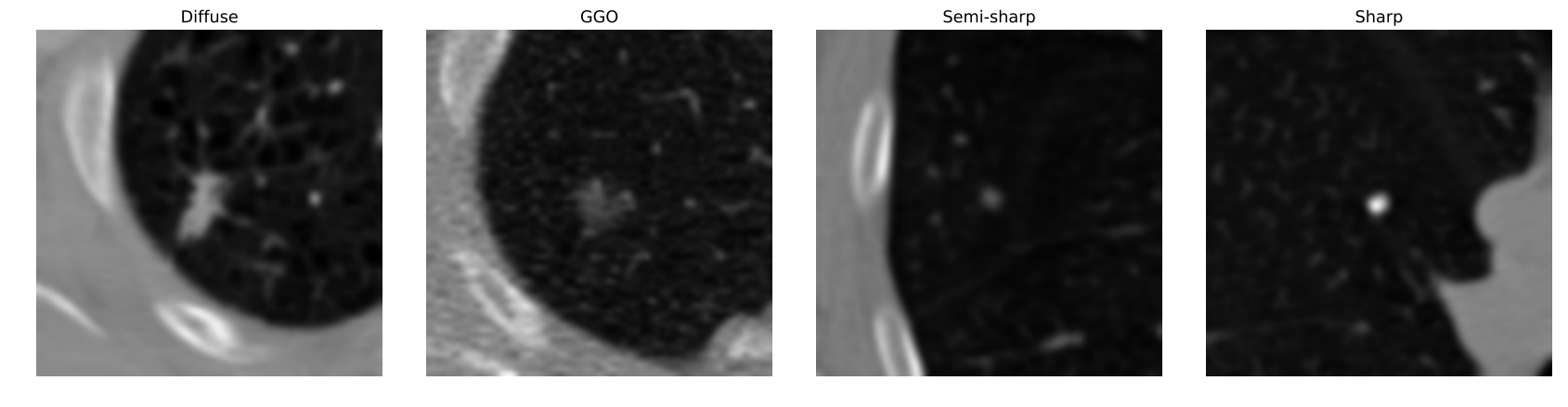

(b) Example nodules of various boundary density types.

Lung Nodule Segmentation: Initialization Routine

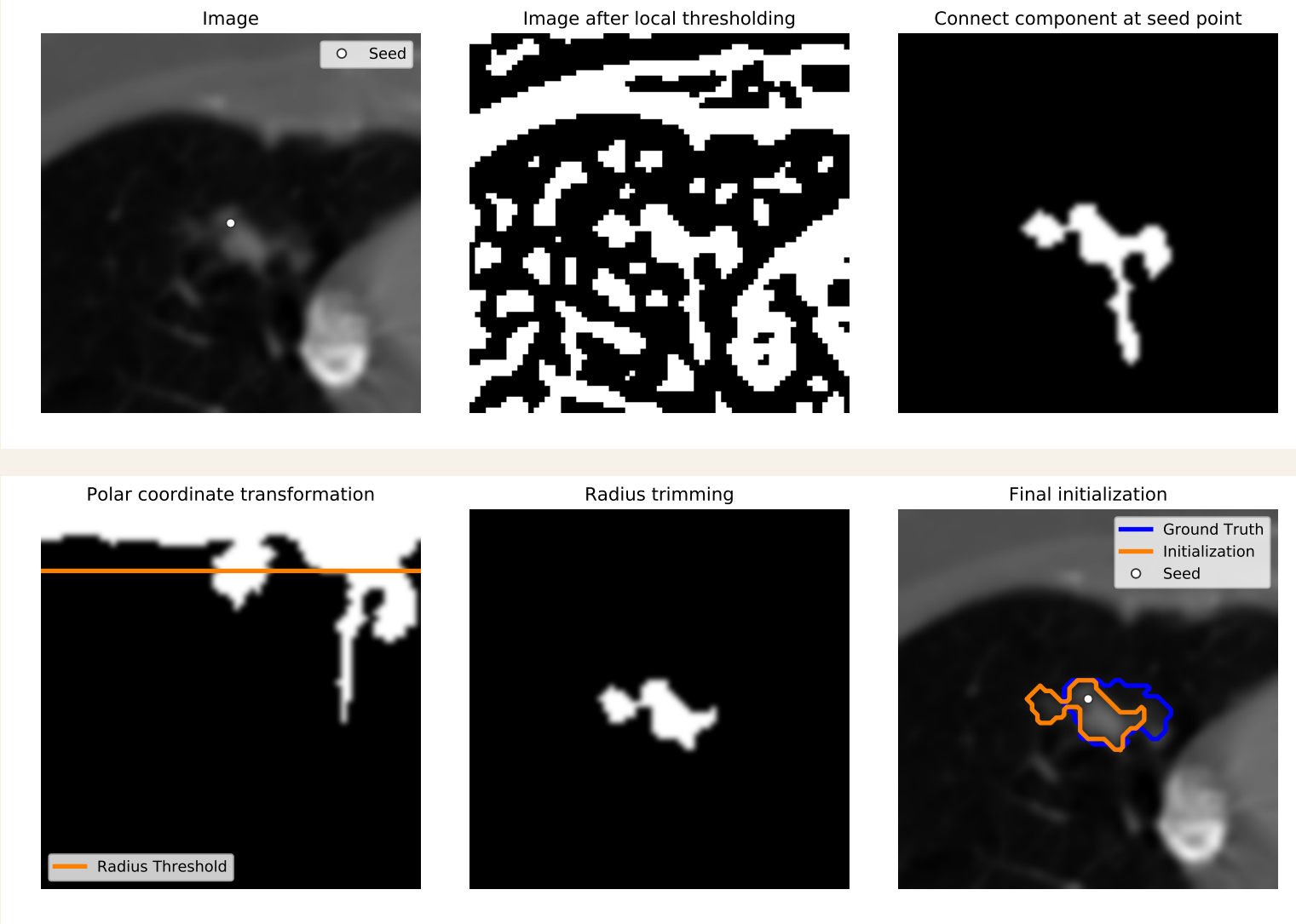

Lung Nodule Segmentation: Feature Maps Tested

Table: Feature Map 1

Feature	Local	Global
Area		✓
Boundary length		✓
Isoperimetric ratio		✓
Seg. moments, $p = 1, 2$		✓
Dist. from center of mass	✓	✓
Image value mean in seg.		✓
Image value std. in seg.		✓
Image value	✓	
Image edge	✓	

Table: Feature Map 2

Feature	Local	Global
Area		✓
Boundary length		✓
Isoperimetric ratio		✓
Seg. moments, $p = 1, 2$		✓
Dist. from center of mass	✓	✓
Image value mean in seg.		✓
Image value std. in seg.		✓
Image value	✓	
Image edge	✓	
Average Image Edge		✓
Frenet frame	✓	

Image features are computed at four scales, $\sigma \in \{0, 1, 2, 3\}$

Lung Nodule Segmentation: Results

Table: Results for Feature Map 1.

N_h	n^*	$\bar{J}$
8	14	0.7128 ($\pm$ 0.1708)
16	14	0.7127 ($\pm$ 0.1680)
32	24	**0.7219** ($\pm$ 0.1591)

Table: Results for Feature Map 2.

N_h	n^*	$\bar{J}$
8	18	0.7241 ($\pm$ 0.1594)
16	22	0.7359 ($\pm$ 0.1532)
32	30	**0.7468** ($\pm$ 0.1428)

Lung Nodule Segmentation: Results

Table: Performance of various lung nodule segmentation methods on the LIDC dataset (table of results reproduced from reference [14])

Authors	Year	Number of Nodules		Jaccard overlap
		Training	Testing	
Tachibana and Kido [11]	2006	-	23	0.5070 ($\pm$0.2190)
Wang et al. [13]	2009	23	64	0.5800
Messay et al. [9]	2010	-	68	0.6300 ($\pm$0.1600)
Kubota et al. [5]	2011	-	23	0.6900 ($\pm$0.1800)
Tan et al. [12]	2013	-	23	0.6500
Lassen et al. [6]	2015	-	19	0.5200 ($\pm$0.0700)
Messay et al. [10]	2015	300	66	0.7170 ($\pm$0.1989)
Wang et al. [14]	2017	350	493	0.7160 ($\pm$0.1222)
SCLS Method (our work)**	-	200 ($\times$10)	100 ($\times$10)	**0.7468** ($\pm$ 0.1428)

**Our work is presently in 2D; results in table are 3D

Lung Nodule Segmentation: Results

Table: Results by type for Feature Map 2.

Density Type Location Type	Diffuse	GGO	Semi-sharp	Sharp	
Isolated	(5) 0.7124	(5) 0.7267	(26) 0.7798	(14) 0.8507	(50) 0.7876
Juxta-pleural	(1) 0.8178	(2) 0.5730	(17) 0.6430	(7) 0.7960	(27) 0.6840
Juxta-vascular	(0) -	(0) -	(9) 0.7462	(4) 0.6552	(13) 0.7182
Pleural-tail	(2) 0.5539	(0) -	(6) 0.7829	(2) 0.8436	(10) 0.7493
	(8) 0.6859	(7) 0.6828	(58) 0.7348	(27) 0.8070	(100) 0.7468

Lung Nodule Segmentation: Training Time / Run Time

Training times (in hours):

N_h	Feature Map 1	Feature Map 2
8	1.12	1.65
17	1.39	3.17
32	3.37	7.17
Total	5.88	12

Average test time (in milliseconds):

Feature Map 1	Feature Map 2
270.20 ($\pm$ 47.16)	545.09 ($\pm$ 208.64)

Lung Nodule Segmentation: Results, Example 1

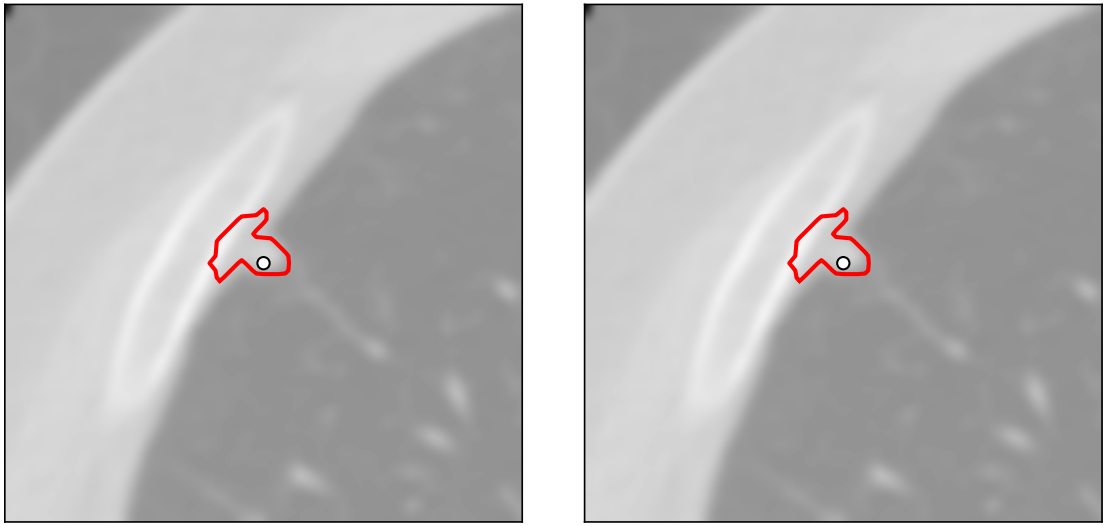

Lung Nodule Segmentation: Results, Example 1

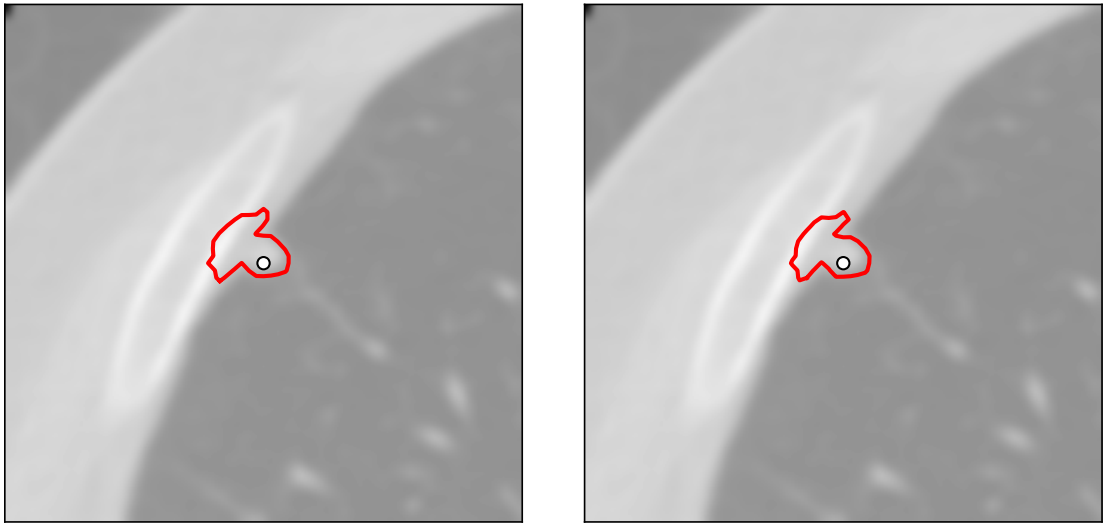

Lung Nodule Segmentation: Results, Example 1

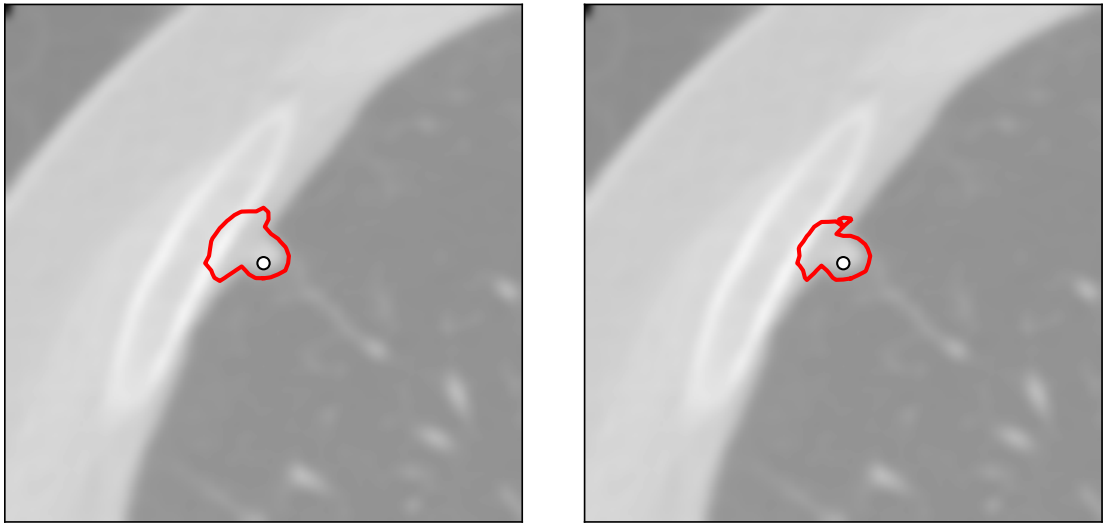

n = 9, Overlap = 0.2785

n = 9, Overlap = 0.3729

Lung Nodule Segmentation: Results, Example 1

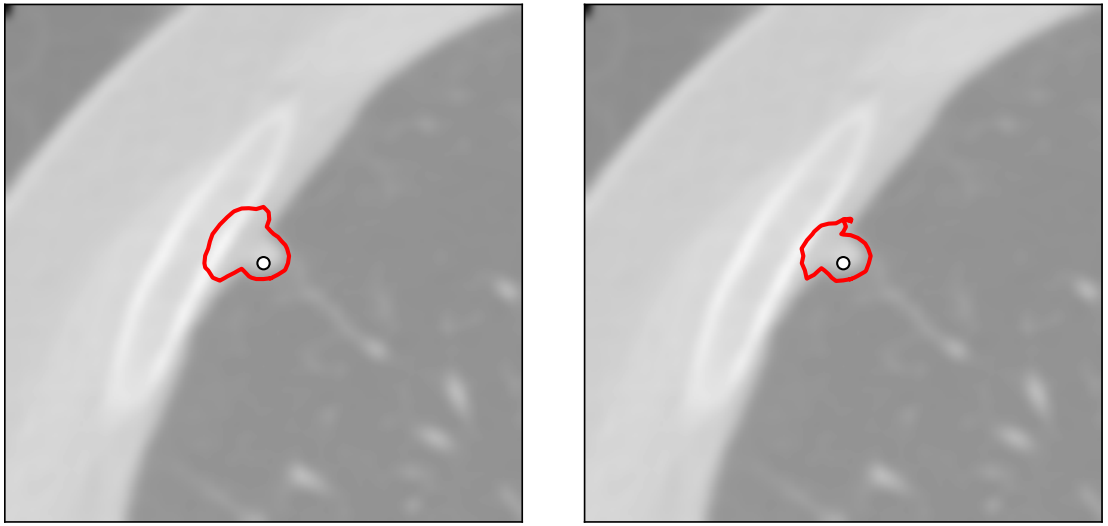

n = 13, Overlap = 0.2619

n = 13, Overlap = 0.3929

Lung Nodule Segmentation: Results, Example 1

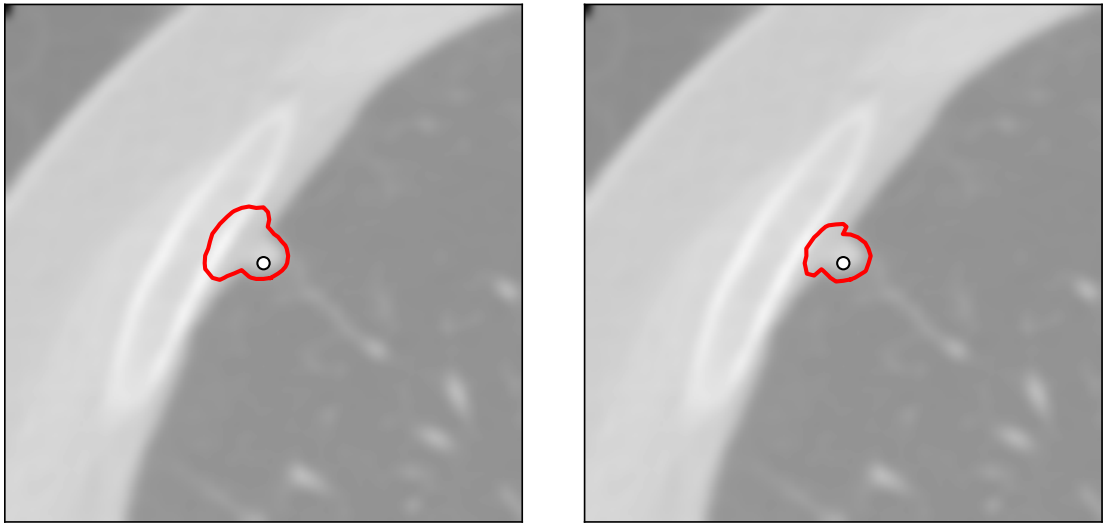

n = 17, Overlap = 0.2558

n = 17, Overlap = 0.4314

Lung Nodule Segmentation: Results, Example 1

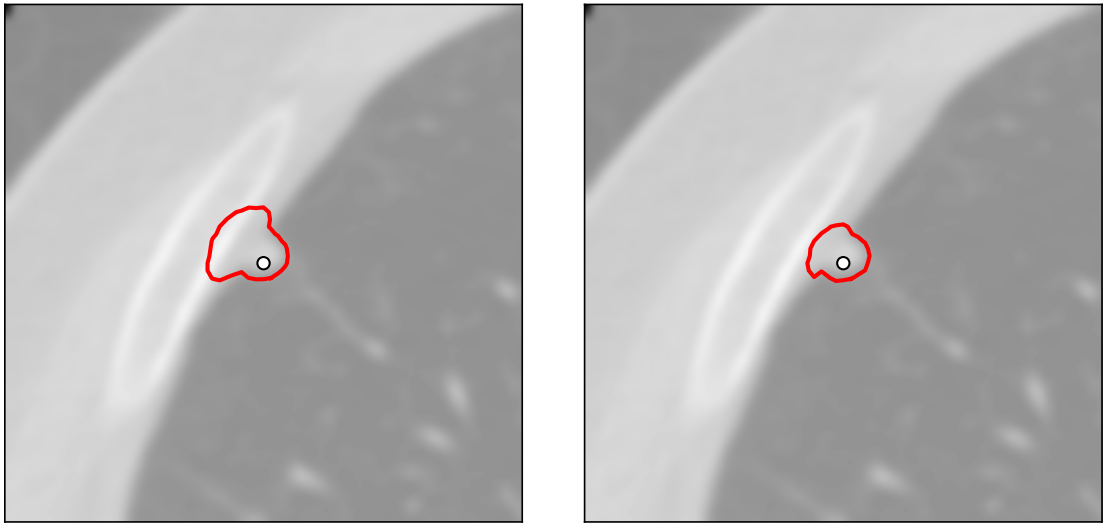

n = 21, Overlap = 0.2619

n = 21, Overlap = 0.4583

Lung Nodule Segmentation: Results, Example 1

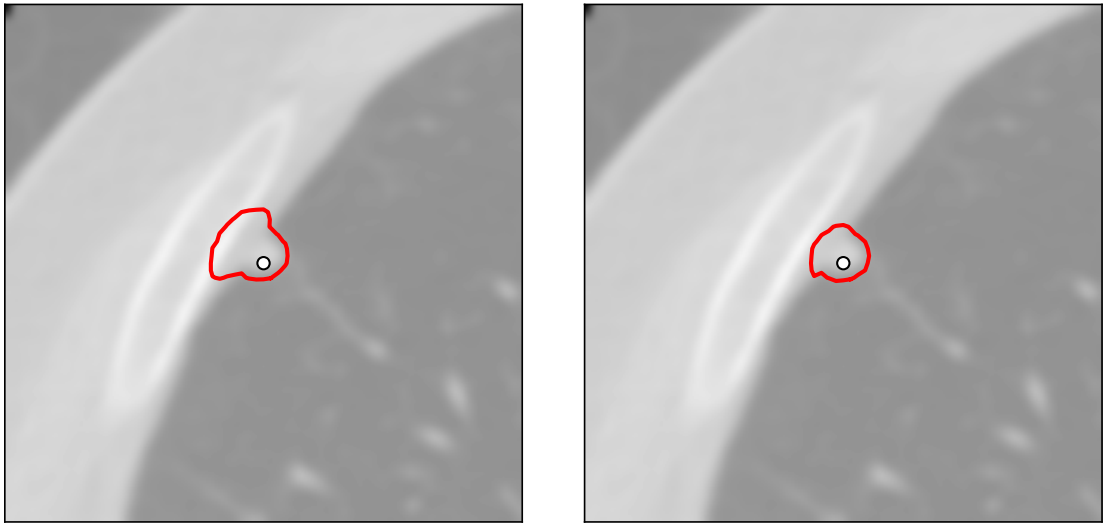

n = 24, Overlap = 0.2750

n = 26, Overlap = 0.4681

Lung Nodule Segmentation: Results, Example 1

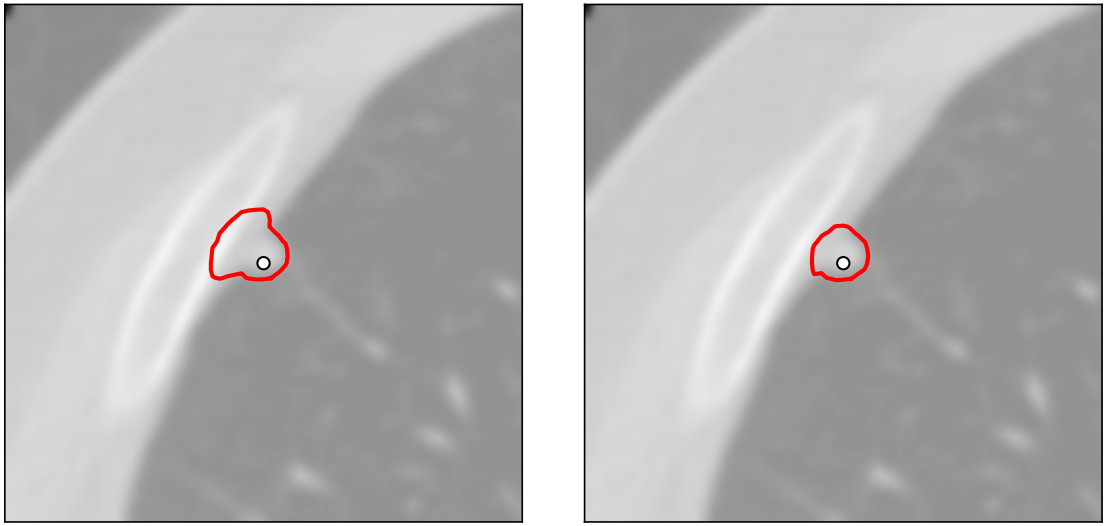

n = 24, Overlap = 0.2750

n = 30, Overlap = 0.4681

Lung Nodule Segmentation: Results, Example 2

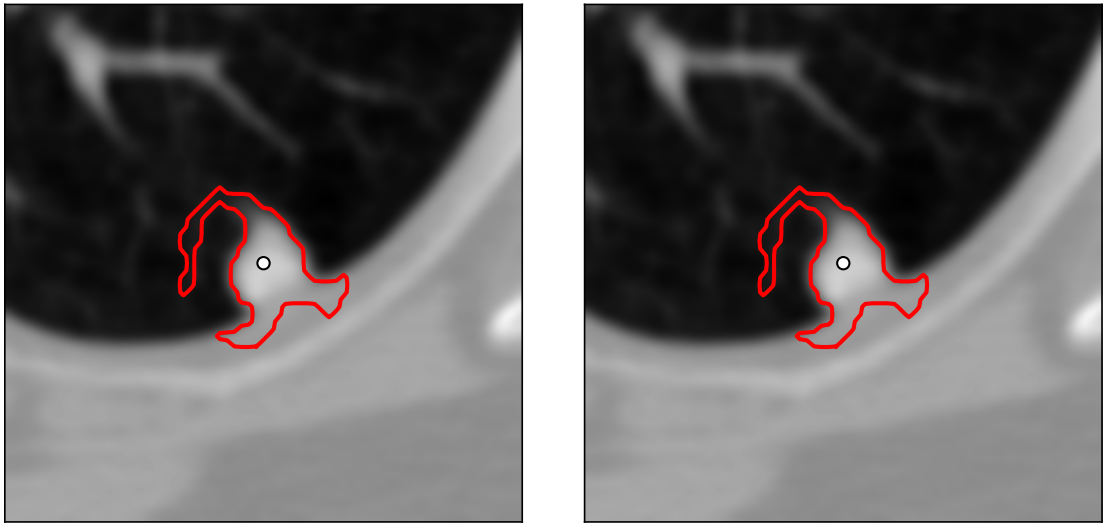

Lung Nodule Segmentation: Results, Example 2

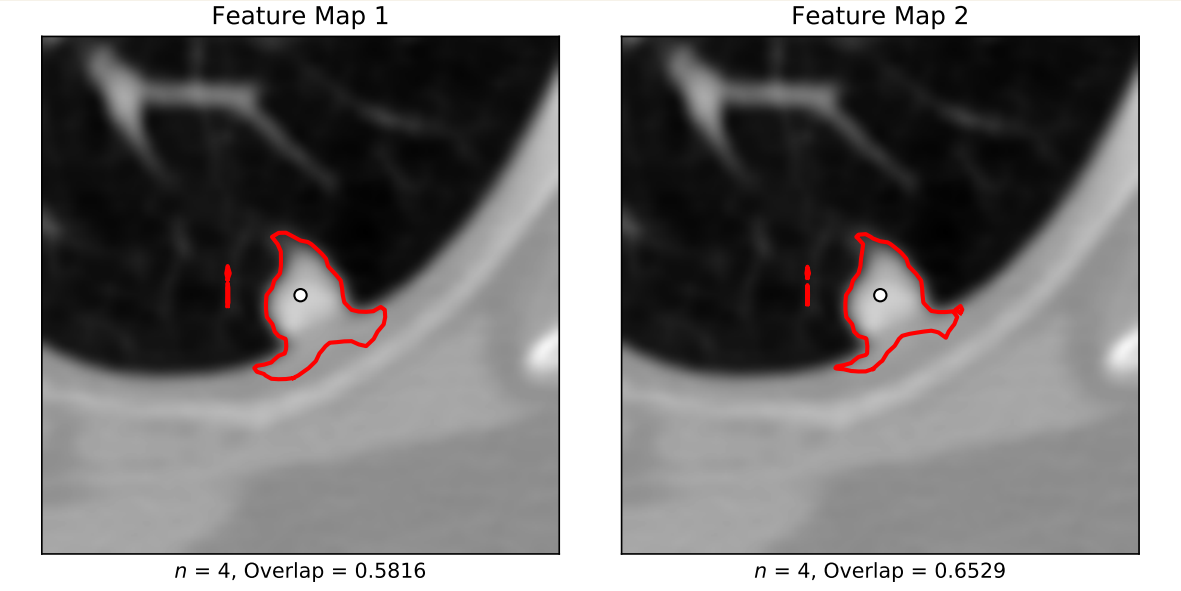

Lung Nodule Segmentation: Results, Example 2

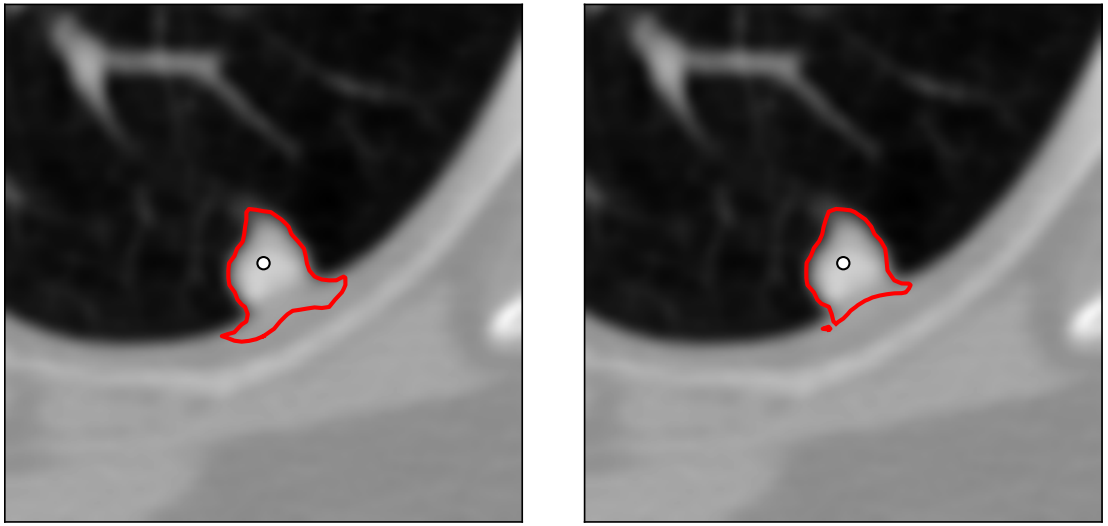

n = 9, Overlap = 0.6066

n = 9, Overlap = 0.7785

Lung Nodule Segmentation: Results, Example 2

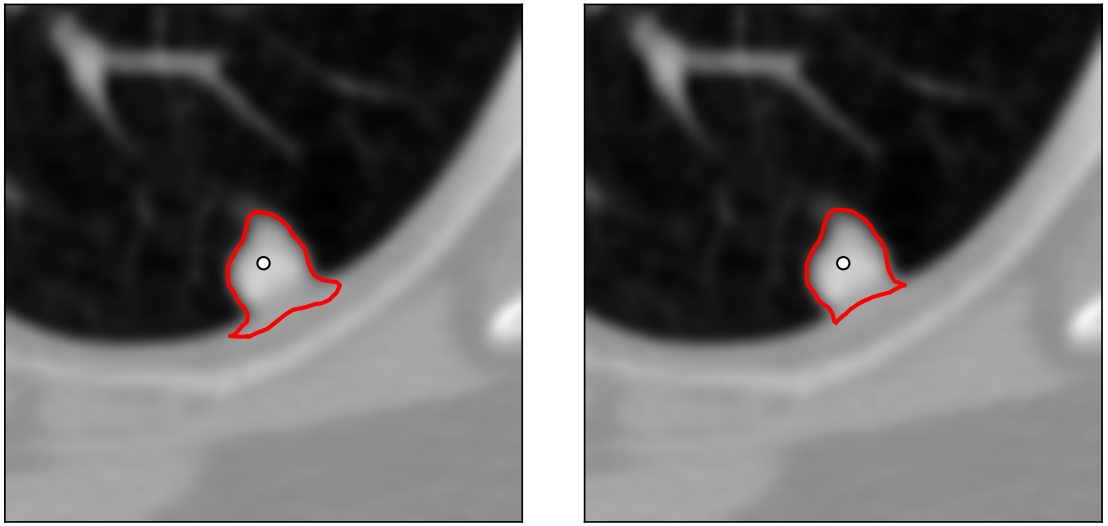

n = 13, Overlap = 0.6453

n = 13, Overlap = 0.8000

Lung Nodule Segmentation: Results, Example 2

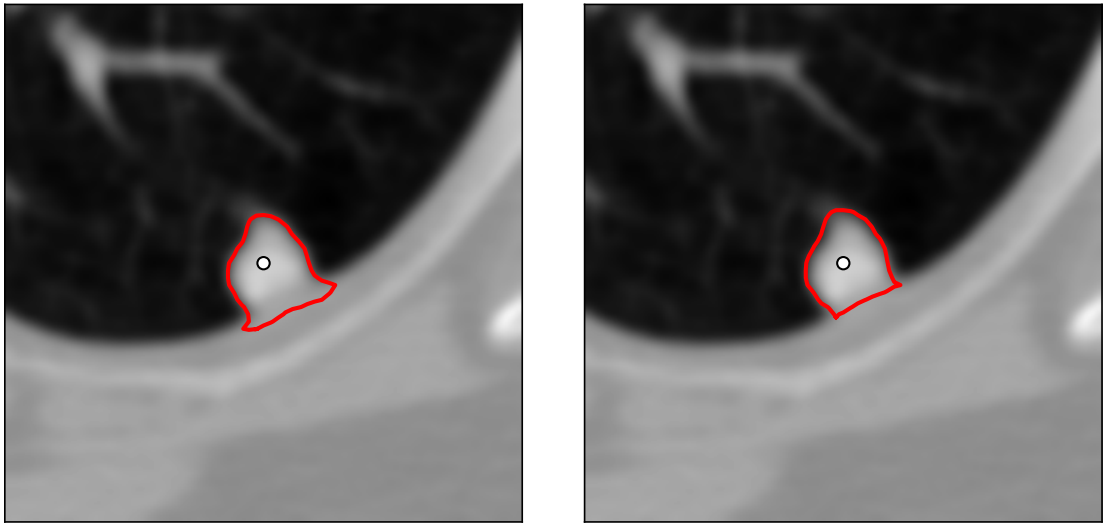

Lung Nodule Segmentation: Results, Example 2

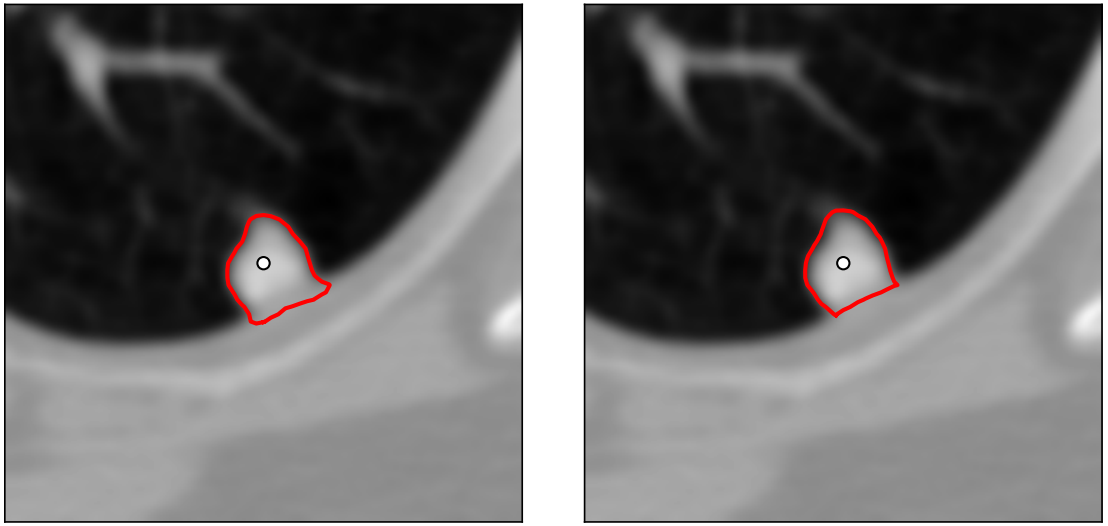

Lung Nodule Segmentation: Results, Example 2

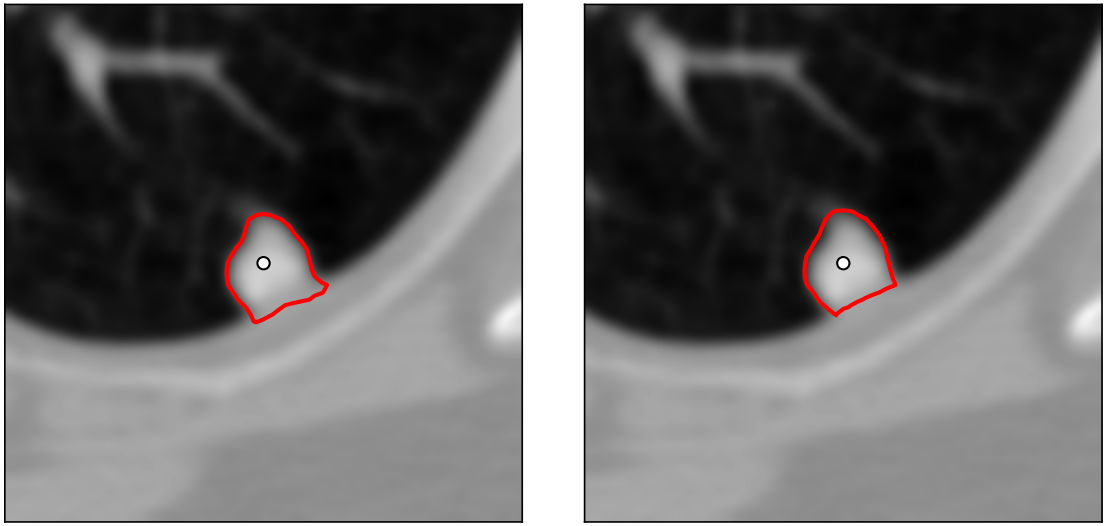

n = 24, Overlap = 0.7368

n = 26, Overlap = 0.8169

Lung Nodule Segmentation: Results, Example 2

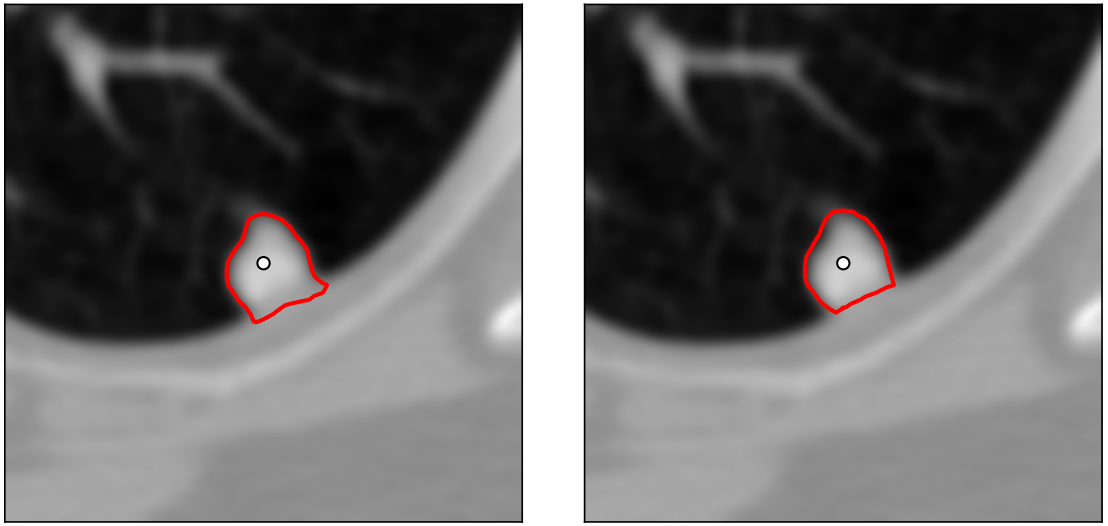

n = 24, Overlap = 0.7368

n = 30, Overlap = 0.8156

Lung Nodule Segmentation: Results, Example 3

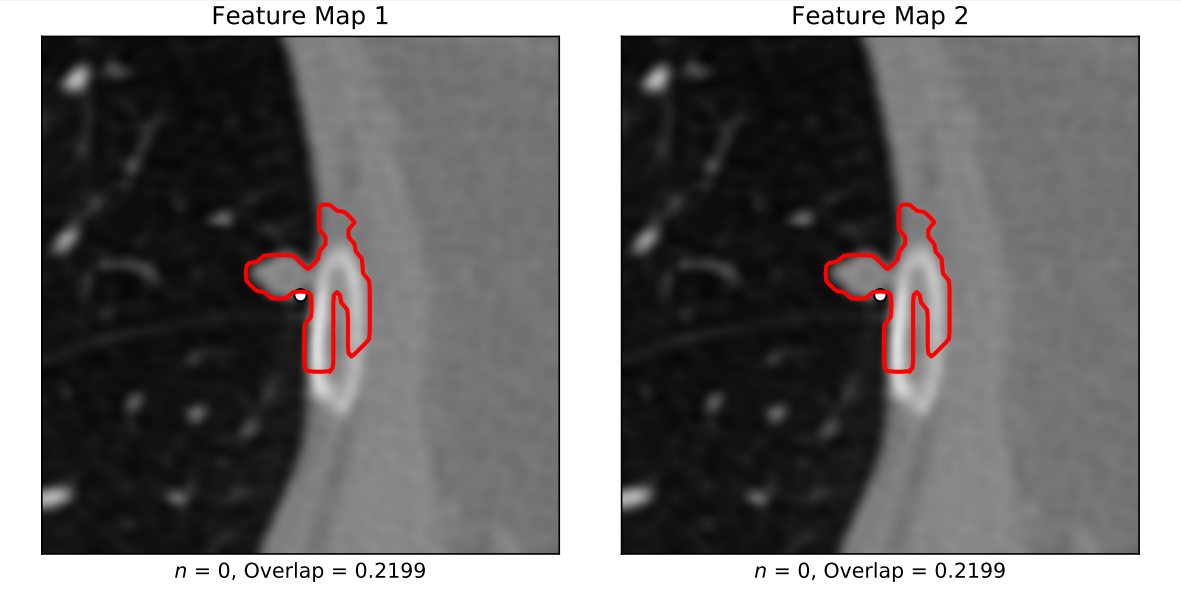

Lung Nodule Segmentation: Results, Example 3

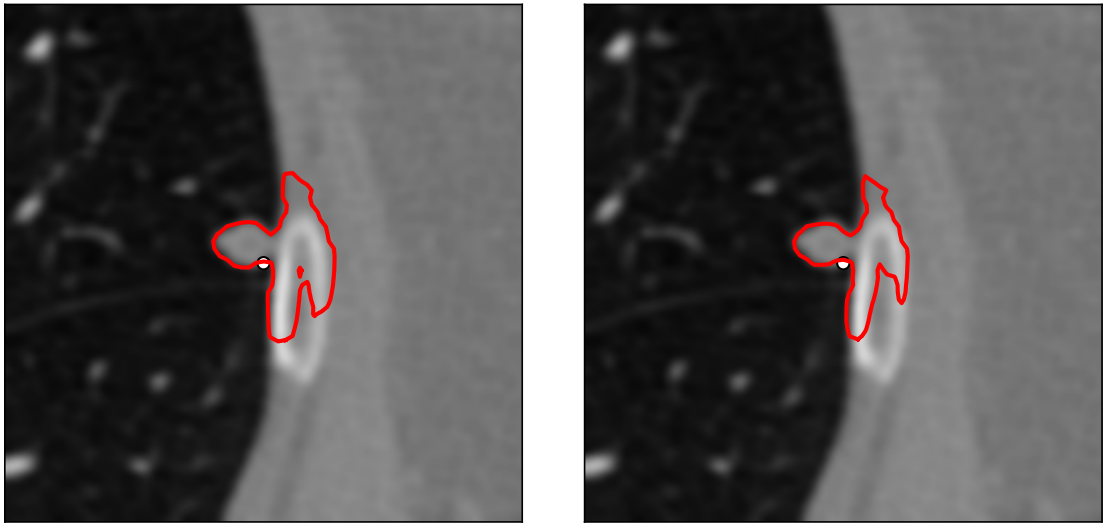

n = 4, Overlap = 0.2063

n = 4, Overlap = 0.2436

Lung Nodule Segmentation: Results, Example 3

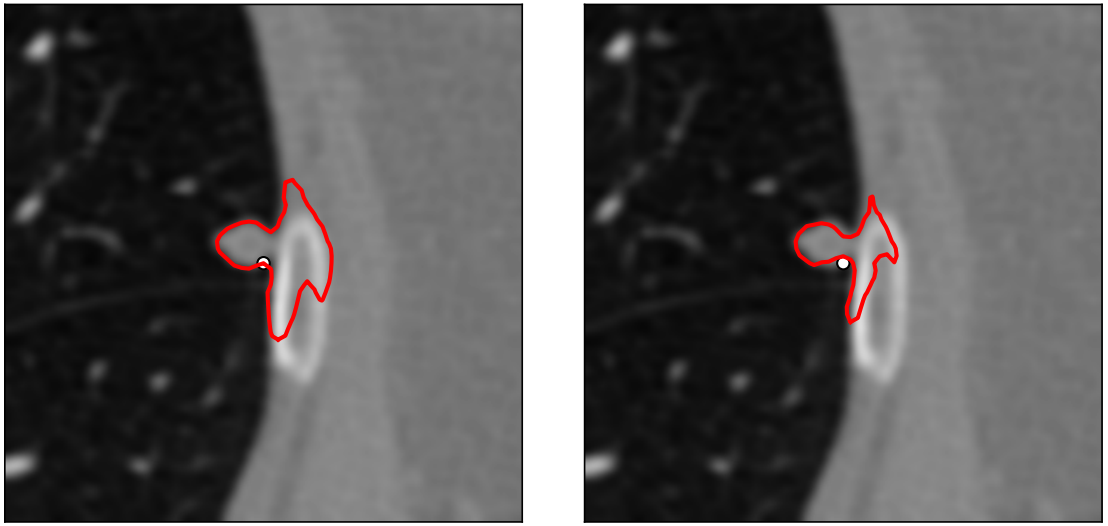

n = 9, Overlap = 0.2286

n = 9, Overlap = 0.3036

Lung Nodule Segmentation: Results, Example 3

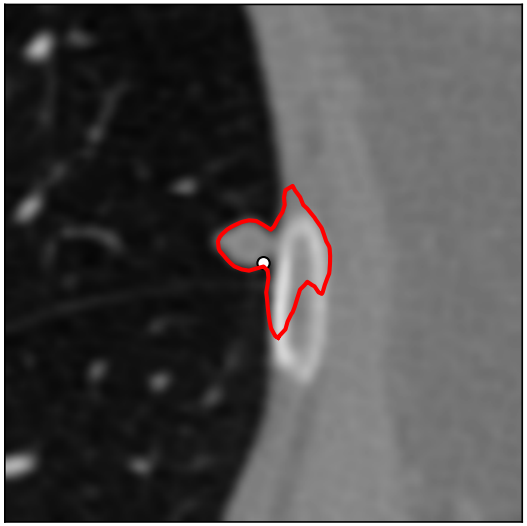

n = 13, Overlap = 0.2471

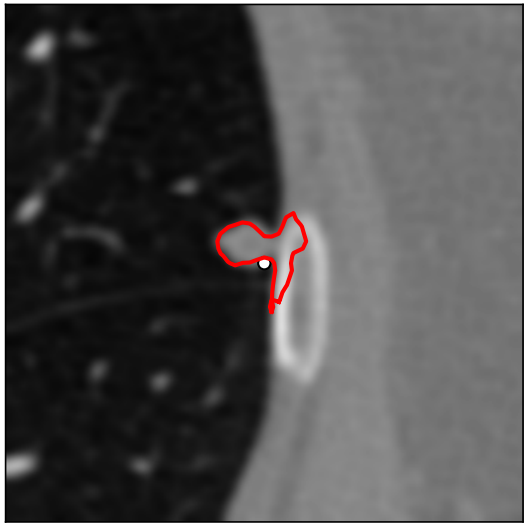

n = 13, Overlap = 0.3587

Lung Nodule Segmentation: Results, Example 3

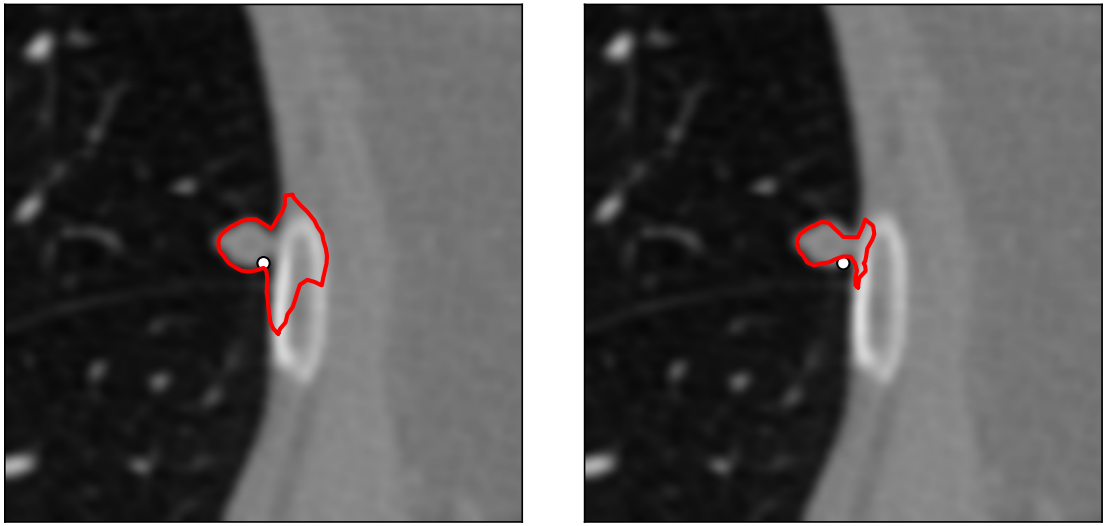

n = 17, Overlap = 0.2866

n = 17, Overlap = 0.4286

Lung Nodule Segmentation: Results, Example 3

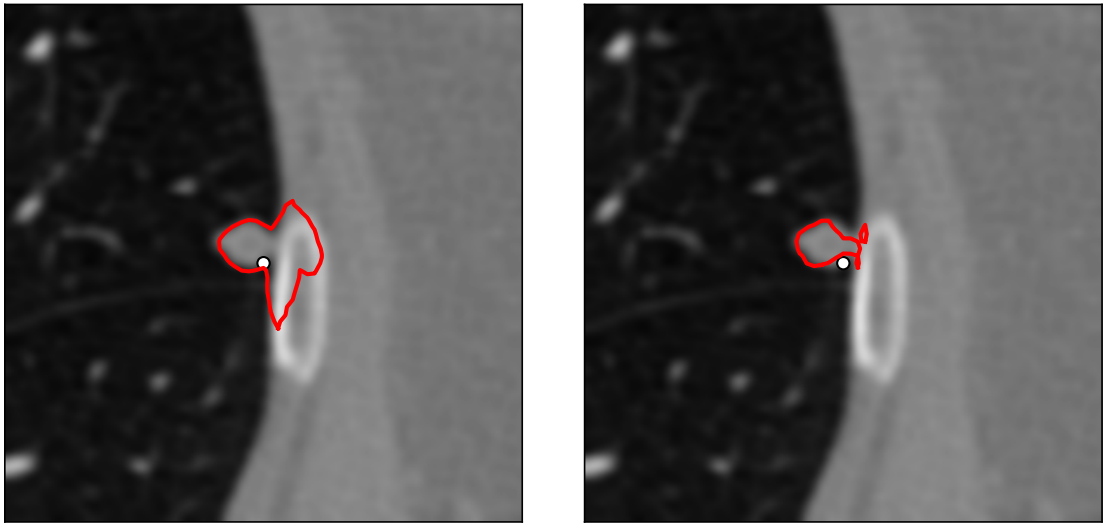

n = 21, Overlap = 0.3209

n = 21, Overlap = 0.4925

Lung Nodule Segmentation: Results, Example 3

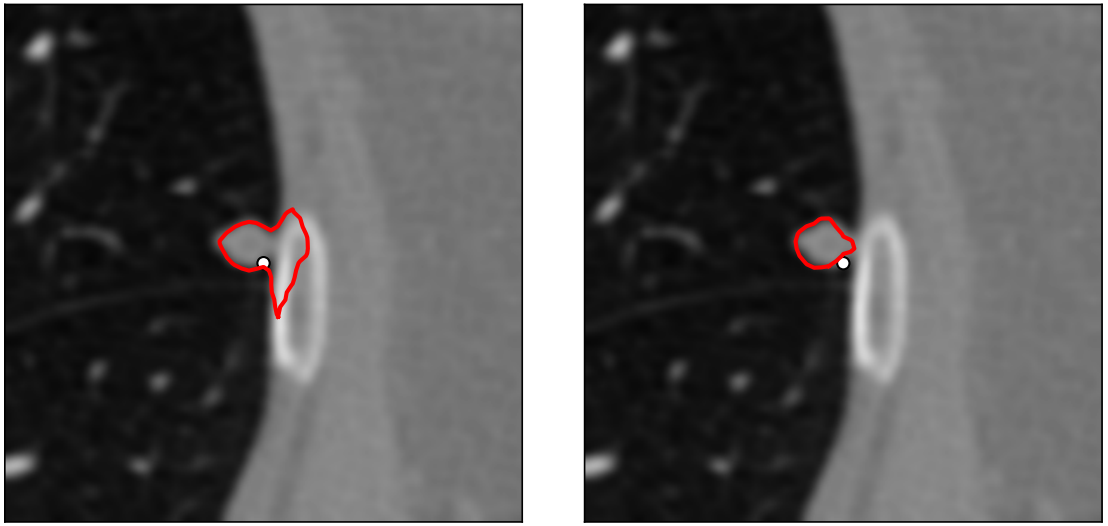

n = 24, Overlap = 0.3774

n = 26, Overlap = 0.6129

Lung Nodule Segmentation: Results, Example 3

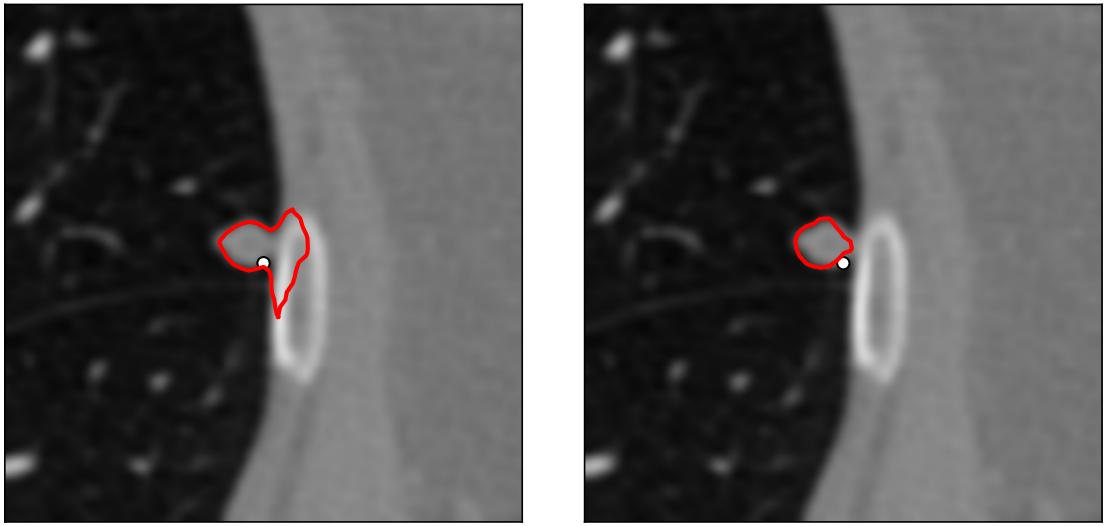

n = 24, Overlap = 0.3774

n = 30, Overlap = 0.5968

Lung Nodule Segmentation: Results, Example 4

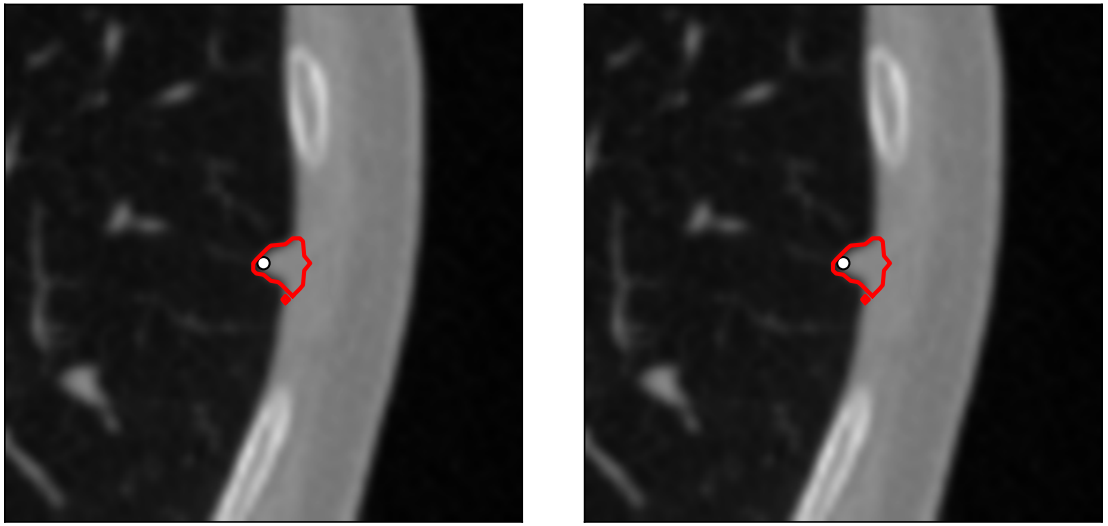

Lung Nodule Segmentation: Results, Example 4

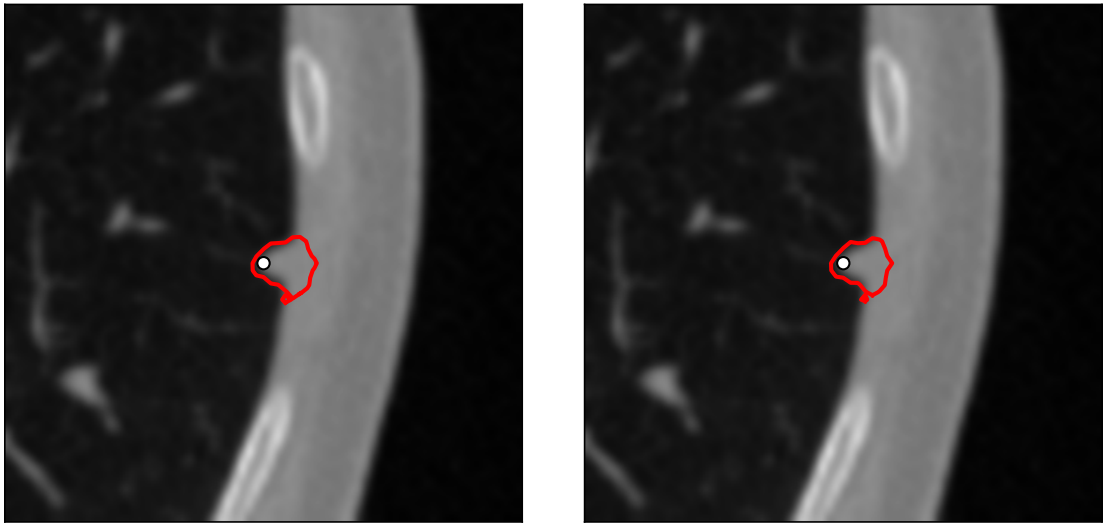

n = 4, Overlap = 0.4468

n = 4, Overlap = 0.5116

Lung Nodule Segmentation: Results, Example 4

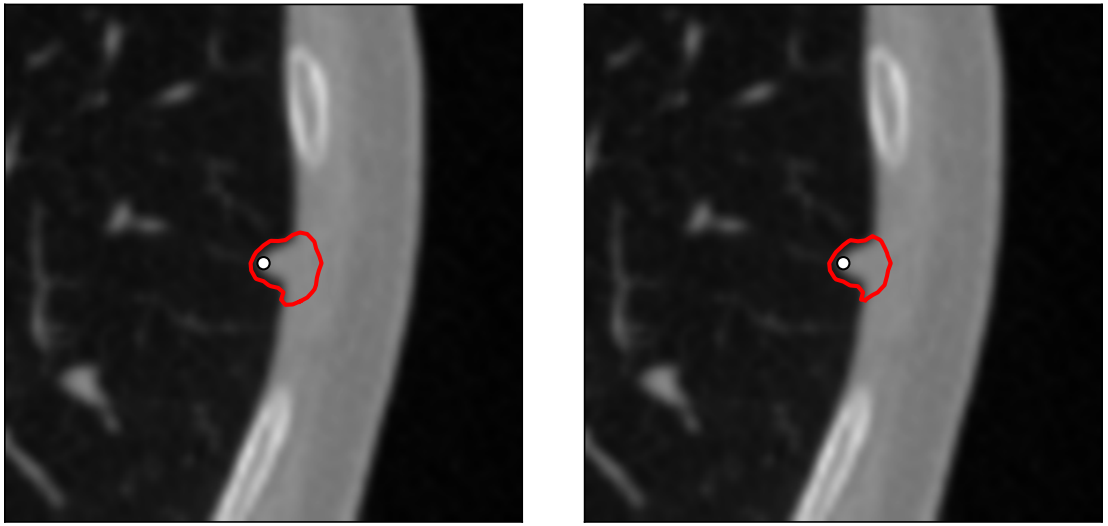

n = 9, Overlap = 0.3538

n = 9, Overlap = 0.4600

Lung Nodule Segmentation: Results, Example 4

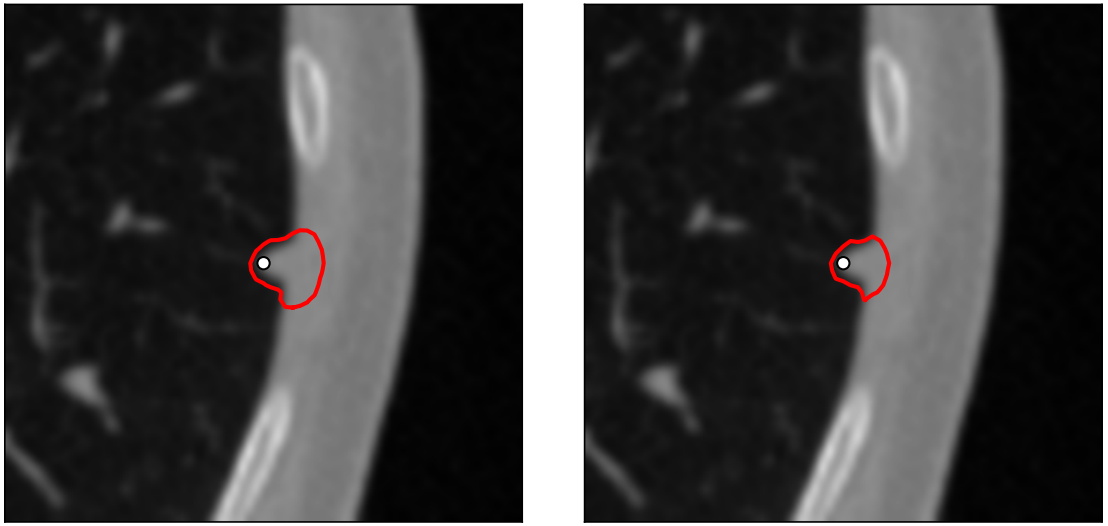

n = 13, Overlap = 0.3067

n = 13, Overlap = 0.4694

Lung Nodule Segmentation: Results, Example 4

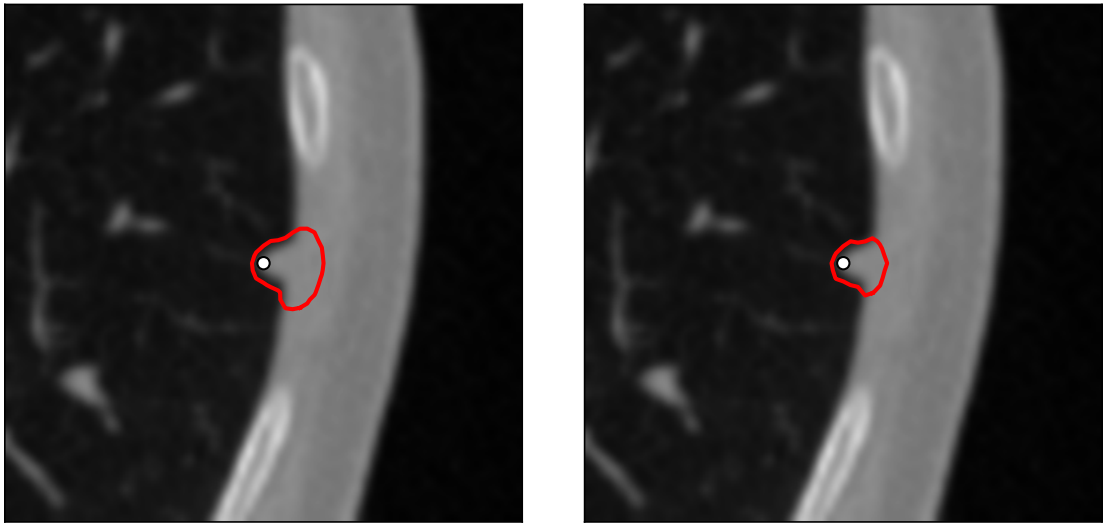

n = 17, Overlap = 0.2949

n = 17, Overlap = 0.5227

Lung Nodule Segmentation: Results, Example 4

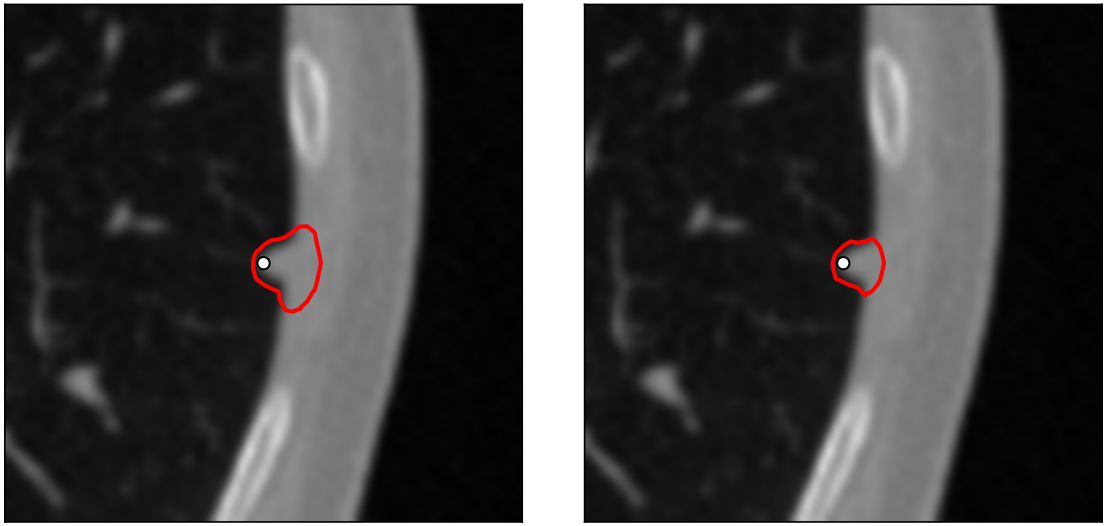

n = 21, Overlap = 0.3067

n = 21, Overlap = 0.5750

Lung Nodule Segmentation: Results, Example 4

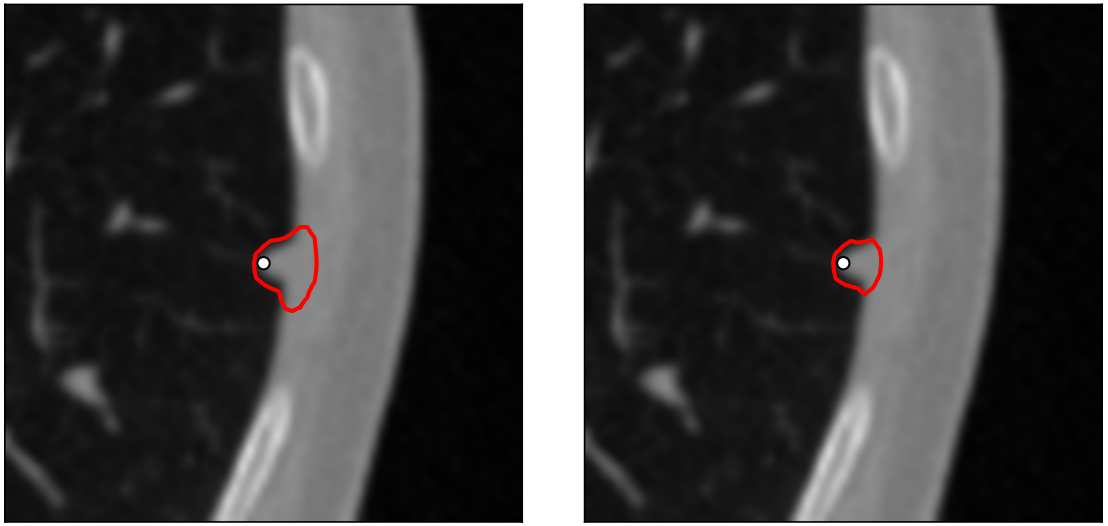

n = 24, Overlap = 0.3286

n = 26, Overlap = 0.5897

Lung Nodule Segmentation: Results, Example 4

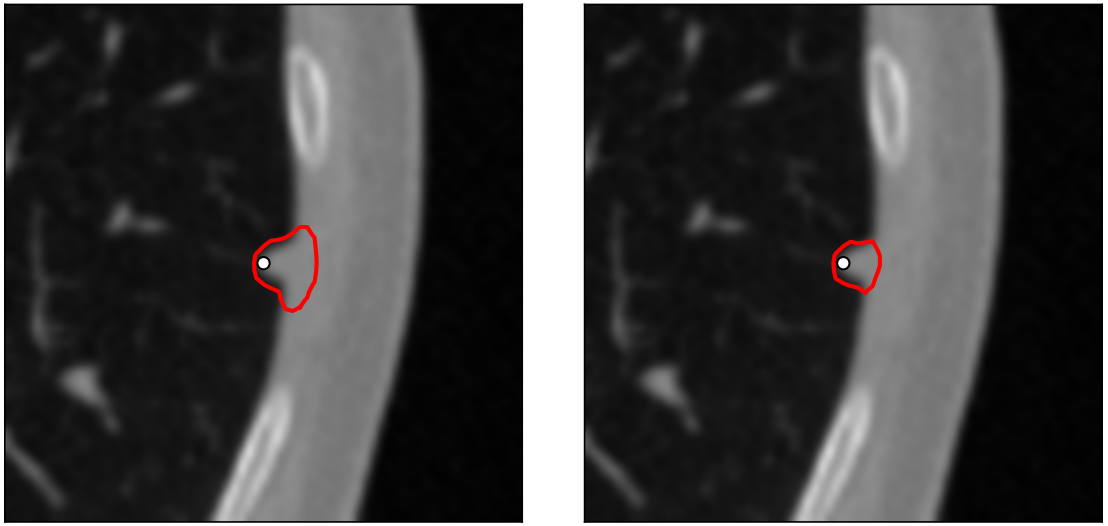

n = 24, Overlap = 0.3286

n = 30, Overlap = 0.6216

Lung Nodule Segmentation: Results, Example 5

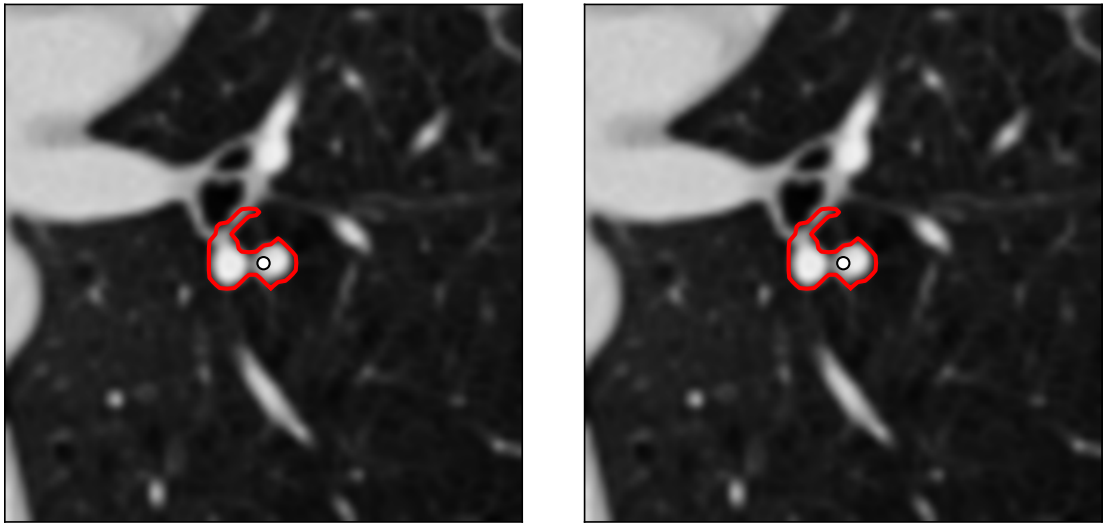

Lung Nodule Segmentation: Results, Example 5

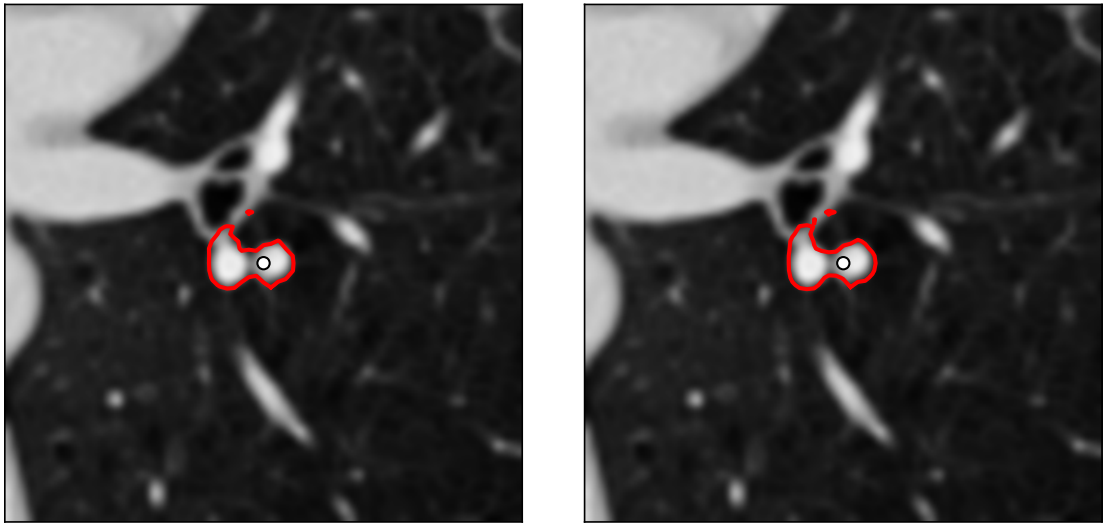

n = 4, Overlap = 0.3485

n = 4, Overlap = 0.3433

Lung Nodule Segmentation: Results, Example 5

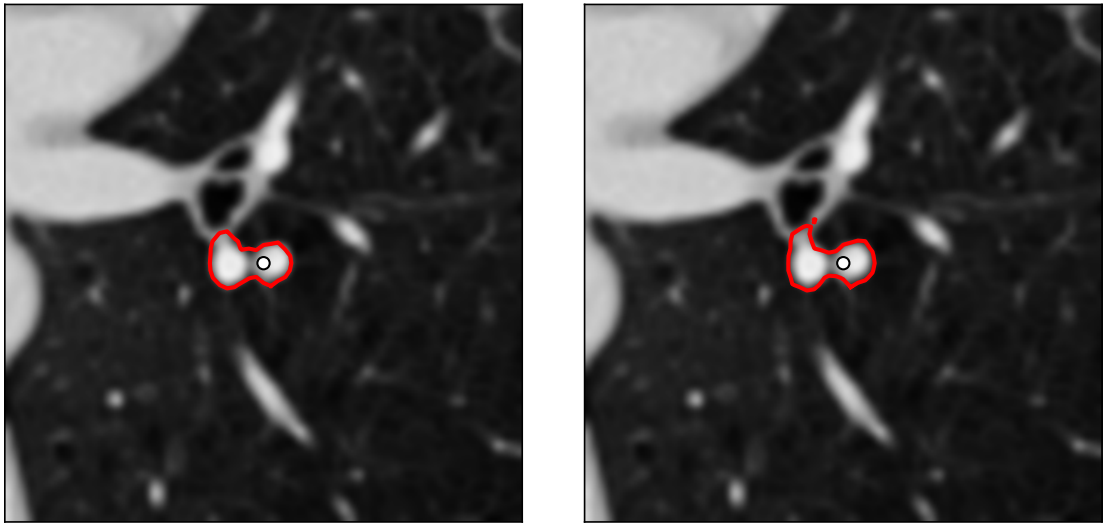

n = 9, Overlap = 0.3729

n = 9, Overlap = 0.3485

Lung Nodule Segmentation: Results, Example 5

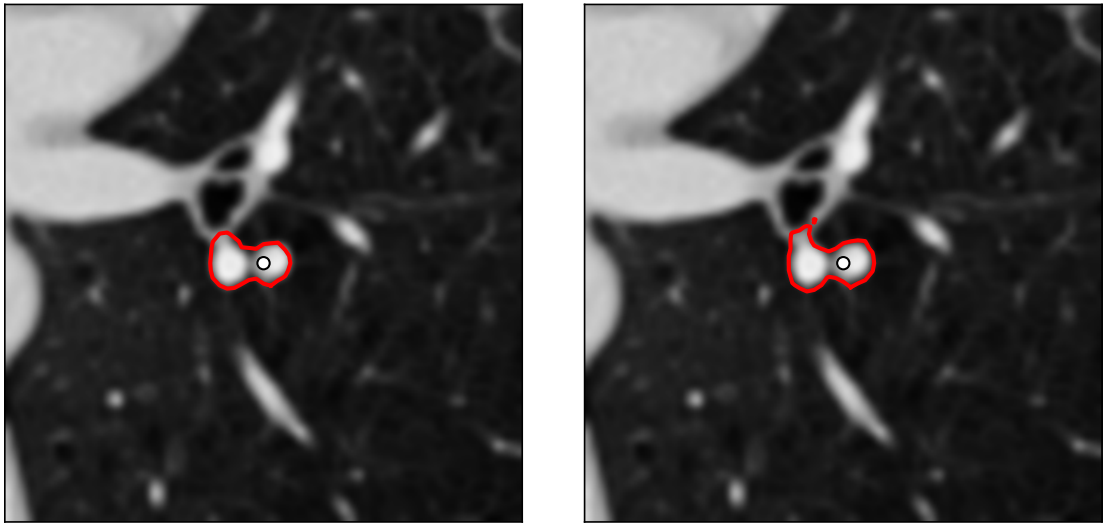

n = 13, Overlap = 0.3607

n = 13, Overlap = 0.3286

Lung Nodule Segmentation: Results, Example 5

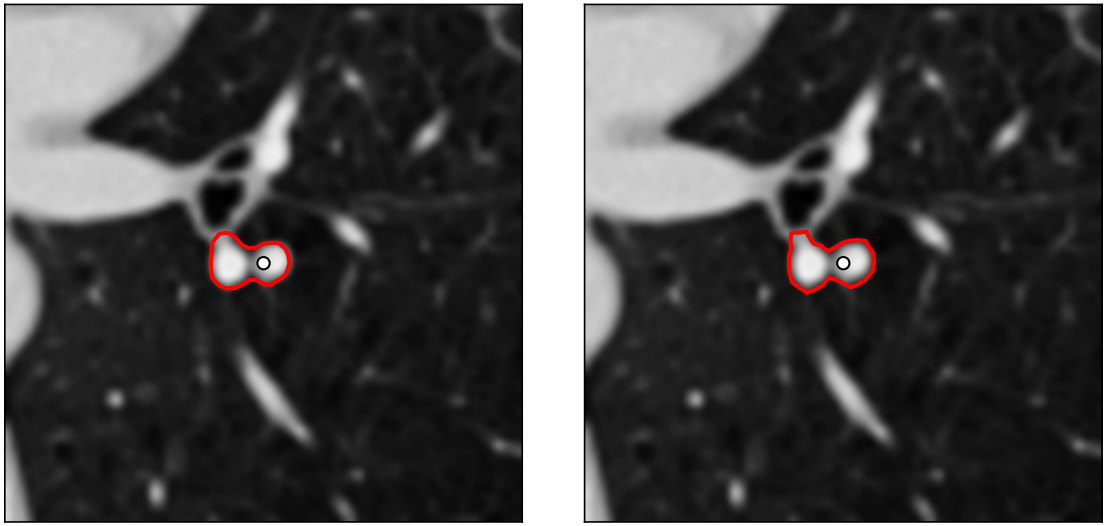

n = 17, Overlap = 0.3492

n = 17, Overlap = 0.3239

Lung Nodule Segmentation: Results, Example 5

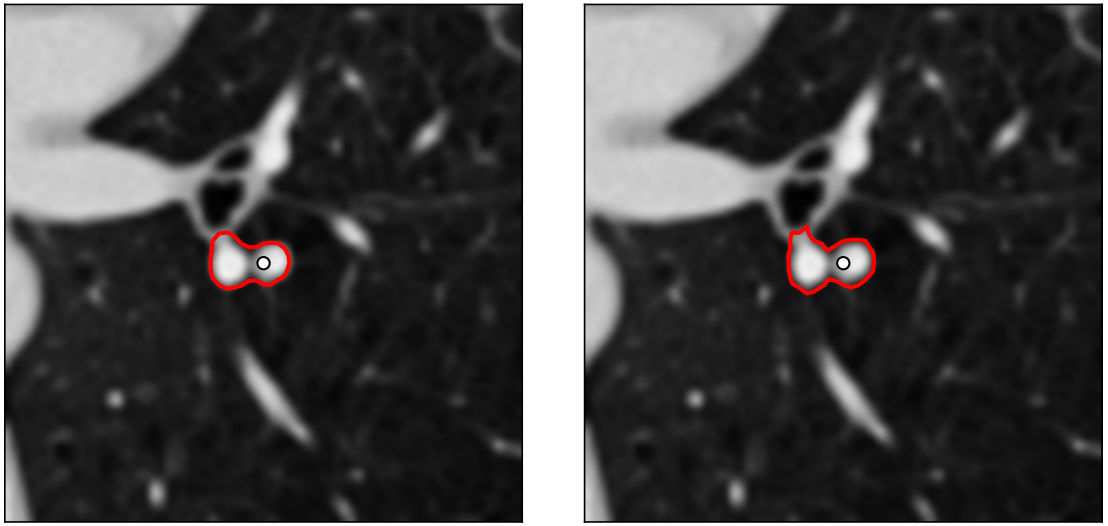

n = 21, Overlap = 0.3231

n = 21, Overlap = 0.3026

Lung Nodule Segmentation: Results, Example 5

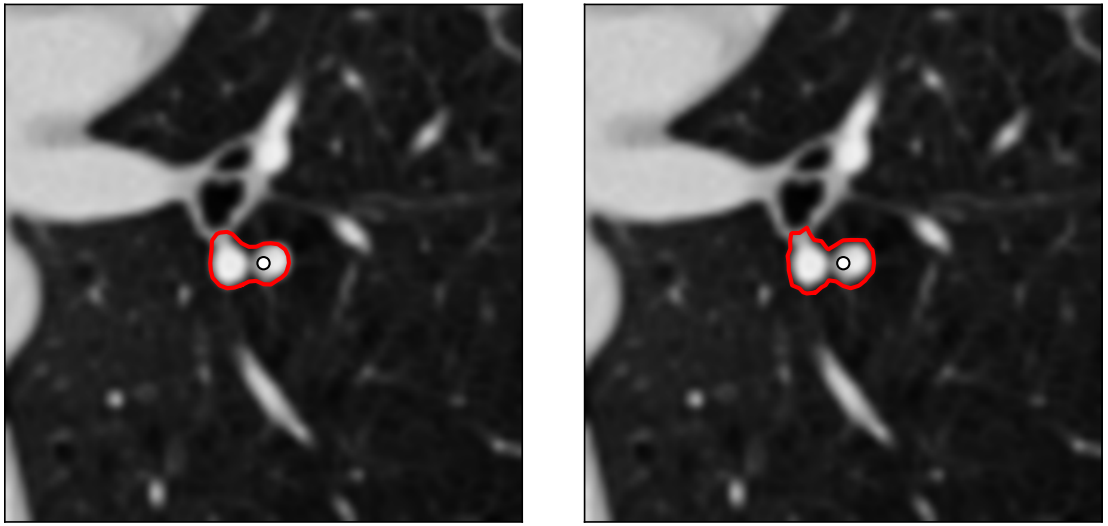

n = 24, Overlap = 0.3281

n = 26, Overlap = 0.2911

Lung Nodule Segmentation: Results, Example 5

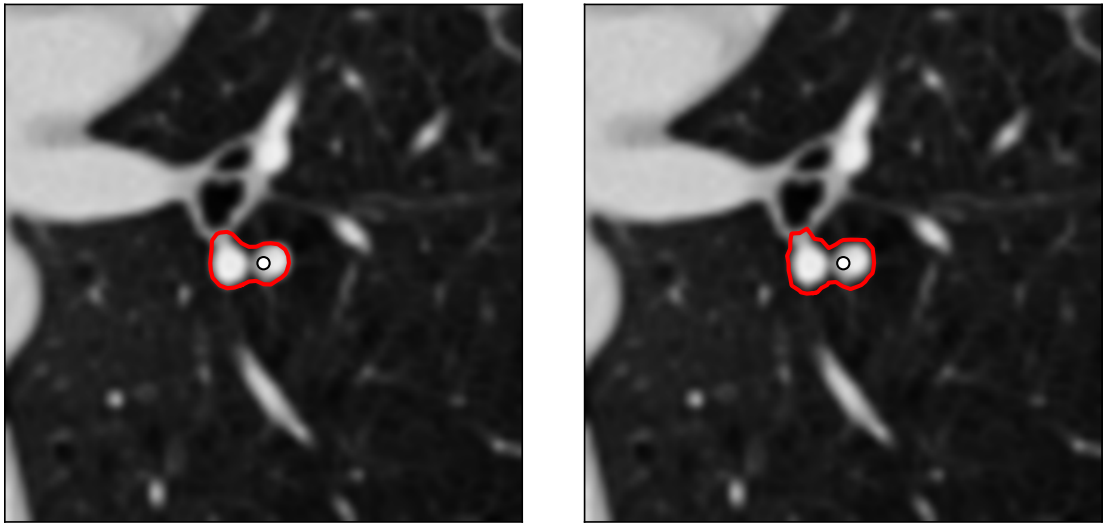

n = 24, Overlap = 0.3281

n = 30, Overlap = 0.2840

Lung Nodule Segmentation: Results, Example 6

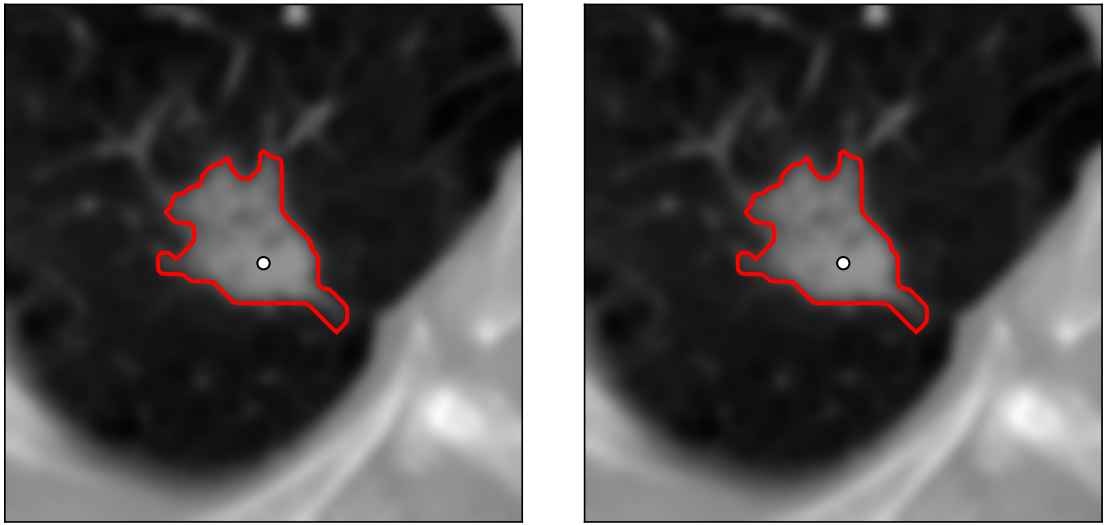

Lung Nodule Segmentation: Results, Example 6

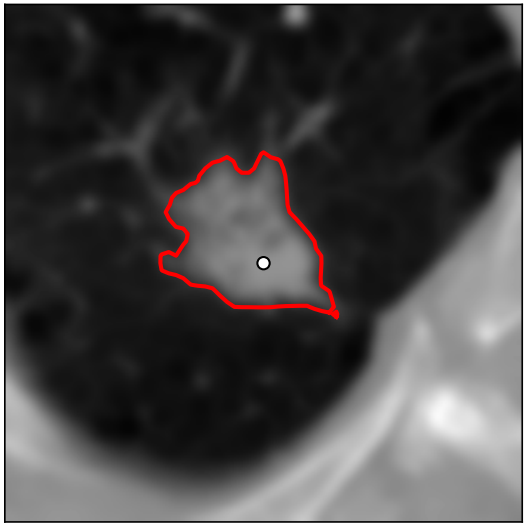

n = 4, Overlap = 0.7335

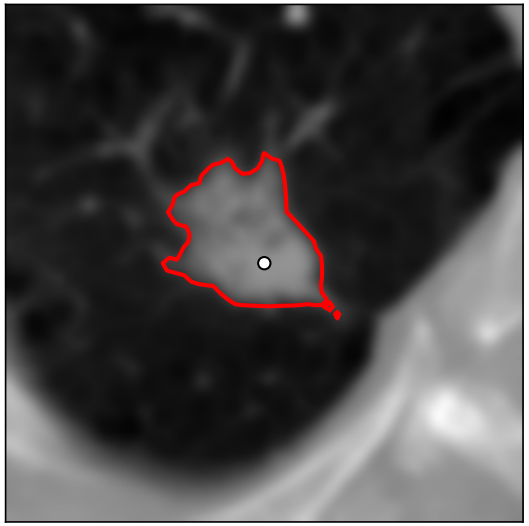

n = 4, Overlap = 0.7184

Lung Nodule Segmentation: Results, Example 6

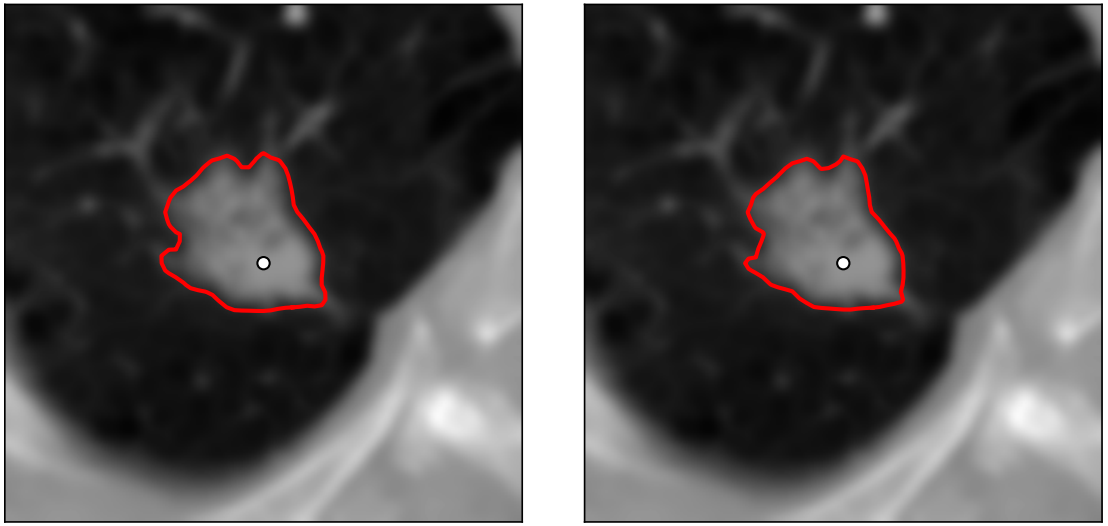

n = 9, Overlap = 0.7227

n = 9, Overlap = 0.6968

Lung Nodule Segmentation: Results, Example 6

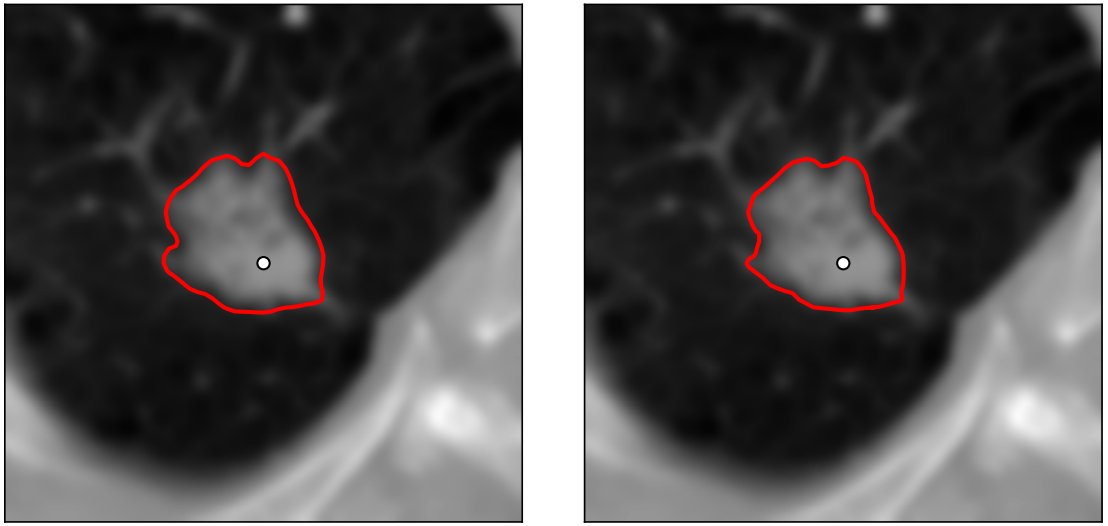

Lung Nodule Segmentation: Results, Example 6

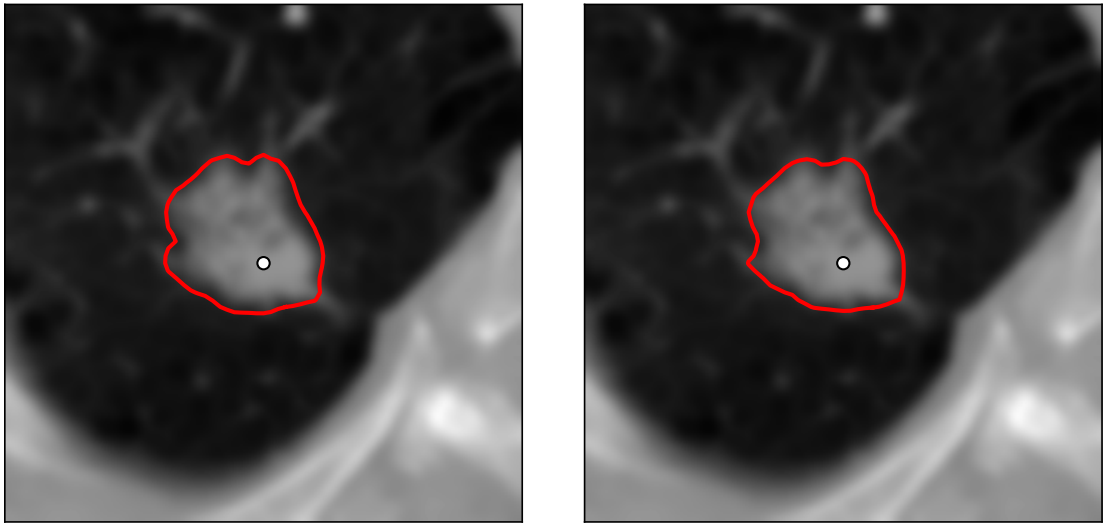

Lung Nodule Segmentation: Results, Example 6

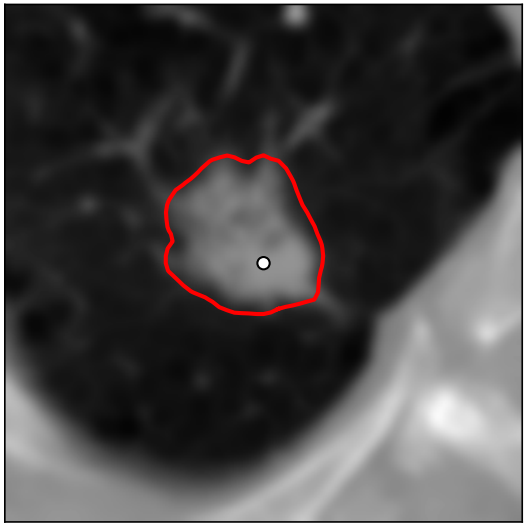

n = 21, Overlap = 0.7042

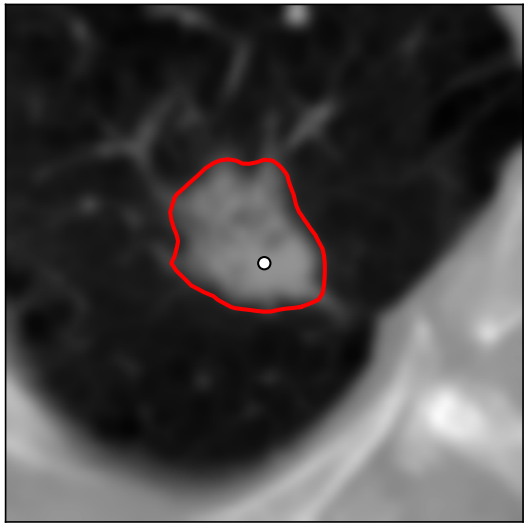

n = 21, Overlap = 0.6953

Lung Nodule Segmentation: Results, Example 6

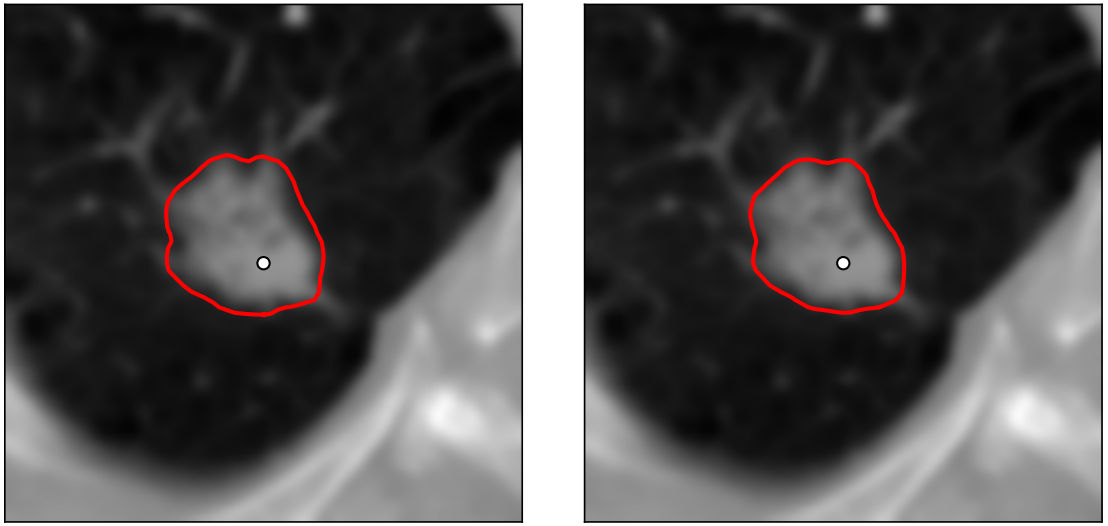

Lung Nodule Segmentation: Results, Example 6

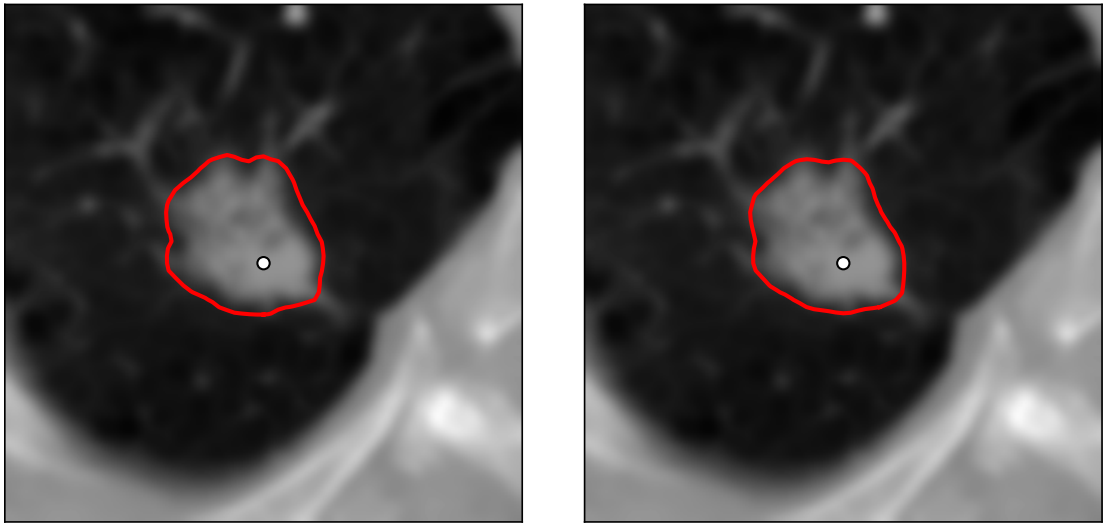

n = 24, Overlap = 0.7024

n = 30, Overlap = 0.6920

Lung Nodule Segmentation: Results, Example 7

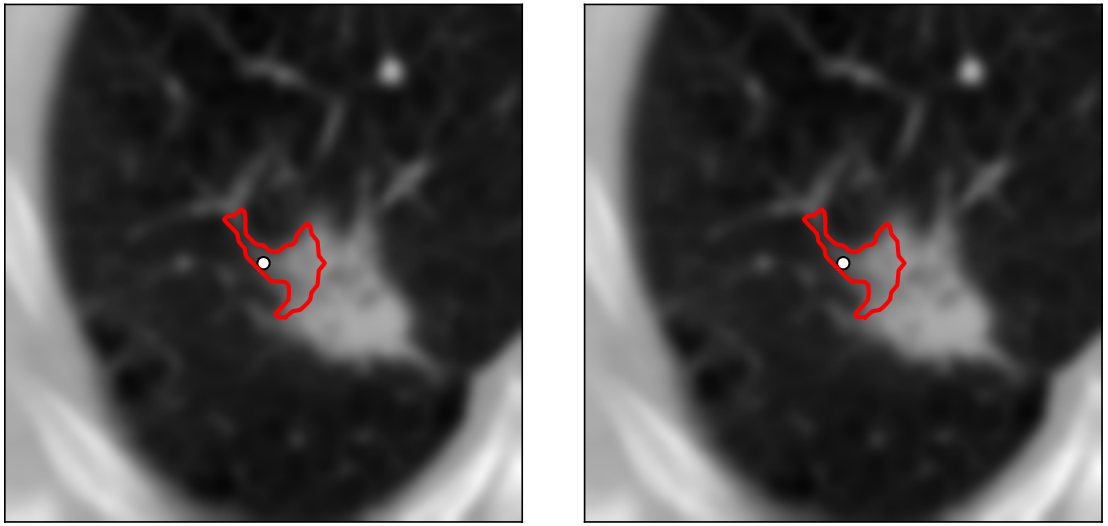

Lung Nodule Segmentation: Results, Example 7

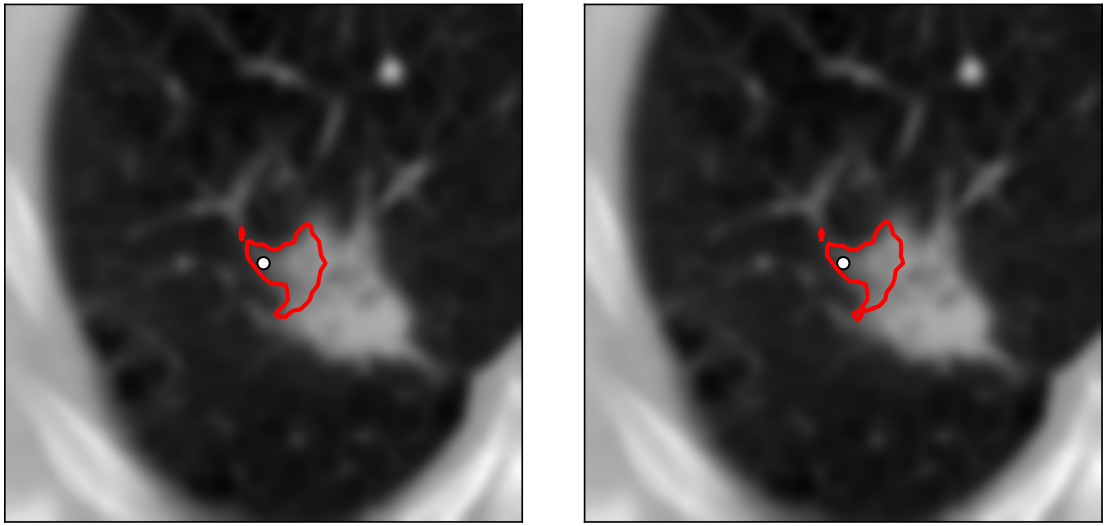

n = 4, Overlap = 0.1605

n = 4, Overlap = 0.1481

Lung Nodule Segmentation: Results, Example 7

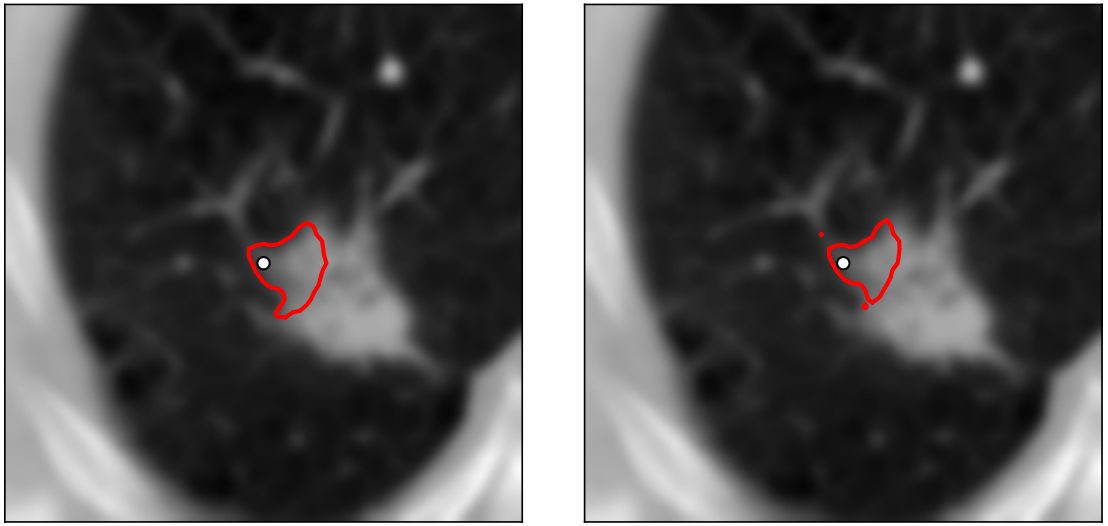

Lung Nodule Segmentation: Results, Example 7

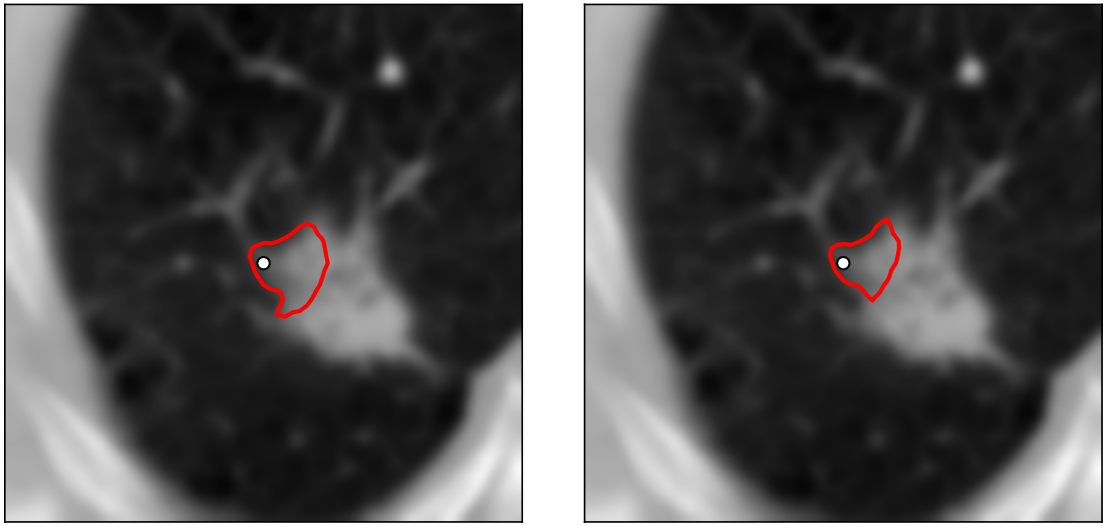

n = 13, Overlap = 0.1912

n = 13, Overlap = 0.1425

Lung Nodule Segmentation: Results, Example 7

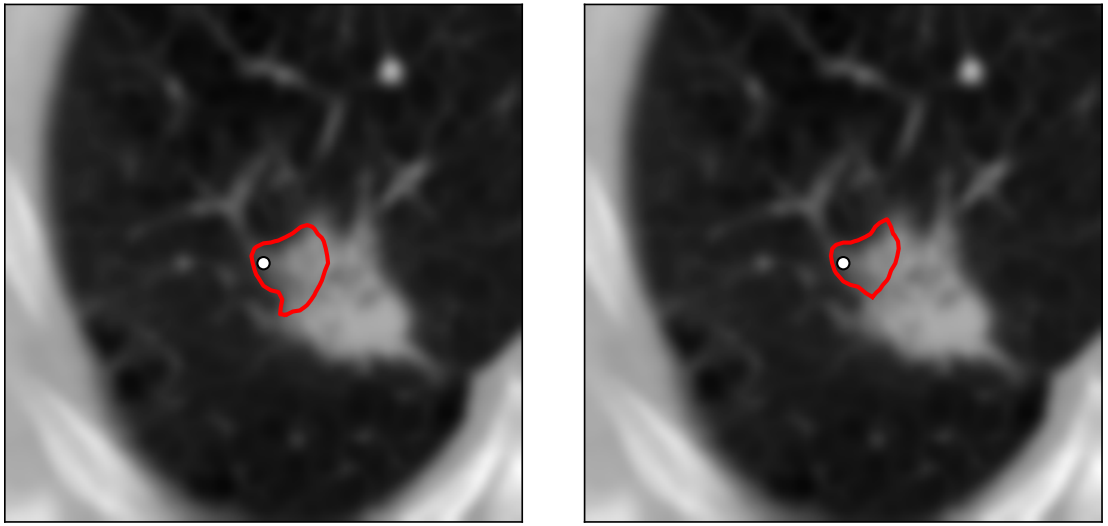

n = 17, Overlap = 0.1883

n = 17, Overlap = 0.1400

Lung Nodule Segmentation: Results, Example 7

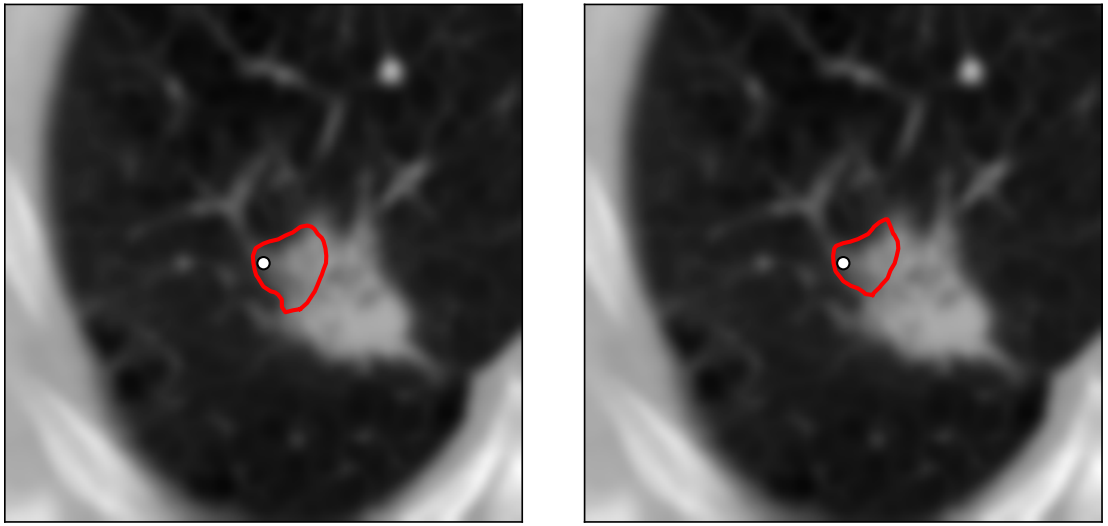

n = 21, Overlap = 0.1858

n = 21, Overlap = 0.1397

Lung Nodule Segmentation: Results, Example 7

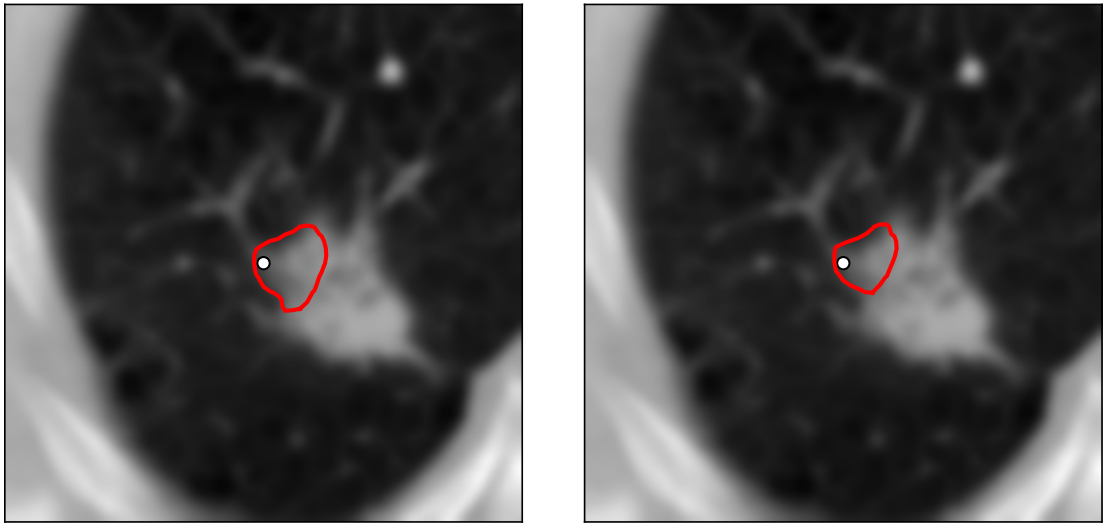

n = 24, Overlap = 0.1858

n = 26, Overlap = 0.1324

Lung Nodule Segmentation: Results, Example 7

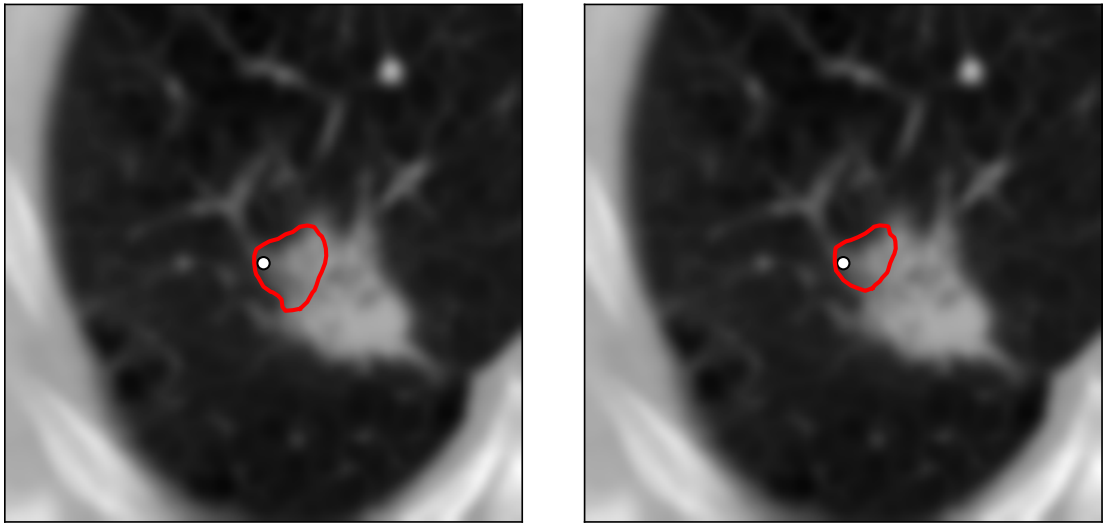

n = 24, Overlap = 0.1858

n = 30, Overlap = 0.1247

References I

[1] Reduced Lung-Cancer Mortality with Low-Dose Computed Tomographic Screening. *New England Journal of Medicine*, 365(5):395–409, August 2011.

[2] Samuel G. Armato III, Geoffrey McLennan, Luc Bidaut, Michael F. McNitt-Gray, Charles R. Meyer, Anthony P. Reeves, Binsheng Zhao, Denise R. Aberle, Claudia I. Henschke, Eric A. Hoffman, and others. The lung image database consortium (LIDC) and image database resource initiative (IDRI): a completed reference database of lung nodules on CT scans. *Medical physics*, 38(2):915–931, 2011.

[3] Claudia I. Henschke, David F. Yankelevitz, Daniel M. Libby, and Mark W. Pasmantier. Survival of Patients with Stage I Lung Cancer Detected on CT Screening. *New England Journal of Medicine*, 355(17), 2006.

[4] Michael Kass, Andrew Witken, and Demetri Terzopoulos. Snakes: active contour models. *International Journal of Computer Vision*, 1(4):321–331, 1988.

References II

[5] Toshiro Kubota, Anna K. Jerebko, Maneesh Dewan, Marcos Salganicoff, and Arun Krishnan. Segmentation of pulmonary nodules of various densities with morphological approaches and convexity models. *Medical Image Analysis*, 15(1):133–154, February 2011.

[6] B C Lassen, C Jacobs, J-M Kuhnigk, B van Ginneken, and E M van Rikxoort. Robust semi-automatic segmentation of pulmonary subsolid nodules in chest computed tomography scans. *Physics in Medicine and Biology*, 60(3):1307–1323, February 2015.

[7] R Malladi and JA Sethian. Shape modeling with front propagation: A level set approach. *IEEE Transactions on Pattern Analysis and Machine Intelligence*, 17(2), 1995.

References III

[8] Michael F. McNitt-Gray, Samuel G. Armato, Charles R. Meyer, Anthony P. Reeves, Geoffrey McLennan, Richie C. Pais, John Freymann, Matthew S. Brown, Roger M. Engelmann, Peyton H. Bland, Gary E. Laderach, Chris Piker, Junfeng Guo, Zaid Towfic, David P.-Y. Qing, David F. Yankelevitz, Denise R. Aberle, Edwin J.R. van Beek, Heber MacMahon, Ella A. Kazerooni, Barbara Y. Croft, and Laurence P. Clarke. The Lung Image Database Consortium (LIDC) Data Collection Process for Nodule Detection and Annotation. *Academic Radiology*, 14(12): 1464–1474, December 2007.

[9] Temesguen Messay, Russell C. Hardie, and Steven K. Rogers. A new computationally efficient CAD system for pulmonary nodule detection in CT imagery. *Medical Image Analysis*, 14(3):390–406, June 2010.

[10] Temesguen Messay, Russell C. Hardie, and Timothy R. Tuinstra. Segmentation of pulmonary nodules in computed tomography using a regression neural network approach and its application to the Lung Image Database Consortium and Image Database Resource Initiative dataset. *Medical Image Analysis*, 22(1):48–62, May 2015.

References IV

[11] Rie Tachibana and Shoji Kido. Automatic segmentation of pulmonary nodules on CT images by use of NCI lung image database consortium. March 2006.

[12] Yongqiang Tan, Lawrence H. Schwartz, and Binsheng Zhao. Segmentation of lung lesions on CT scans using watershed, active contours, and Markov random field. *Medical physics*, 40(4):043502, 2013.

[13] Qian Wang, Enmin Song, Renchao Jin, Ping Han, Xiaotong Wang, Yanying Zhou, and Jianchao Zeng. Segmentation of Lung Nodules in Computed Tomography Images Using Dynamic Programming and Multidirection Fusion Techniques1. *Academic Radiology*, 16(6):678–688, June 2009.

[14] Shuo Wang, Mu Zhou, Zaiyi Liu, Zhenyu Liu, Dongsheng Gu, Yali Zang, Di Dong, Olivier Gevaert, and Jie Tian. Central focused convolutional neural networks: Developing a data-driven model for lung nodule segmentation. *Medical Image Analysis*, 40:172–183, August 2017.